ORNL/SUB/98-85B99398V-2

ornl

OAK RIDGE
NATIONAL
LABORATORY

LOCKHEED MARTIN

Results of Parametric Design Studies of VVER-1000 Core with MOX Lead Test Assemblies

Project Manager

A. M. Pavlovitchev

Executed by

A. A. Aleshin
S. N. Bolshagin
N. A. Bychkova
Y. A. Styrin
M. Y. Tomilov

MANAGED AND OPERATED BY
LOCKHEED MARTIN ENERGY RESEARCH CORPORATION
FOR THE UNITED STATES
DEPARTMENT OF ENERGY

ORNL-27 (3-96)

This report has been reproduced from the best available copy.

Reports are available to the public from the following source.

National Technical Information Service
5285 Port Royal Road
Springfield, VA 22161
Telephone 703-605-6000 (1-800-553-6847)
TDD 703-487-4639
Fax 703-605-6900
E-mail orders@ntis.fedworld.gov
Web site http://www.ntis.gov/ordering.htm

Reports are available to U.S. Department of Energy (DOE) employees, DOE contractors, Energy Technology Data Exchange (ETDE) representatives, and International Nuclear Information System (INIS) representatives from the following source.

Office of Scientific and Technical Information
P.O. Box 62
Oak Ridge, TN 37831
Telephone 423-576-8401
Fax 423-576-5728
E-mail reports@adonis.osti.gov
Web site http://www.osti.gov/products/sources.html

Reports produced after January 1, 1996, are generally available via the DOE Information Bridge.
Web site http://www.doe.gov/bridge

This report was prepared as an account of work sponsored by an agency of the United States Government. Neither the United States Government nor any agency thereof, nor any of their employees, makes any warranty, express or implied, or assumes any legal liability or responsibility for the accuracy, completeness, or usefulness of any information, apparatus, product, or process disclosed, or represents that its use would not infringe privately owned rights. Reference herein to any specific commercial product, process, or service by trade name, trademark, manufacturer, or otherwise, does not necessarily constitute or imply its endorsement, recommendation, or favoring by the United States Government or any agency thereof. The views and opinions of authors expressed herein do not necessarily state or reflect those of the United States Government or any agency thereof.

ORNL/SUB/98-85B99398V-2

RESULTS OF PARAMETRIC DESIGN STUDIES OF VVER-1000 CORE WITH MOX LEAD TEST ASSEMBLIES

Project Manager

A. M. Pavlovitchev

Executed by

A. A. Aleshin
S. N. Bolshagin
N. A. Bychkova
Y. A. Styrin
M. Y. Tomilov

Date Published: December 1998

Report Prepared by
LOCKHEED MARTIN ENERGY RESEARCH CORP.
P.O. Box 2008
Oak Ridge, Tennessee 37831-6363
under
Subcontract Number 85B99398V

Funded by
Office of Fissile Materials Disposition
United States Department of Energy

Prepared for

Computational Physics and Engineering Division
Oak Ridge National Laboratory
Oak Ridge, Tennessee 37831
managed by
LOCKHEED MARTIN ENERGY RESEARCH CORP.
for the
U.S. DEPARTMENT OF ENERGY
under contract DE-96OR22464

Russian Research Center "Kurchatov Institute"
Institute of Nuclear Reactors
VVER Division

Joint U.S. / Russian Project to Update, Verify and Validate Reactor Design/Safety Computer Codes Associated with Weapons-Grade Plutonium Disposition in VVER Reactors.

Results of Parametric Design Studies of VVER-1000 Core with MOX Lead Test Assemblies

(Report for FY98)

Project Manager

A.M.Pavlovitchev

Executed by

A.A.Aleshin
S.N.Bolshagin
N.A.Bychkova
Y.A.Styrin
M.Y.Tomilov

Moscow 1998

ACRONYMS

BOC	beginning of cycle
BPR	boron poison rod
CR	control rods
DTC	Doppler coefficient
EFPD	effective full power day
EOC	end of cycle
FP	fission products
LWR	light water reactor
LTA	lead test assembly
MCL	minimum controllable level
MDC	moderator density coefficient
MOX	mixed oxide
MTC	moderator temperature coefficient
PWR	pressurized-water reactor
SOR	system of regulation
UOX	uranium oxide
VVER	Russian water-water reactor

EXECUTIVE SUMMARY

In this document the results of neutronics calculations of VVER-1000 core with 3 MOX LTA are presented. Performance of MOX LTA in core is studied for two options of LTA design: 100% plutonium and of "plutonium island" type. The coarse-mesh (assembly-by-assembly) core calculations are carried out by the Russian code BIPR-7A and fine-mesh (pin-by-pin) core calculations – by the Russian code PERMAK-A.

CONTENTS

INTRODUCTION 9

1. DEFINITIONS 9

2. COARSE-MESH CODE BIPR-7A 15

3. FINE-MESH CODE PERMAK-A 16

4. RESULTS OF URANIUM CORE CALCULATIONS 17

5. RESULTS OF MOX CORE CALCULATIONS 18

5.1. CORE WITH 100% PLUTONIUM MOX LTAS 18
5.2. CORE WITH "ISLAND" TYPE MOX LTAS 19
5.3. CALCULATIONS IN ZERO POWER STATES AND CONTROL RODS WORTH 19

CONCLUSION 21

REFERENCES 22

TABLE 1. LIMITING PARAMETERS FOR VVER-1000 23

TABLE 2. LIMITS RECOMMENDED FOR TOTAL POWER PEAKING FACTOR KOJ LIM 23

TABLE 3. RECOMMENDED LIMITING PARAMETERS FOR VVER-1000 WITH MOX FUEL 24

TABLE 4. LIMITS RECOMMENDED FOR TOTAL POWER PEAKING FACTOR KOJ LIM FOR VVER-1000 WITH MOX FUEL 24

TABLE 5. EVOLUTION OF MAIN NEUTRONICS PARAMETERS. REFERENCE URANIUM CORE EQUILIBRIUM CYCLE. CORE 60° SECTOR 25

TABLE 6. MAIN NEUTRONICS PARAMETERS IN ZERO POWER STATES. REFERENCE URANIUM CORE EQUILIBRIUM CYCLE 26

TABLE 7. EVOLUTION OF MAIN NEUTRONICS PARAMETERS. CYCLE 1-MOX. "ISLAND-2" TYPE PU(3.8-2.8) – U3.7% 27

TABLE 8. MAIN NEUTRONICS PARAMETERS IN ZERO POWER STATES. CYCLE 1-MOX. "ISLAND-2" TYPE PU(3.8-2.8) – U3.7% 28

TABLE 9. EVOLUTION OF MAIN NEUTRONICS PARAMETERS. CYCLE-1 MOX. 100%PU(4.2-3.0-2.0) 29

TABLE 10. MAIN NEUTRONICS PARAMETERS IN ZERO POWER STATES. CYCLE-1 MOX. 100%PU(4.2-3.0-2.0) 30

TABLE 11. EVOLUTION OF MAIN NEUTRONICS PARAMETERS. CYCLE 2-MOX. 100%PU(4.2-3.0-2.0) 31

TABLE 12. MAIN NEUTRONICS PARAMETERS IN ZERO POWER STATES. CYCLE-2 MOX. 100%PU(4.2-3.0-2.0) 32

TABLE 13. EVOLUTION OF MAIN NEUTRONICS PARAMETERS. CYCLE 3-MOX. 100%PU(4.2-3.0-2.0)33

TABLE 14. MAIN NEUTRONICS PARAMETERS IN ZERO POWER STATES. CYCLE-3 MOX. 100%PU(4.2-3.0-2.0) 34

TABLE 15A. CONTROL RODS WORTH CALCULATION. STATES DESCRIPTION 35

TABLE 15B. CONTROL RODS WORTH IN URANIUM REFERENCE CORE AND IN 3 MOX LTAS LOADED CORES (PCM) 35

FIG. 1. SIMPLIFIED DESIGN FOR 3 ZONES MOX LTA 36

FIG. 2. SIMPLIFIED DESIGN FOR "ISLAND-2" TYPE MOX LTA 37

FIG. 3. SIMPLIFIED DESIGN FOR VVER-1000 FUEL ASSEMBLY. TYPE A 38

FIG. 4. SIMPLIFIED DESIGN FOR VVER-1000 FUEL ASSEMBLY. TYPES B AND BA 39

FIG. 5. SIMPLIFIED DESIGN FOR VVER-1000 FUEL ASSEMBLY. TYPE C 40

FIG. 6. EQUILIBRIUM LOADING PATTERN FOR REFERENCE URANIUM CORE WITH BORON BPRS, CORE 60 ° SECTOR 41

FIG. 7. EQUILIBRIUM CYCLE FOR REFERENCE URANIUM CORE. ASSEMBLY-BY-ASSEMBLY BURNUP AND POWER DISTRIBUTION, CORE 60 ° SECTOR 42

FIG. 8. BEGINNING OF THE EQUILIBRIUM CYCLE FOR REFERENCE URANIUM CORE. ASSEMBLY-BY-ASSEMBLY PIN POWER PEAKING FACTOR, CORE 60 ° SECTOR 43

FIG. 9. END OF THE EQUILIBRIUM CYCLE FOR REFERENCE URANIUM CORE. ASSEMBLY-BY-ASSEMBLY PIN POWER PEAKING FACTOR, CORE 60 ° SECTOR 44

FIG. 10. BEGINNING OF THE EQUILIBRIUM CYCLE FOR REFERENCE URANIUM CORE. ASSEMBLY-BY-ASSEMBLY MAXIMUM PIN LINEAR POWER, CORE 60 ° SECTOR 45

FIG. 11. END OF THE EQUILIBRIUM CYCLE FOR REFERENCE URANIUM CORE. ASSEMBLY-BY-ASSEMBLY MAXIMUM PIN LINEAR POWER, CORE 60 ° SECTOR 46

FIG. 12. BEGINNING OF THE EQUILIBRIUM CYCLE FOR REFERENCE URANIUM CORE. RELATIVE POWER DISTRIBUTION IN THE MOST POWERED ASSEMBLY 47

FIG. 13. END OF THE EQUILIBRIUM CYCLE FOR REFERENCE URANIUM CORE. RELATIVE POWER DISTRIBUTION IN THE MOST POWERED ASSEMBLY 48

FIG. 14. LOADING PATTERN FOR THE FIRST CYCLE WITH 3 MOX LTAS 49

FIG. 15. FIRST CYCLE WITH 3 MOX LTAS OF "ISLAND-2" TYPE (PU3.8-2.8-U3.7). ASSEMBLY-BY-ASSEMBLY BURNUP DISTRIBUTION 50

FIG. 16. FIRST CYCLE WITH 3 MOX LTAS OF "ISLAND-2" TYPE (PU3.8-2.8-U3.7). ASSEMBLY-BY-ASSEMBLY POWER DISTRIBUTION 51

FIG. 17. BEGINNNING OF THE FIRST CYCLE WITH 3 MOX LTAS OF "ISLAND-2" TYPE (PU3.8-2.8-U3.7). ASSEMBLY-BY-ASSEMBLY PIN POWER PEAKING FACTOR 52

FIG. 18. END OF THE FIRST CYCLE WITH 3 MOX LTAS OF "ISLAND-2" TYPE (PU3.8-2.8-U3.7). ASSEMBLY-BY-ASSEMBLY PIN POWER PEAKING FACTOR 53

FIG. 19. BEGINNING OF THE FIRST CYCLE WITH 3 MOX LTAS OF "ISLAND-2" TYPE (PU3.8-2.8-U3.7). ASSEMBLY-BY-ASSEMBLY MAXIMUM PIN LINEAR POWER 54

FIG. 20. END OF THE FIRST CYCLE WITH 3 MOX LTAS OF "ISLAND-2" TYPE (PU3.8-2.8-U3.7). ASSEMBLY-BY-ASSEMBLY MAXIMUM PIN LINEAR POWER 55

FIG. 21. BEGINNING OF THE FIRST CYCLE WITH 3 MOX LTAS OF "ISLAND-2" TYPE (PU3.8-2.8-U3.7). RELATIVE POWER DISTRIBUTION IN THE MOST POWERED ASSEMBLY 56

FIG. 22. END OF THE FIRST CYCLE WITH 3 MOX LTAS OF "ISLAND-2" TYPE (PU3.8-2.8-U3.7). RELATIVE POWER DISTRIBUTION IN THE MOST POWERED ASSEMBLY 57

FIG. 23. BEGINNING OF THE FIRST CYCLE WITH 3 MOX LTAS OF "ISLAND-2" TYPE (PU3.8-2.8-U3.7). RELATIVE POWER DISTRIBUTION IN THE MOX ASSEMBLY 58

FIG. 24. END OF THE FIRST CYCLE WITH 3 MOX LTAS OF "ISLAND-2" TYPE (PU3.8-2.8-U3.7). RELATIVE POWER DISTRIBUTION IN THE MOX ASSEMBLY 59

FIG. 25. END OF THE FIRST CYCLE WITH 3 MOX LTAS OF "ISLAND-2" TYPE (PU3.8-2.8-U3.7). RELATIVE BURNUP DISTRIBUTION IN THE MOX ASSEMBLY 60

FIG. 26. FIRST CYCLE WITH 3 MOX LTAS 100%PU (4.2-3.0-2.0). ASSEMBLY-BY-ASSEMBLY BURNUP DISTRIBUTION 61

FIG. 27. FIRST CYCLE WITH 3 MOX LTAS 100%PU (4.2-3.0-2.0). ASSEMBLY-BY-ASSEMBLY POWER DISTRIBUTION 62

FIG. 28. BEGINNING OF THE FIRST CYCLE WITH 3 MOX LTAS 100%PU (4.2-3.0-2.0). ASSEMBLY-BY-ASSEMBLY PIN POWER PEAKING FACTOR 63

FIG. 29. END OF THE FIRST CYCLE WITH 3 MOX LTAS 100%PU (4.2-3.0-2.0). ASSEMBLY-BY-ASSEMBLY PIN POWER PEAKING FACTOR 64

FIG. 30. BEGINNING OF THE FIRST CYCLE WITH 3 MOX LTAS 100%PU (4.2-3.0-2.0). ASSEMBLY-BY-ASSEMBLY MAXIMUM PIN LINEAR POWER 65

FIG. 31. END OF THE FIRST CYCLE WITH 3 MOX LTAS 100%PU (4.2-3.0-2.0). ASSEMBLY-BY-ASSEMBLY MAXIMUM PIN LINEAR POWER 66

FIG. 32. BEGINNING OF THE FIRST CYCLE WITH 3 MOX LTAS 100%PU (4.2-3.0-2.0). RELATIVE POWER DISTRIBUTION IN THE MOST POWERED ASSEMBLY 67

FIG. 33. END OF THE FIRST CYCLE WITH 3 MOX LTAS 100%PU (4.2-3.0-2.0). RELATIVE POWER DISTRIBUTION IN THE MOST POWERED ASSEMBLY 68

FIG. 34. BEGINNING OF THE FIRST CYCLE WITH 3 MOX LTAS 100%PU (4.2-3.0-2.0). RELATIVE POWER DISTRIBUTION IN THE MOX ASSEMBLY 69

FIG. 35. END OF THE FIRST CYCLE WITH 3 MOX LTAS 100%PU (4.2-3.0-2.0). RELATIVE POWER DISTRIBUTION IN THE MOX ASSEMBLY 70

FIG. 36. END OF THE FIRST CYCLE WITH 3 MOX LTAS 100%PU (4.2-3.0-2.0). RELATIVE BURNUP DISTRIBUTION IN THE MOX ASSEMBLY 71

FIG. 37. LOADING PATTERN FOR THE SECOND CYCLE WITH 3 MOX LTAS 72

FIG. 38. SECOND CYCLE WITH 3 MOX LTAS 100%PU (4.2-3.0-2.0). ASSEMBLY-BY-ASSEMBLY BURNUP DISTRIBUTION 73

FIG. 39. SECOND CYCLE WITH 3 MOX LTAS 100%PU (4.2-3.0-2.0). ASSEMBLY-BY-ASSEMBLY POWER DISTRIBUTION 74

FIG. 40. BEGINNING OF THE SECOND CYCLE WITH 3 MOX LTAS 100%PU (4.2-3.0-2.0). ASSEMBLY-BY-ASSEMBLY PIN POWER PEAKING FACTOR 75

FIG. 41. END OF THE SECOND CYCLE WITH 3 MOX LTAS 100%PU (4.2-3.0-2.0). ASSEMBLY-BY-ASSEMBLY PIN POWER PEAKING FACTOR 76

FIG. 42. BEGINNING OF THE SECOND CYCLE WITH 3 MOX LTAS 100%PU (4.2-3.0-2.0). ASSEMBLY-BY-ASSEMBLY MAXIMUM PIN LINEAR POWER 77

FIG. 43. END OF THE SECOND CYCLE WITH 3 MOX LTAS 100%PU (4.2-3.0-2.0). ASSEMBLY-BY-ASSEMBLY MAXIMUM PIN LINEAR POWER 78

FIG. 44. BEGINNING OF THE SECOND CYCLE WITH 3 MOX LTAS 100%PU (4.2-3.0-2.0). RELATIVE POWER DISTRIBUTION IN THE MOST POWERED ASSEMBLY 79

FIG. 45. END OF THE SECOND CYCLE WITH 3 MOX LTAS 100%PU (4.2-3.0-2.0). RELATIVE POWER DISTRIBUTION IN THE MOST POWERED ASSEMBLY 80

FIG. 46. BEGINNING OF THE SECOND CYCLE WITH 3 MOX LTAS 100%PU (4.2-3.0-2.0). RELATIVE POWER DISTRIBUTION IN THE MOX ASSEMBLY 81

FIG. 46A. BEGINNING OF THE SECOND CYCLE WITH 3 MOX LTAS OF "ISLAND-2" TYPE (PU3.8-2.8-U3.7). RELATIVE POWER DISTRIBUTION IN THE MOX ASSEMBLY 81

FIG. 47. END OF THE SECOND CYCLE WITH 3 MOX LTAS 100%PU (4.2-3.0-2.0). RELATIVE POWER DISTRIBUTION IN THE MOX ASSEMBLY 82

FIG. 47A. END OF THE SECOND CYCLE WITH 3 MOX LTAS OF "ISLAND-2" TYPE (PU3.8-2.8-U3.7). RELATIVE POWER DISTRIBUTION IN THE MOX ASSEMBLY 82

FIG. 48. BEGINNING OF THE SECOND CYCLE WITH 3 MOX LTAS 100%PU (4.2-3.0-2.0). RELATIVE BURNUP DISTRIBUTION IN THE MOX ASSEMBLY 83

FIG. 48A. BEGINNING OF THE SECOND CYCLE WITH 3 MOX LTAS OF "ISLAND-2" TYPE (PU3.8-2.8-U3.7). RELATIVE BURNUP DISTRIBUTION IN THE MOX ASSEMBLY 83

FIG. 49. END OF THE SECOND CYCLE WITH 3 MOX LTAS 100%PU (4.2-3.0-2.0). RELATIVE BURNUP DISTRIBUTION IN THE MOX ASSEMBLY 84

FIG. 49A. END OF THE SECOND CYCLE WITH 3 MOX LTAS OF "ISLAND-2" TYPE (PU3.8-2.8-U3.7). RELATIVE BURNUP DISTRIBUTION IN THE MOX ASSEMBLY 84

FIG. 50. LOADING PATTERN FOR THE THIRD CYCLE WITH 3 MOX LTAS 85

FIG. 51. THIRD CYCLE WITH 3 MOX LTAS 100%PU (4.2-3.0-2.0). ASSEMBLY-BY-ASSEMBLY BURNUP DISTRIBUTION 86

FIG. 52. THIRD CYCLE WITH 3 MOX LTAS 100%PU (4.2-3.0-2.0). ASSEMBLY-BY-ASSEMBLY POWER DISTRIBUTION 87

FIG. 53. BEGINNING OF THE THIRD CYCLE WITH 3 MOX LTAS 100%PU (4.2-3.0-2.0). ASSEMBLY-BY-ASSEMBLY PIN POWER PEAKING FACTOR 88

FIG. 54. END OF THE THIRD CYCLE WITH 3 MOX LTAS 100%PU (4.2-3.0-2.0). ASSEMBLY-BY-ASSEMBLY PIN POWER PEAKING FACTOR 89

FIG. 55. BEGINNING OF THE THIRD CYCLE WITH 3 MOX LTAS 100%PU (4.2-3.0-2.0). ASSEMBLY-BY-ASSEMBLY MAXIMUM PIN LINEAR POWER 90

FIG. 56. END OF THE THIRD CYCLE WITH 3 MOX LTAS 100%PU (4.2-3.0-2.0). ASSEMBLY-BY-ASSEMBLY MAXIMUM PIN LINEAR POWER 91

FIG. 57. BEGINNING OF THE THIRD CYCLE WITH 3 MOX LTAS 100%PU (4.2-3.0-2.0). RELATIVE POWER DISTRIBUTION IN THE MOST POWERED ASSEMBLY 92

FIG. 58. END OF THE THIRD CYCLE WITH 3 MOX LTAS 100%PU (4.2-3.0-2.0). RELATIVE POWER DISTRIBUTION IN THE MOST POWERED ASSEMBLY 93

FIG. 59. BEGINNING OF THE THIRD CYCLE WITH 3 MOX LTAS 100%PU (4.2-3.0-2.0). RELATIVE POWER DISTRIBUTION IN THE MOX ASSEMBLY 94

FIG. 59A. BEGINNING OF THE THIRD CYCLE WITH 3 MOX LTAS OF "ISLAND-2" TYPE (PU3.8-2.8-U3.7). RELATIVE POWER DISTRIBUTION IN THE MOX ASSEMBLY 94

FIG. 60. END OF THE THIRD CYCLE WITH 3 MOX LTAS 100%PU (4.2-3.0-2.0). RELATIVE POWER DISTRIBUTION IN THE MOX ASSEMBLY 95

FIG. 60A. END OF THE THIRD CYCLE WITH 3 MOX LTAS OF "ISLAND-2" TYPE (PU3.8-2.8-U3.7). RELATIVE POWER DISTRIBUTION IN THE MOX ASSEMBLY 95

FIG. 61. BEGINNING OF THE THIRD CYCLE WITH 3 MOX LTAS 100%PU (4.2-3.0-2.0). RELATIVE BURNUP DISTRIBUTION IN THE MOX ASSEMBLY 96

FIG. 61A. BEGINNING OF THE THIRD CYCLE WITH 3 MOX LTAS OF "ISLAND-2" TYPE (PU3.8-2.8-U3.7). RELATIVE BURNUP DISTRIBUTION IN THE MOX ASSEMBLY 96

FIG. 62. END OF THE THIRD CYCLE WITH 3 MOX LTAS 100%PU (4.2-3.0-2.0). RELATIVE BURNUP DISTRIBUTION IN THE MOX ASSEMBLY 97

FIG. 62A. BEGINNING OF THE THIRD CYCLE WITH 3 MOX LTAS OF "ISLAND-2" TYPE (PU3.8-2.8-U3.7). RELATIVE BURNUP DISTRIBUTION IN THE MOX ASSEMBLY 97

FIG. 63. CONTROL RODS GROUPING AND POSITIONS OF IN-CORE SELF-POWERED DETECTORS98

INTRODUCTION

The present work is a part of Joint U.S. / Russian Project with Weapons-Grade Plutonium Disposition in VVER Reactor and presents the neutronics calculations of VVER-1000 core with 3 introduced MOX LTAs.

In [3-4] MOX LTA design has been studied for two options of MOX LTA: 100% plutonium and of "island" type. As a result, zoning (fissile plutonium enrichments in different plutonium zones) has been defined.

In present work, VVER-1000 core with 3 introduced MOX LTAs is studied for two above-mentioned MOX LTA options with the chosen zoning.

In [2] the volume and sequence of these studies were defined. The preliminary results of the first part of these studies are presented in [5]. This document is a final report on these studies that comprises:

1. ***"Uranium Core"***. Calculation of the so-called Advanced VVER-1000 core with boron BPRs for the equilibrium fuel cycle [2] that was defined as basic for 3 MOX LTAs introduction.

Evolution of average assembly powers, average fuel pins powers, boron acid concentrations, reactivity coefficients and kinetics parameters during fuel cycles has been calculated. The results are described in Chapter 4.

2. ***"MOX Core"***. Studies of VVER-1000 core with introduction of 3 MOX LTAs of two above-mentioned design. Three cycles till MOX LTAs discharge have been studied. Corresponding loading patterns for every cycle have been chosen to minimize power peaking factors.

The same parameters as for Uranium core have been defined. Inter-assembly pin-by-pin power distribution has been presented both for the most powered assemblies and MOX assemblies. The results are described in Chapter 5.

Control rods worth and reactivity margin while reactor shutdown for "Uranium Core" and "MOX Core" have been also defined. The results are described in Chapter 6.

Coarse-mesh (assembly-by-assembly) core calculations have been made by the Russian code BIPR-7A [8] briefly evoked in Chapter 2.

Fine-mesh (pin-by-pin) calculations have been made by the Russian code PERMAK-A [8] briefly described in Chapter 3.

The corresponding neutronics constants libraries for BIPR-7A and PERMAK-A have been prepared by the cell code TVS-M [7].

1. DEFINITIONS

In the following table the parameters used in current studies are described according to [2].

Parameter	Abbreviation	Units	Remarks
Calculational system	CS		core
Reactivity of CS	RO	pcm	RO = (Keff-1)/Keff*1.E5
Calculational volume	Vij		Axial fraction j of assembly number i. In VVER-1000 calculations, 10 axial fractions of equal volume are usually used.
Effective multiplication factor of CS	Keff		
Multiplication factor of CS	Ko		Relation of neutron generation to neutron absorption. For core calculations Ko values are attributed to Vij
3-D power distribution in core	q_{ij}		Power in Vij normalized by average Vij power
Volume power peaking factor	Kv		Maximum in qij values
Radial position of volume power peaking factor	N (Kv)		Number of assembly in calculational core sector where Kv is realized
Axial position of volume power peaking factor	M (Kv)		Number of axial level where Kv is realized (numerating from core bottom)
2-D power distribution in core	q_i		Assembly powers normalized by average assembly power in core.
Radial power peaking factor	Kq		Maximum in q_i values
Radial position of radial power peaking factor	N (Kq)		Number of assembly in calculational core sector where Kq is realized
3-D burnup distribution in core	BUij	MWd/kg	Burnup in Vij.
2-D burnup distribution in core	BUi	MWd/kg	Averaged-assembly burnup distribution in core.
Pin power peaking factor in assembly	Kk_i		For an assembly number i for a fraction number j where maximum q_{ij} for this assembly is realized. In fine-mesh 2-D calculations by PERMAK-A

			fraction 4 (level 4) is usually chosen as the most powered.
Radial pin power peaking factor	Kr		max (q_i * Kki)
Radial position of radial pin power peaking factor	N (Kr)		Number of assembly in calculational core sector where Kr is realized
Total power peaking factor	Ko		max (q_{ij} * Kki) ij
Radial position of total power peaking factor	N (Ko)		Number of assembly in calculational core sector where Ko is realized
Axial position of total power peaking factor	M (Ko)		Number of axial level where Ko is realized
Pin linear power	Q_l	Wt/cm	Pin power for 1 cm of an axial calculational fraction
Average Boron acid (H_3BO_3) concentration[a] in coolant	Cb	ppm	H_3BO_3 fraction in coolant (mg of boron acid in 1 Kg of H_2O)
Critical boron acid concentration in coolant	Cb_{CRIT}	ppm	Cb value ensuring Keff=1
2-D power distribution in assembly	Kk		Power of fuel pins normalized by average fuel pin power in assembly.
2-D pin burnup distribution in CS	BUk	MWd/kg	Averaged-pin burnup distribution in CS.
2-D power peaking factor in assembly	$(Kk)_{max}$		Maximum relative power of fuel pins (maximum of Kk values)
Control rods worth (in core)	$(RO)_{SOR}$	ppm	Effect of control rods insertion in core supposing the most effective single CR/SOR stuck in upper position.

[a] Boron acid concentration divided by the coefficient 5.72 means natural boron (nat B) concentration. In VVER-1000 calculations the term of boron acid concentration is widely used. Below, Cb means boron acid concentration if there is no special indication.

			It is defined as a reactivity difference in two states: (RO)SOR= RO1-RO2. The second state differs from the first one only by additional CRs inserted in core. All the other parameters correspond to the first state: Cb (that is equal to Cb crit for the first state), temperature and FP distribution in core.
Moderator temperature coefficient (in core)	MTC	pcm/°C	
Moderator density coefficient (in core)	MDC	pcm/g/cc	
Doppler coefficient (in core)	DTC	pcm/°C	
Boron reactivity coefficient (in core)	DRO/DCB	pcm/ppm	
Effective fraction of delayed neutrons	βeff		General characteristic of core
Prompt neutrons lifetime	λm	s	General characteristic of core
Reactor thermal power	W	MW	
Specific reactor thermal power in CS	Wv	kW/ litre	Reactor thermal power in CS volume unit
Nominal reactor thermal power	W nom	MW	Equal to 3000 MW for VVER-1000
Minimum controllable level of reactor power	MCL	MW	In calculations corresponds to Zero Power and uniform temperature 280°C in core.
Average entry core temperature	Tentry	°C	
Average coolant-moderator temperature	T mod	°C	
Average fuel temperature	T fuel	°K	
Average temperature of other CS components	T con	°C	
Xenon-135 concentration distribution	Xe	10*24 /cc	For 1 cc in fuel

Equilibrium Xenon-135 concentration distribution	Xe eq (W)	10*24 /cc	Concentration formed during long working with W power, regulation group in nominal position
Sm-149 concentration distribution	Sm	10*24 /cc	For 1 cc in fuel
Equilibrium Sm-149 concentration distribution	Sm eq	10*24 /cc	Concentration formed during long working, regulation group in nominal position
Samarium-149 concentration distribution, all Prometium-149 decayed in Sm	Smh	10*24 /cc	
Core reactivity while reactor shut-down	RO_{STOP}	pcm	Under conditions: W=0, Xe=0,Sm=Smh, Tmod= Tfuel= Tcon=20°C, Cb= 16000 ppm

2. COARSE-MESH CODE BIPR-7A

BIPR-7A is a 3-dimensional hexagonal coarse-mesh code intended to calculate neutronics characteristics of VVER-type reactor core.

Calculational cell represents assembly transversal section in horizontal plane and usually one-tenth of core height in axial direction i.e. there are 1630 cells in VVER-1000 core. Neutronics parameters are homogeneous within a cell.

Radial, upper and lower reflectors are described by border conditions.

Calculation is performed in two energetic groups using the so-called modal presentation of group fluxes [6].

Cell constants, prepared by the code TBC-M [7], form a library and represent a number of polynomials that reflect the two-group neutronics cross sections dependence on moderator density, moderator temperature, fuel temperature, FP concentrations in fuel, boron acid concentration in coolant, Xe and Sm concentration in fuel.

BIPR-7A is a part of industrial super-code KASKAD that allows obtaining in convenient formats all the parameters necessary for reactor safety estimations and licensing.

As a result BIPR-7A calculate the following parameters:

- q_i,
- q_{ij},
- BUi,
- BUij,
- MTC,
- MDC,
- DTC,
- DRO/DCB,
- βeff,
- λm,
- Cb_{CRIT} ,
- RO_{STOP},
- $(RO)_{SOR}$.

3. FINE-MESH CODE PERMAK-A

PERMAK-A is a 2-dimensional fine-mesh code intended to calculate neutronics characteristics of VVER-type reactor core.

Calculational cell represents fuel pin-type hexagonal cell with homogeneous neutronics parameters within it.

Diffusion finite-differencies neutron balance equation in few energetic groups are resolved.

Radial reflector is described by the same manner as a core.

Neutron flux axial gradients, obtained by BIPR-7A, are used while calculating one (as usual) the most powered core axial level.

Cell (fuel and non-fuel) constants, prepared by the code TBC-M [7], form a special library and represent a number of polynomials that reflect the group neutronics cross sections dependence on moderator density, moderator temperature, fuel temperature, FP concentrations in fuel, boron acid concentration in coolant, Xe and Sm concentration in fuel.

PERMAK-A is a part of industrial super-code KASKAD that allows obtaining in convenient formats all the parameters necessary for reactor safety estimations and licensing.

As a result PERMAK-A calculates the following parameters:

- Kk_i,
- Kr;
- BUk,
- Q_l.

4. RESULTS of URANIUM CORE CALCULATIONS

The uranium core with BPRs has been calculated for the equilibrium cycle (Fig.6) using neutronics constants libraries obtained from the cell code TVS-M calculations for assembly types presented in Fig. 3-5.

The results of averaged-assembly burnup and power distribution calculations are presented in Fig.7. They have been carried up by the code BIPR-7A.

The distribution of pin power peaking factors (qi * Kki) is presented in Fig. 8 and 9 correspondingly for BOC and EOC. The distribution of maximum pin linear powers Q_L is presented in Fig. 10 and 11 correspondingly for BOC and EOC. Relative power distributions in the interior of the most powered assemblies are presented in Fig. 12 and 13 correspondingly for BOC and EOC. All the parameters here mentioned have been calculated by the code PERMAK-A.

The evolution of main core neutronics parameters in the process of uranium core irradiation is presented in Table 5. Irradiation simulation has been performed in the following conditions:

- constant reactor power W=Wnom;
- 20% insertion of CR regulation bank (see Fig. 63), other banks are out of the core.

5. RESULTS of MOX CORE CALCULATIONS

3 MOX assemblies have been located in uranium reference core (Fig. 6) according to principals adopted in [2].

The positions 8, 88 and 150 for the first MOX loading (Fig. 14) have been chosen because they possess self-powered detectors (see Fig. 63). Other assemblies have been replaced to ensure a minimum value of Kq calculated by BIPR-7A. Besides, several fresh assemblies of "Ba" type (it is described in Fig. 6) have been added to the first MOX loading.

5.1. Core with 100% Plutonium MOX LTAs

The design of 3-zones MOX LTA has been chosen in [3-4].

The chosen core loading pattern for the first fuel cycle with such MOX LTAs is presented in Fig. 14.

Calculated averaged-assembly power and burnup distributions in BOC and EOC are presented in Fig. 27 and 26.

Evolution of main neutronics parameters is presented in Table 9. It is seen that Kq in the first fuel cycle with 3 MOX LTA is equal to 1.31 in BOC and it is found in Uranium assembly. It meets the requirements adopted [1] for Uranium cores and presented in Tables 1 and 2. Then during the cycle Kq does not exceed 1.28 meeting safety requirements adopted in [2] for MOX fueled cores and presented in Tables 3 and 4.

In the second (Fig. 39 and Table 9) and the third (Fig. 52 and Table 11) cycles, Kq in BOC is equal correspondingly to 1.33 and 1.32. Further in the process of fuel loading irradiation its values do not exceed 1.27.

In all presented calculations qi in MOX LTAs are sufficiently lower than Kq.

Pin power peaking factors distributions (qi * Kki) in core for BOC and EOC are presented in Fig. 28 and 29 for the first cycle with MOX LTAs, in Fig. 40 and 41 - for the second cycle, in Fig. 53 and 54 - for the third cycle. The values of Kr are presented in Tables 9, 11 and 13. It is seen that they are lower than adopted limiting values 1.50 for Uranium assemblies and 1.45 for MOX assemblies.

Maximum pin linear power Q_l distributions in core for BOC and EOC are presented in Fig. 30 and 31 for the first cycle with MOX LTAs, in Fig. 42 and 43 - for the second cycle, in Fig. 55 and 56 - for the third cycle.

Relative power distributions in the interior of the most powered assemblies are presented in Fig. 32 and 33 correspondingly in BOC and EOC for the first cycle, in Fig. 44 and 45 - for the second cycle, in Fig. 57 and 58 - for the third cycle.

Relative power distributions in the interior of the MOX assemblies are presented in Fig. 34 and 35 correspondingly in BOC and EOC for the first cycle, in Fig. 46 and 47 - for the second cycle, in Fig. 59 and 60 - for the third cycle.

Relative burnup distributions in the interior of the MOX assemblies are presented in Fig. 36 in EOC for the first cycle, in Fig. 48 and 49 - correspondingly in BOC and EOC for the second cycle, in Fig. 61 and 62 - for the third cycle.

The values of total power peaking factor Ko presented in Tables 9, 11 and 13 also meet the requirements described in Tables 2 and 4.

5.2. Core with "Island" Type MOX LTAs

According to the studies [3-4] MOX LTA of "Island-2" type has been chosen with the zoning shown in Fig. 2. The core loading pattern chosen in p.5.1 can be also used for this MOX LTA design because multiplication factor Ko are close in two options of MOX LTA [3-4]. Tables 7 and 9 and Fig. 16 and 27 confirm this fact for the first cycle with 3 MOX LTAs. "Island" type design influences only "inter-assembly" parameters. So for "Island-2" type MOX LTA the most part of results is presented only for the first fuel cycle.

Pin power peaking factors distributions (qi * Kki) in core for BOC and EOC are presented in Fig. 17 and 18.

Maximum pin linear power Q_L distributions in core for BOC and EOC are presented in Fig. 19 and 20.

Relative power distributions in the interior of the most powered assemblies are presented in Figures 21 and 22 correspondingly in BOC and EOC.

Relative power distributions in the interior of the MOX assemblies are presented in Figures 23 and 24 correspondingly in BOC and EOC for the first fuel cycle, Figures 46a and 47a - for the second fuel cycle, Figures 59a and 60a - for the third fuel cycle.

Relative burnup distribution in the interior of the MOX assemblies is presented in Fig. 25 in EOC for the first fuel cycle, Figures 48a and 49a - for the second fuel cycle, Figures 61a and 62a - for the third fuel cycle..

The values of total power peaking factor Ko are presented in Table 7.

5.3. Calculations in zero power states and control rods worth

According to [2] a number of neutronics parameters has been calculated for the range of discrete zero power states: Cb_{CRIT}, reactivity coefficients and reactivity margin RO_{STOP}. Their values are accumulated in Tables 6, 8, 10, 8 and 12. It is seen that MTC is negative in all cases.

$(RO)_{SOR}$ in different core states is presented in Table 15 supposing one the most effective rod stuck in the upper position. Stuck rod has been defined separately for nominal power state and for zero power state.

It can be seen that presence of 3 MOX LTAs does not influence $(RO)_{SOR}$ in clear manner. Its value is determined first of all by core loading pattern. It may be supposed that

only significant value of MOX assemblies in core could lead to lowering of control rods worth because of strong absorbing capacity of MOX fuel. In all calculated cases $(RO)_{SOR}$ values meet the adopted limitating values 5500 ppm [1] for Uranium cores and 5800 ppm [2] for MOX loaded cores.

CONCLUSION

The report presents the calculation results of VVER-1000 core with 3 MOX LTAs. Uranium core with boron burnable poison rods has been used as a reference core for MOX fuel introduction.

MOX LTAs of 100% Plutonium (graded by three enrichments zones) and of "Island" type have been considered. Core loadings have been optimized to ensure minimum value of power peaking factor Kq.

Evolution of main neutronics parameters during 3 successive cycles with MOX LTAs is presented. It is shown that MOX loaded cores meet the safety requirements preliminary adopted for MOX fuel concerning power peaking factors, reactivity coefficients and control rods worth.

REFERENCES

1. Y.A. Styrin. Fuel Assembly and Core Model for Neutronics Calculations of VVER-1000.
Moscow, Kurchatov Institute 1998.
2. Y.A. Styrin, I.K.Levina. Design of Lead Test MOX Assemblies for Pilot Irradiation in VVER-1000 and Related Parametric Studies.
Moscow, Kurchatov Institute 1998.
3. S.A. Bichkov, Y.A. Styrin. Results of Parametric Design Studies of MOX Lead Test Assembly (Progress Report).
Moscow, Kurchatov Institute 1998.
4. S.A. Bichkov, A.G. Kalashnikov, Y.A. Styrin. Results of Parametric Design Studies of MOX Lead Test Assembly (Final Report).
Moscow, Kurchatov Institute 1998.
5.Y.A. Styrin. Calculations of MOX LTA Performance in VVER-1000 Core. (Progress Report)
Moscow, Kurchatov Institute 1998.
6. Kaloinen E., Siltanen P., Terasvirta R. Two-group nodal calculations in hexagonal fuel assembly geometry. – In: Proc. of NFACRP Specialists' Meeting on Calculation of 3-D Rating Distributions in Operating Reactors.
Paris, 1979.
7. V.D.Sidorenko et al. Spectral Code TBC-M for calculation of Characteristics of Cells, Super-cells and Fuel Assemblies of VVER-Type Reactors. 5-th Symposium of the AER.
Dobogoko, Hungary, October 15-20, 1995.
8. In-core fuel management code package validation for WWERs. IAEA-TECDOC-847. November 1995.

Table 1. Limiting parameters for VVER-1000

Criterion	Limiting Value	Remarks
Kq	<=1.35	For nominal power W=3000 MW
Kr	<=1.50	For nominal power W=3000 MW
Koj lim	Tabl. 2	For nominal power W=3000 MW
MTC	< 0	
MDC	> 0	
RO stop	<= -2%	T=20°C, Xe=0, Sm=Smh, Cb=16g/Kg, all control rods extracted
RCT	< 220°C	
Control rods worth	> 5.5%	

Table 2. Limits recommended for total power peaking factor Koj lim

Layer (from bottom to top)	1	2	3	4	5	6	7	8	9	10
Koj lim	2.24	2.24	2.24	2.24	2.24	2.14	1.96	1.80	1.69	1.58

Table 3. Recommended limiting parameters for VVER-1000 with MOX fuel

Criterion	Limiting Value	Remarks
Kq	<=1.30	For nominal power W=3000 MW
Kr	<=1.45	For nominal power W=3000 MW
Koj lim	Tabl. 4	For nominal power W=3000 MW
MTC	< 0	
MDC	> 0	
RO stop	<= -2%	T=20°C, Xe=0, Sm=Smh, Cb=16g/Kg, all control rods extracted
RCT	< 210°C	
Control rods worth	> 5.8%	

Table 4. Limits recommended for total power peaking factor Koj lim for VVER-1000 with MOX fuel

Layer (from bottom to top)	1	2	3	4	5	6	7	8	9	10
Koj lim	2.15	2.15	2.15	2.15	2.15	2.15	1.86	1.81	1.60	1.50

Table 5. Evolution of main neutronics parameters. Reference Uranium Core Equilibrium Cycle. Core 60° Sector

T, EFPD	Cb, ppm	Kq	N Kq	Kv	N Kv	M Kv	Kr	N Kr	Ko	N Ko	M Ko	MTC, pcm/°C	MDC, pcm/g/cc	DTC, pcm/°C	DRO/DCB pcm/ppm	λm $*10^5$s	βeff *100
0.0	6020	1.31	19	1.59	19	4	1.50	10	1.82	19	4	-25.78	12180	-2.94	-1.53	2.22	0.65
20.0	5670	1.31	19	1.56	19	4	1.49	10	1.77	19	4	-26.82	12790	-2.93	-1.53	2.23	0.64
40.0	5230	1.31	19	1.54	19	4	1.48	10	1.73	19	4	-29.12	13910	-2.91	-1.54	2.24	0.63
60.0	4790	1.31	19	1.52	19	3	1.47	10	1.69	19	3	-31.61	15100	-2.91	-1.55	2.25	0.62
80.0	4340	1.31	19	1.50	19	3	1.45	10	1.66	19	3	-34.15	16300	-2.91	-1.56	2.27	0.61
100.0	3910	1.31	19	1.49	19	3	1.44	10	1.64	19	3	-36.71	17490	-2.92	-1.58	2.29	0.61
120.0	3480	1.30	19	1.48	19	3	1.43	10	1.62	19	3	-39.21	18660	-2.93	-1.59	2.31	0.60
140.0	3050	1.30	19	1.47	19	3	1.42	10	1.59	19	3	-41.71	19820	-2.95	-1.60	2.34	0.59
160.0	2630	1.30	19	1.46	19	3	1.41	10	1.58	19	3	-44.17	20960	-2.97	-1.62	2.36	0.59
180.0	2220	1.30	19	1.46	19	2	1.39	10	1.56	19	2	-46.65	22090	-2.99	-1.63	2.39	0.58
200.0	1810	1.30	19	1.46	19	2	1.38	6	1.55	19	2	-49.10	23210	-3.02	-1.65	2.41	0.57
220.0	1410	1.30	19	1.46	19	2	1.38	6	1.54	19	2	-51.58	24340	-3.04	-1.66	2.44	0.57
240.0	1000	1.29	19	1.45	19	2	1.37	6	1.53	19	2	-54.09	25470	-3.06	-1.68	2.47	0.56
260.0	600	1.29	19	1.45	19	2	1.36	6	1.52	19	2	-56.60	26600	-3.08	-1.69	2.50	0.56
280.0	210	1.29	19	1.44	19	2	1.35	6	1.51	19	2	-59.13	27740	-3.09	-1.71	2.53	0.55
290.6	0	1.28	19	1.44	19	2	1.35	6	1.50	19	2	-60.49	28340	-3.10	-1.72	2.55	0.55

Table 6. Main neutronics parameters in zero power states. Reference Uranium Core Equilibrium Cycle

T	RO pcm	Cb ppm	Bank 10	Other banks↓↑	Xe	Sm	Tmod °C	MTC pcm/°C	MDC pcm/g/cc	DTC pcm/°C	DRO/DCB pcm/ppm	λm $*10^5$s	βeff *100
BOC	0	9390	100% ↑	100% ↑	0	Smh	280	-1.07	2090	-2.93	-1.46	2.08	0.65
EOC	0	2150	100% ↑	100% ↑	eq	Sm eq	280	-27.57	18680	-3.32	-1.75	2.43	0.56
BOC	-11926 (RO_{STOP})	16000	100% ↑	100% ↑	0	Smh	20						

Table 7. Evolution of main neutronics parameters. Cycle 1-MOX. "Island-2" Type Pu(3.8-2.8) – U3.7%

T, EFPD	Cb, ppm	Kq	N Kq	q_l MOX	Kv	N Kv	M Kv	Kr	N Kr	Ko	N Ko	M Ko	MTC, pcm/°C	MDC, pcm/g/cc	DTC, pcm/°C	DRO/DCB pcm/ppm	λm $*10^5$s	βeff *100
0.0	6140	1.31	38	1.00	1.57	38	4	1.45	38	1.75	38	4	-24.70	11850	-2.85	-1.54	2.23	0.65
20.0	5790	1.26	38	0.97	1.48	38	4	1.41	40	1.65	40	4	-25.71	12450	-2.85	-1.54	2.24	0.64
40.0	5350	1.26	38	0.96	1.46	38	4	1.40	40	1.62	40	4	-28.08	13590	-2.85	-1.55	2.25	0.63
60.0	4900	1.26	40	0.96	1.44	47	3	1.39	40	1.59	132	3	-30.63	14800	-2.85	-1.57	2.27	0.62
80.0	4460	1.26	72	0.96	1.43	72	3	1.38	72	1.57	132	3	-33.22	16010	-2.85	-1.58	2.29	0.61
100.0	4020	1.26	72	0.96	1.43	132	3	1.38	72	1.56	72	3	-35.83	17220	-2.86	-1.59	2.31	0.60
120.0	3580	1.26	132	0.96	1.42	132	3	1.37	72	1.55	72	3	-38.40	18420	-2.88	-1.60	2.33	0.60
140.0	3150	1.26	132	0.96	1.42	132	3	1.37	72	1.53	72	3	-40.96	19600	-2.90	-1.60	2.35	0.59
160.0	2710	1.27	132	0.96	1.42	132	2	1.36	72	1.53	124	2	-43.54	20780	-2.92	-1.63	2.38	0.58
180.0	2290	1.27	132	0.96	1.42	124	2	1.36	124	1.52	124	2	-46.06	21940	-2.94	-1.65	2.40	0.58
200.0	1870	1.27	124	0.96	1.43	124	2	1.35	124	1.52	124	2	-48.61	23100	-2.96	-1.66	2.43	0.57
220.0	1450	1.27	124	0.96	1.43	124	2	1.34	124	1.52	124	2	-51.18	24270	-2.98	-1.68	2.46	0.57
240.0	1040	1.27	124	0.96	1.43	124	2	1.34	124	1.51	124	2	-53.73	25420	-3.00	-1.69	2.49	0.56
260.0	630	1.27	124	0.96	1.43	124	2	1.33	124	1.50	124	2	-56.31	26580	-3.02	-1.71	2.52	0.56
280.0	220	1.27	124	0.96	1.43	124	2	1.33	124	1.50	124	2	-58.90	27740	-3.04	-1.72	2.55	0.55
290.8	0	1.27	124	0.96	1.43	124	2	1.33	124	1.49	124	2	-60.29	28360	-3.05	-1.73	2.57	0.55

Table 8. Main neutronics parameters in zero power states. Cycle 1-MOX. "Island-2" Type Pu(3.8-2.8) – U3.7%

T	RO pcm	Cb ppm	Bank 10	Other banks↓↑	Xe	Sm	Tmod °C	MTC pcm/°C	MDC pcm/g/cc	DTC pcm/°C	DRO/DCB pcm/ppm	λm $*10^5$s	βeff *100
BOC	0	9430	100% ↑	100% ↑	0	Smh	280	-0.62	1980	-2.96	-1.47	2.09	0.65
EOC	0	2110	100% ↑	100% ↑	eq	Sm eq	280	-27.67	18790	-3.32	-1.77	2.45	0.56
BOC	-12014 (RO_{STOP})	16000	100% ↑	100% ↑	0	Smh	20						

Table 9. Evolution of main neutronics parameters. Cycle-1 MOX. 100%Pu(4.2-3.0-2.0)

T, EFPD	Cb, ppm	Kq	N Kq	q_l MOX	Kv	N Kv	M Kv	Kr	N Kr	Ko	N Ko	M Ko	MTC, pcm/°C	MDC, pcm/g/cc	DTC, pcm/°C	DRO/DCB pcm/ppm	λm $*10^5$s	βeff *100
0.0	6160	1.31	38	1.03	1.57	38	4	1.46	38	1.76	38	4	-24.89	11950	-2.85	-1.53	2.22	0.64
20.0	5800	1.26	38	0.98	1.48	38	4	1.41	30	1.65	38	4	-25.88	12550	-2.86	-1.53	2.23	0.63
40.0	5350	1.26	38	0.96	1.46	38	4	1.40	30	1.62	40	4	-28.25	13680	-2.86	-1.55	2.24	0.62
60.0	4900	1.26	40	0.94	1.44	117	3	1.39	30	1.60	132	3	-30.80	14880	-2.86	-1.56	2.26	0.62
80.0	4460	1.26	92	0.93	1.44	92	3	1.39	45	1.58	92	3	-33.38	16090	-2.86	-1.57	2.28	0.61
100.0	4020	1.26	92	0.92	1.43	92	3	1.38	45	1.56	92	3	-35.97	17300	-2.88	-1.58	2.30	0.60
120.0	3570	1.27	92	0.92	1.43	92	3	1.37	45	1.55	32	3	-38.56	18490	-2.89	-1.60	2.32	0.59
140.0	3130	1.27	92	0.91	1.43	92	3	1.37	65	1.54	124	3	-41.14	19690	-2.91	-1.61	2.34	0.59
160.0	2700	1.27	92	0.91	1.42	124	2	1.36	134	1.53	124	2	-43.69	20860	-2.93	-1.62	2.37	0.58
180.0	2270	1.27	92	0.91	1.43	124	2	1.36	134	1.53	124	2	-46.24	22020	-2.95	-1.64	2.39	0.58
200.0	1850	1.27	124	0.90	1.43	124	2	1.35	134	1.52	124	2	-48.78	23180	-2.97	-1.65	2.42	0.57
220.0	1430	1.28	124	0.90	1.43	124	2	1.35	134	1.52	124	2	-51.34	24340	-2.99	-1.67	2.45	0.56
240.0	1010	1.28	124	0.90	1.44	124	2	1.34	134	1.51	124	2	-53.92	25500	-3.01	-1.68	2.48	0.56
260.0	600	1.28	124	0.90	1.44	124	2	1.34	134	1.51	124	2	-56.49	26660	-3.03	-1.70	2.51	0.55
280.0	190	1.28	124	0.90	1.44	124	2	1.33	134	1.50	124	2	-59.07	27820	-3.05	-1.72	2.54	0.55
289.6	0	1.28	124	0.90	1.44	124	2	1.33	134	1.50	124	2	-60.31	28370	-3.06	-1.72	2.56	0.55

Table 10. Main neutronics parameters in zero power states. Cycle-1 MOX. 100%Pu(4.2-3.0-2.0)

T	RO pcm	Cb ppm	Bank 10	Other banks↓↑	Xe	Sm	Tmod °C	MTC pcm/°C	MDC pcm/g/cc	DTC pcm/°C	DRO/DCB pcm/ppm	λm $*10^5 s$	βeff *100
BOC	0	9460	100% ↑	100% ↑	0	Smh	280	-0.86	2130	-2.97	-1.46	2.08	0.65
EOC	0	2120	100% ↑	100% ↑	eq	Sm eq	280	-27.62	18770	-3.32	-1.76	2.44	0.56
BOC	-11742 (RO_{STOP})	16000	100% ↑	100% ↑	0	Smh	20						

Table 11. Evolution of main neutronics parameters. Cycle 2-MOX. 100%Pu(4.2-3.0-2.0)

T, EFPD	Cb, ppm	Kq	N Kq	q_i MOX	Kv	N Kv	M Kv	Kr	N Kr	Ko	N Ko	M Ko	MTC, pcm/°C	MDC, pcm/g/cc	DTC, pcm/°C	DRO/DCB pcm/ppm	λm $*10^5$s	βeff *100
0.0	6040	1.33	153	1.22	1.62	153	4	1.48	153	1.80	153	4	-25.96	12390	-2.87	-1.53	2.21	0.64
20.0	5680	1.27	153	1.21	1.52	153	4	1.44	108	1.68	153	4	-27.03	13010	-2.87	-1.53	2.22	0.63
40.0	5240	1.27	153	1.20	1.50	153	4	1.42	108	1.65	153	4	-29.35	14130	-2.86	-1.54	2.24	0.62
60.0	4800	1.27	153	1.19	1.47	153	3	1.40	108	1.62	153	3	-31.85	15310	-2.86	-1.55	2.25	0.62
80.0	4360	1.26	153	1.19	1.45	153	3	1.39	108	1.59	152	3	-34.39	16500	-2.86	-1.57	2.27	0.61
100.0	3920	1.26	153	1.18	1.43	153	3	1.37	108	1.56	152	3	-36.91	17680	-2.87	-1.58	2.29	0.60
120.0	3490	1.25	153	1.17	1.41	47	3	1.37	153	1.54	50	3	-39.43	18850	-2.88	-1.59	2.31	0.59
140.0	3060	1.24	110	1.17	1.39	47	3	1.36	153	1.53	50	3	-41.95	20020	-2.90	-1.60	2.33	0.59
160.0	2620	1.25	110	1.16	1.38	110	3	1.35	153	1.51	50	3	-44.47	21180	-2.92	-1.62	2.36	0.58
180.0	2210	1.25	110	1.15	1.39	110	2	1.34	153	1.49	50	2	-46.94	22310	-2.94	-1.63	2.39	0.58
200.0	1790	1.25	110	1.15	1.40	110	2	1.33	153	1.49	50	2	-49.42	23450	-2.96	-1.65	2.41	0.57
220.0	1370	1.25	110	1.15	1.40	110	2	1.33	50	1.48	50	2	-51.92	24590	-2.98	-1.66	2.44	0.56
240.0	9700	1.26	110	1.14	1.41	110	2	1.32	50	1.47	110	2	-54.41	25720	-2.99	-1.68	2.47	0.56
260.0	560	1.26	110	1.14	1.41	110	2	1.31	50	1.47	110	2	-56.92	26850	-3.01	-1.69	2.50	0.55
280.0	150	1.26	110	1.14	1.41	56	2	1.31	50	1.46	110	2	-59.46	27990	-3.03	-1.71	2.53	0.55
287.8	0	1.26	110	1.13	1.41	56	2	1.30	50	1.46	110	2	-60.43	28430	-3.04	-1.71	2.54	0.55

Table 12. Main neutronics parameters in zero power states. Cycle-2 MOX. 100%Pu(4.2-3.0-2.0)

T	RO pcm	Cb ppm	Bank 10	Other banks↓↑	Xe	Sm	Tmod °C	MTC pcm/°C	MDC pcm/g/cc	DTC pcm/°C	DRO/DCB pcm/ppm	λm $*10^5$ s	βeff *100
BOC	0	9330	100% ↑	100% ↑	0	Smh	280	-1.71	2590	-2.97	-1.46	2.08	0.64
EOC	0	2090	100% ↑	100% ↑	eq	Sm eq	280	-27.86	18880	-3.32	-1.75	2.43	0.56
BOC	-11857 (RO_{STOP})	16000	100% ↑	100% ↑	0	Smh	20						

Table 13. Evolution of main neutronics parameters. Cycle 3-MOX. 100%Pu(4.2-3.0-2.0)

T, EFPD	Cb, ppm	Kq	N Kq	q_l MOX	Kv	N Kv	M Kv	Kr	N Kr	Ko	N Ko	M Ko	MTC, pcm/°C	MDC, pcm/g/cc	DTC, pcm/°C	DRO/DCB pcm/ppm	λm $*10^5$s	βeff *100
0.0	6190	1.32	126	1.07	1.60	126	4	1.47	126	1.78	126	4	-24.66	11820	-2.86	-1.53	2.22	0.65
20.0	5830	1.27	112	1.09	1.51	126	4	1.42	124	1.68	124	4	-25.82	12490	-2.86	-1.53	2.22	0.64
40.0	5390	1.27	11	1.08	1.48	11	4	1.41	124	1.64	124	4	-28.16	13620	-2.85	-1.54	2.23	0.63
60.0	4950	1.27	124	1.07	1.46	126	3	1.39	124	1.61	124	3	-30.68	14800	-2.85	-1.55	2.25	0.62
80.0	4510	1.26	124	1.07	1.44	124	3	1.38	124	1.58	124	3	-33.23	16000	-2.86	-1.56	2.27	0.61
100.0	4070	1.26	124	1.07	1.43	124	3	1.37	124	1.56	124	3	-35.80	17200	-2.87	-1.58	2.29	0.60
120.0	3640	1.26	124	1.06	1.42	124	3	1.36	137	1.53	124	3	-38.33	18380	-2.88	-1.59	2.31	0.60
140.0	3210	1.26	124	1.06	1.42	124	3	1.35	137	1.52	124	3	-40.85	19540	-2.89	-1.60	2.33	0.59
160.0	2780	1.26	124	1.06	1.41	124	3	1.34	137	1.50	124	3	-43.38	20710	-2.91	-1.62	2.36	0.58
180.0	2360	1.26	124	1.06	1.41	124	2	1.33	137	1.49	124	2	-45.87	21850	-2.93	-1.63	2.38	0.58
200.0	1940	1.26	124	1.06	1.41	124	2	1.32	137	1.48	124	2	-48.38	23000	-2.98	-1.65	2.41	0.57
220.0	1530	1.26	124	1.06	1.42	124	2	1.32	137	1.47	124	2	-50.88	24140	-2.97	-1.66	2.44	0.57
240.0	1120	1.26	124	1.06	1.42	124	2	1.31	137	1.47	124	2	-53.41	25280	-2.99	-1.68	2.46	0.56
260.0	700	1.26	124	1.06	1.41	124	2	1.30	137	1.46	124	2	-55.96	26430	-3.01	-1.69	2.49	0.56
280.0	300	1.25	124	1.06	1.41	124	2	1.29	137	1.45	124	2	-58.49	27570	-3.03	-1.71	2.52	0.55
295.0	0	1.25	124	1.06	1.41	124	2	1.29	137	1.45	124	2	-60.41	28430	-3.04	-1.72	2.55	0.55

Table 14. Main neutronics parameters in zero power states. Cycle-3 MOX. 100%Pu(4.2-3.0-2.0)

T	RO pcm	Cb ppm	Bank 10	Other banks↓↑	Xe	Sm	Tmod °C	MTC pcm/°C	MDC pcm/g/cc	DTC pcm/°C	DRO/DCB pcm/ppm	λm $*10^5$s	βeff *100
BOC	0	9470	100% ↑	100% ↑	0	Smh	280	-0.84	2080	-2.96	-1.46	2.08	0.65
EOC	0	2090	100% ↑	100% ↑	eq	Sm eq	280	-27.91	18910	-3.32	-1.75	2.43	0.56
BOC	-11814 (RO_{STOP})	16000	100% ↑	100% ↑	0	Smh	20						

Table 15a. Control rods worth calculation. States description

V1. BOC	V2. BOC	V3. BOC	V1. EOC	V1. EOC	V1. EOC
S1 Wnom, Xe=Xe eq, Tentry=287°C, Cb burnup 100 % 5↓* 30 % 10↓ S2: the same but 100% 1-10↓	S1 MCL, Xe=0, Tentry=280°C Cb crit 30% 10↓ S2: the same but 100% 1-10↓	S1 MCL, Xe=Xe eq, Tentry=280°C Cb crit 30% 10↓ S2: the same but 100% 1-10↓	S1 Wnom, Xe=Xe eq, Tentry=287°C Cb burnup 100 % 5↓ 30% 10↓ S2: the same but 100% 1-10↓	S1 MCL, Xe=Xe eq, Tentry=280°C Cb crit 100 % 5↓ 30 % 10↓ S2: the same but 100% 1-10↓	S1 MCL, Xe=0, Tentry=280°C Cb crit 100 % 5↓ 30 % 10↓ S2: the same but 100% 1-10↓

Table 15b. Control rods worth in Uranium reference core and in 3 MOX LTAs loaded cores (pcm)

		Uranium Core			1-st cycle with 3 MOX LTAs of "Island" type			1-st cycle with 3 MOX LTAs 100% Pu			2-nd cycle with 3 MOX LTAs			3-d cycle with 3 MOX LTAs		
	Variant	V1	V2	V3	V1	V2	V3	V1	V2	V3	V1	V2	V3	V1	V2	V3
BOC	Stuck rod number	55	55	55	67	67	67	67	67	67	109	82	82	112	97	97
	$(RO)_{SOR}$	6930	6770	6730	6980	6830	6800	6980	6860	6820	6960	6790	6730	7700	7150	7120
EOC	Stuck rod number	55	55	55	97	97	97	97	97	97	55	97	97	97	55	55
	$(RO)_{SOR}$	7200	6150	6150	7100	6010	5990	7090	6000	5980	7140	6090	6120	7170	6190	6170

* X% N↓ means that the Bank N is X% inserted in core

Figure 1. Simplified Design for 3 Zones MOX LTA

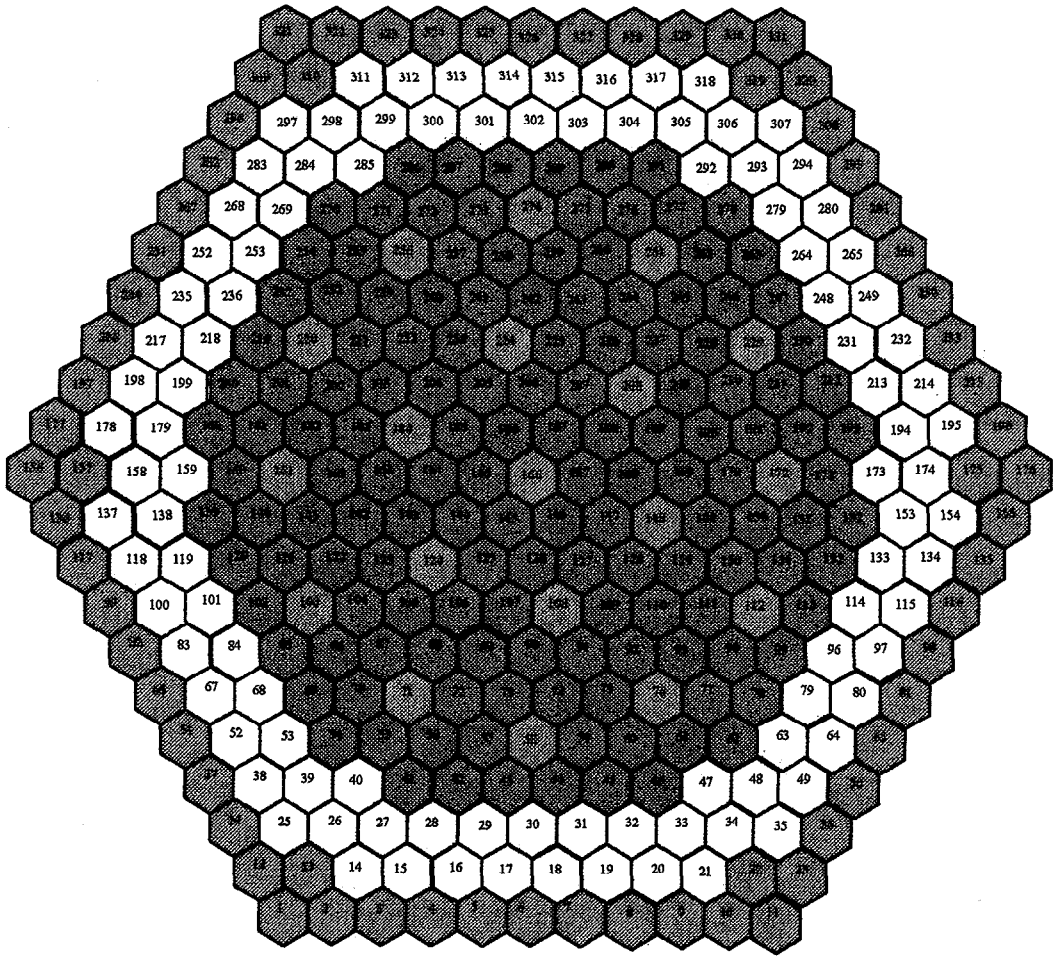

- **2.0% fissile Pu MOX Rods**
- **3.0% fissile Pu MOX Rods**
- **4.2% fissile Pu MOX Rods**
- **Central tube**
- **Control Rods / Burnable Absorbers**

Figure 2. Simplified Design for "Island-2" Type MOX LTA

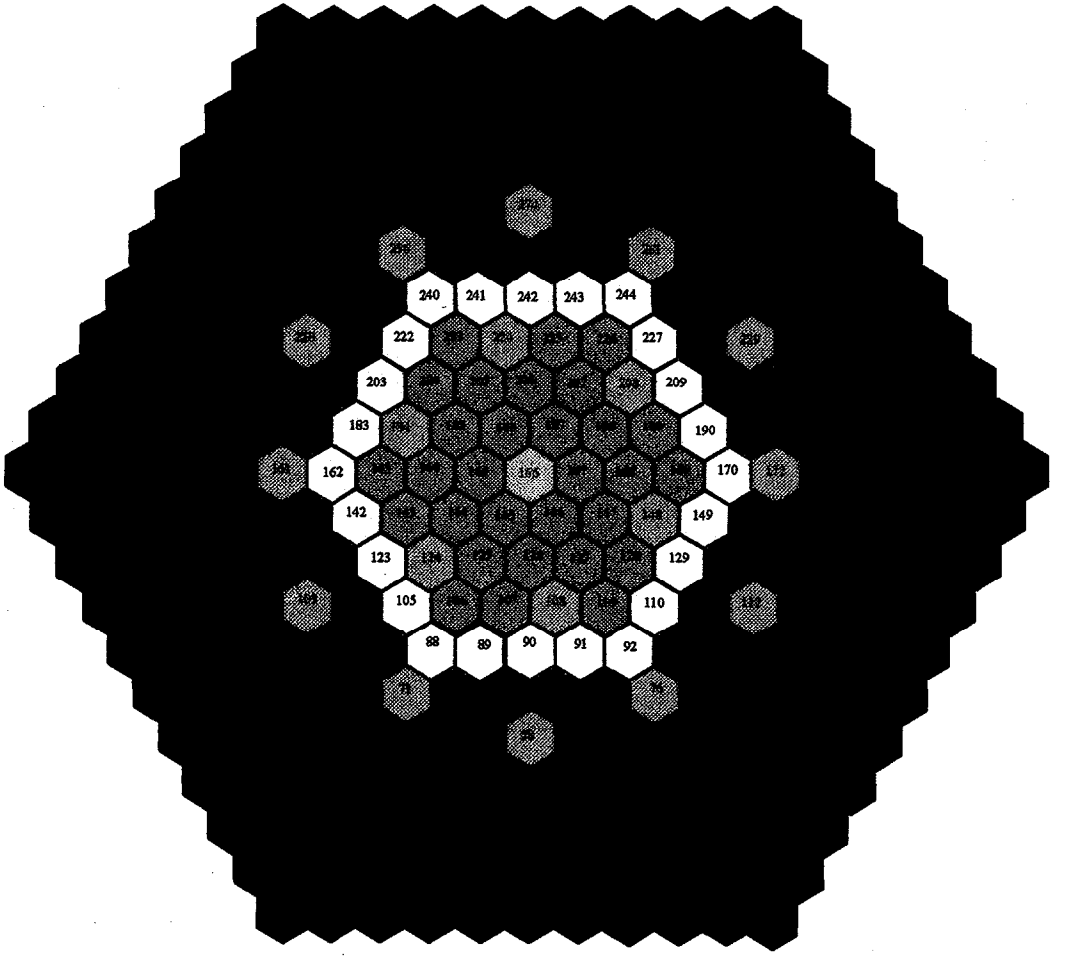

- **3.7% Enriched Uranium Rods**
- **3.8% fissile Pu MOX Rods**
- **2.8% fissile Pu MOX Rods**
- **Central tube**
- **Control Rods / Burnable Absorbers**

Figure 3. Simplified Design for VVER-1000 Fuel Assembly. Type A

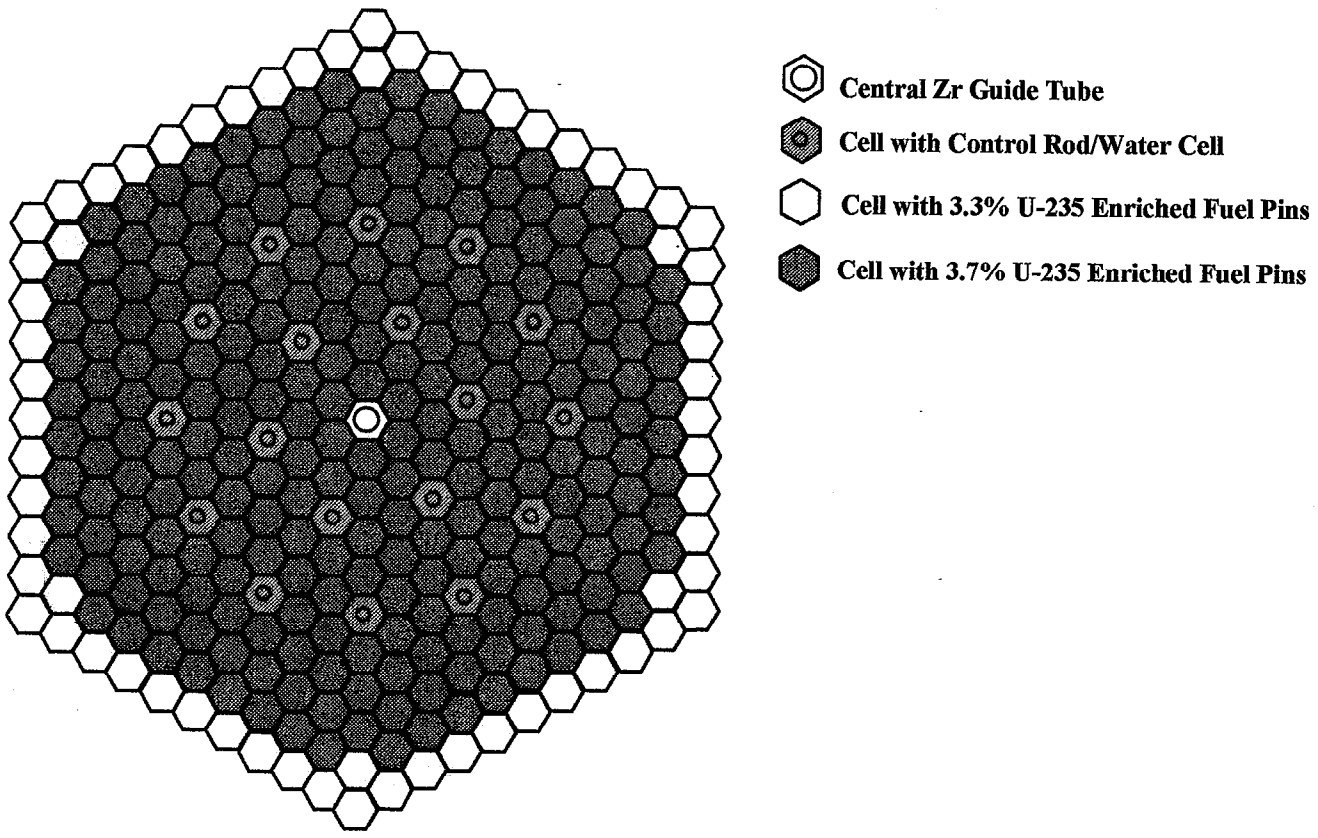

Figure 4. Simplified Design for VVER-1000 Fuel Assembly. Types B and Ba

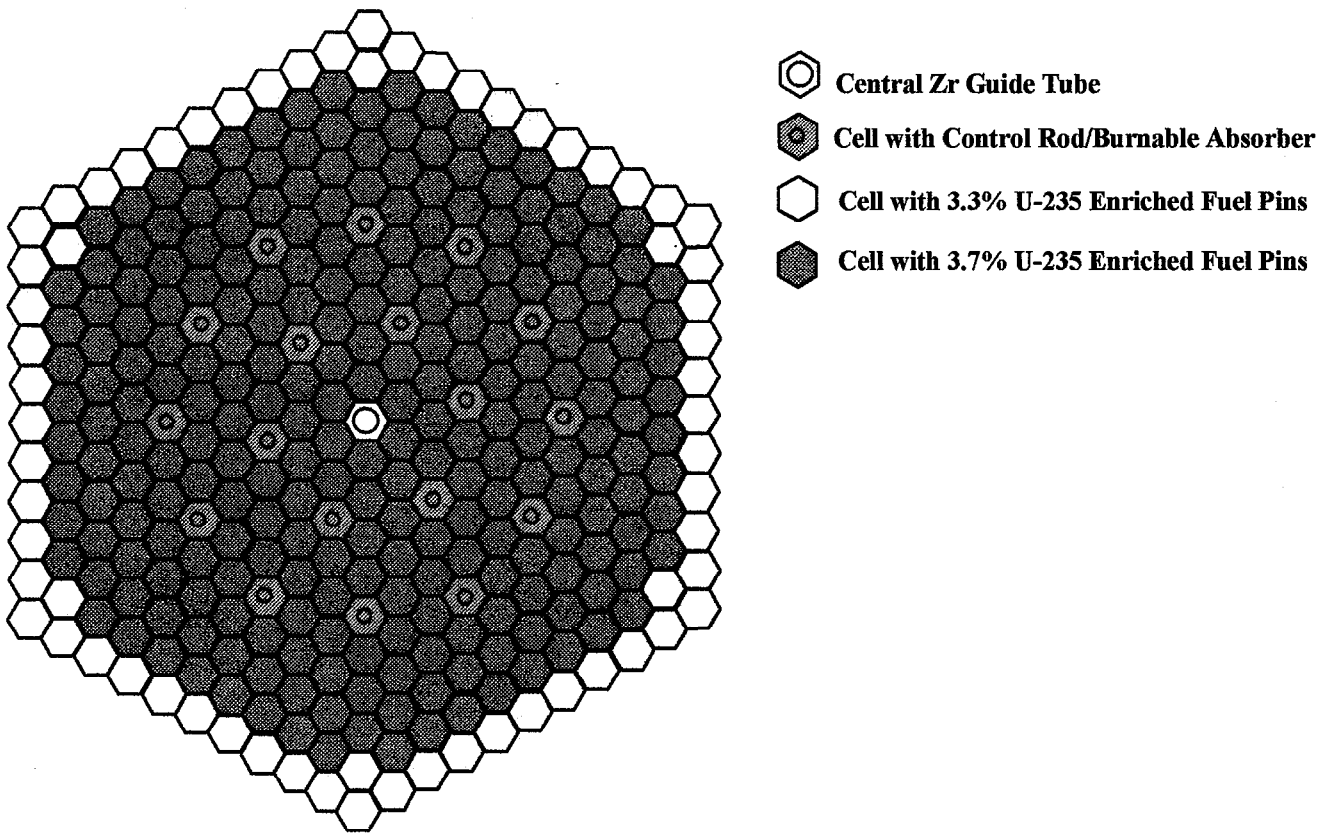

Figure 5. Simplified Design for VVER-1000 Fuel Assembly. Type C

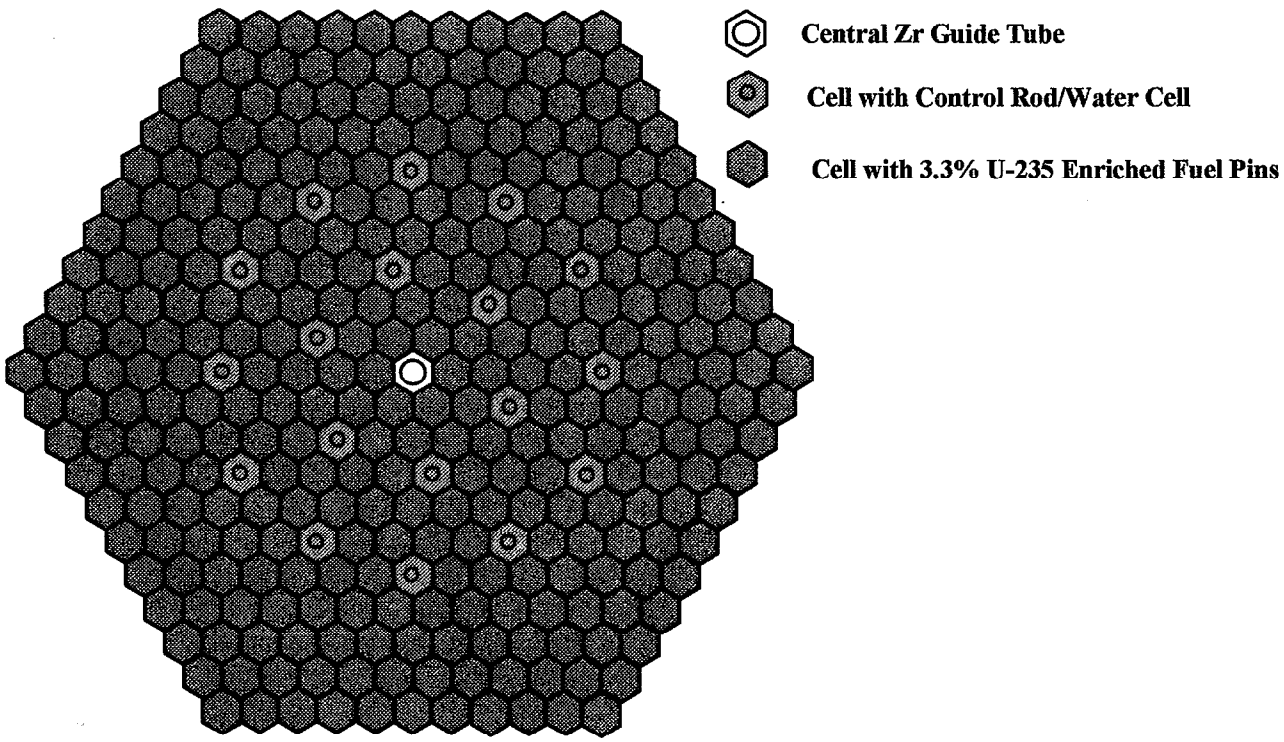

Figure 6. Equilibrium Loading Pattern for Uranium Reference Core with Boron BPRs, Core 60 ° Sector

An - 3,7% Enrichment graded by 3,3% Replaced After 3 Years (No BPRs)

Bn - 3,7% Enrichment graded by 3,3% Replaced After 3/4 Years (0,065 g/cc Boron BPRs, removed after 1st year)

Ba n - 3,7% Enrichment graded by 3,3% Replaced After 3/4 Years (0,036 g/cc Boron BPRs, removed after 1st year)

Cn - 3,3% Enrichment Replaced After 3 Years (No BPRs)

1-28 - Positions in 60 Degree Sector

n - Current Cycle of Fuel Assembly

Symbol e.g. **$** - Position of a Fuel Assembly During Lifetime in Core

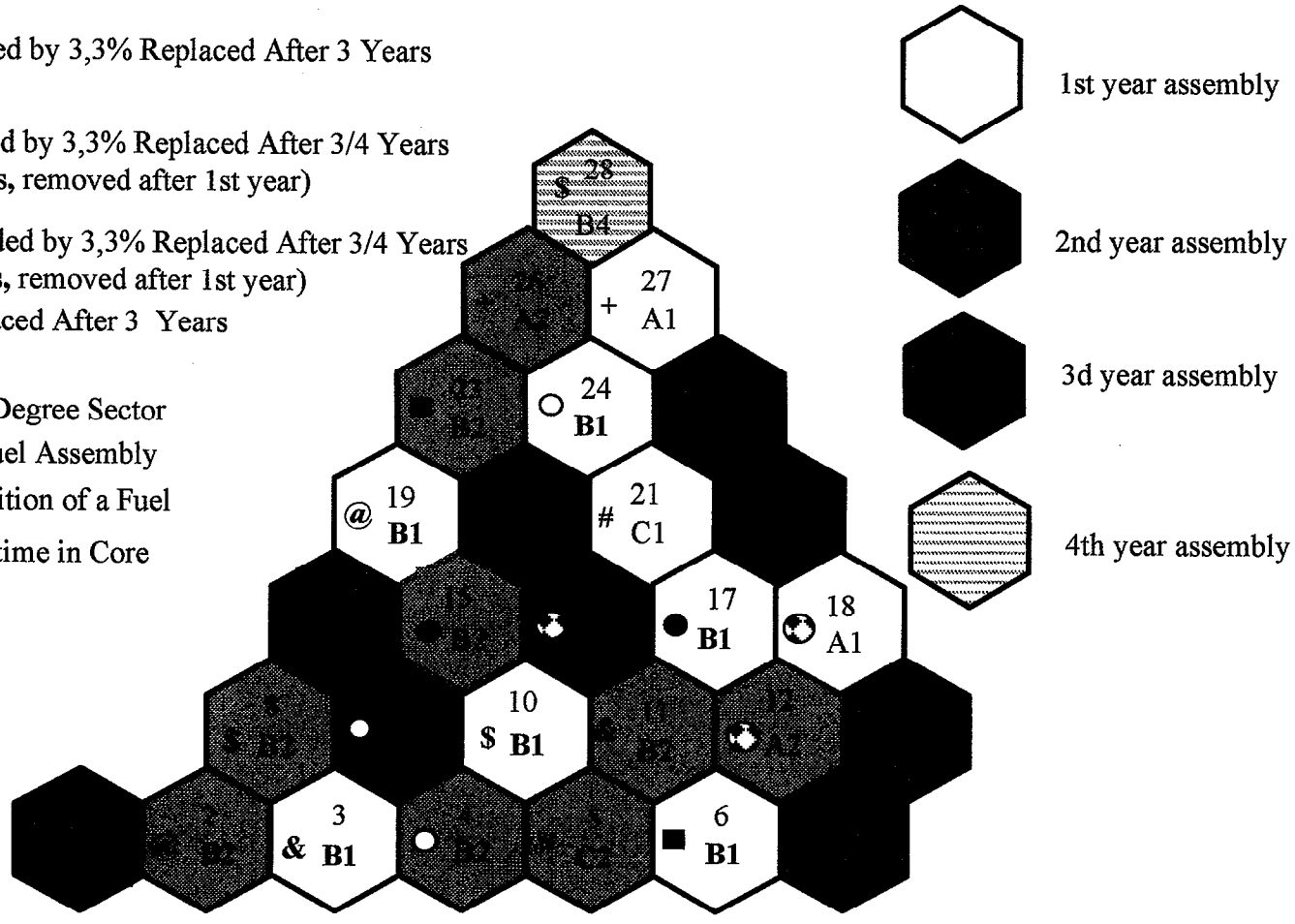

Figure 7. Equilibrium Cycle for Reference Uranium Core. Assembly-by-Assembly Burnup and Power Distribution, Core 60° Sector

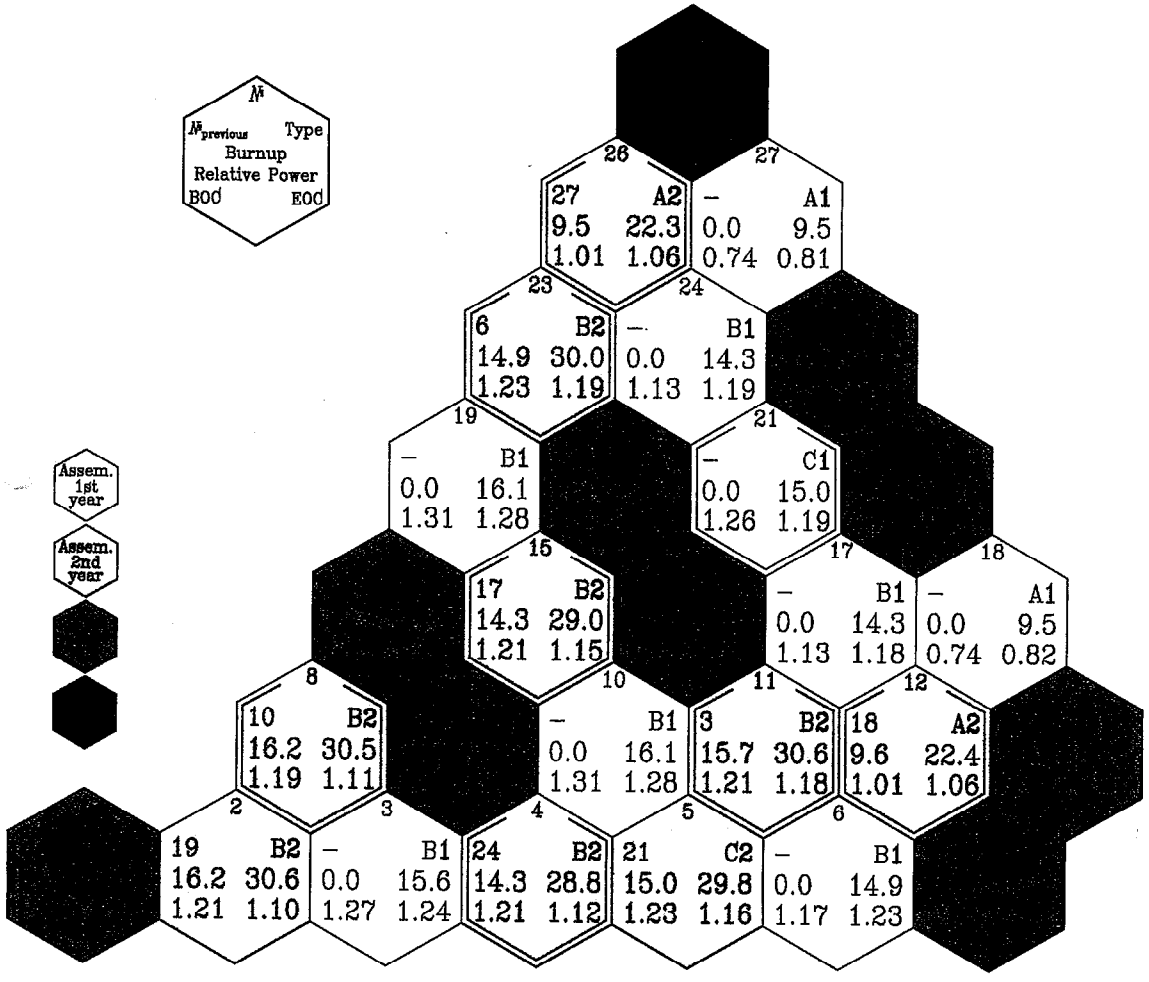

Figure 8. Beginning of the Equilibrium Cycle for Reference Uranium Core. Assembly-by-Assembly Pin Power Peaking Factor, Core 60° Sector

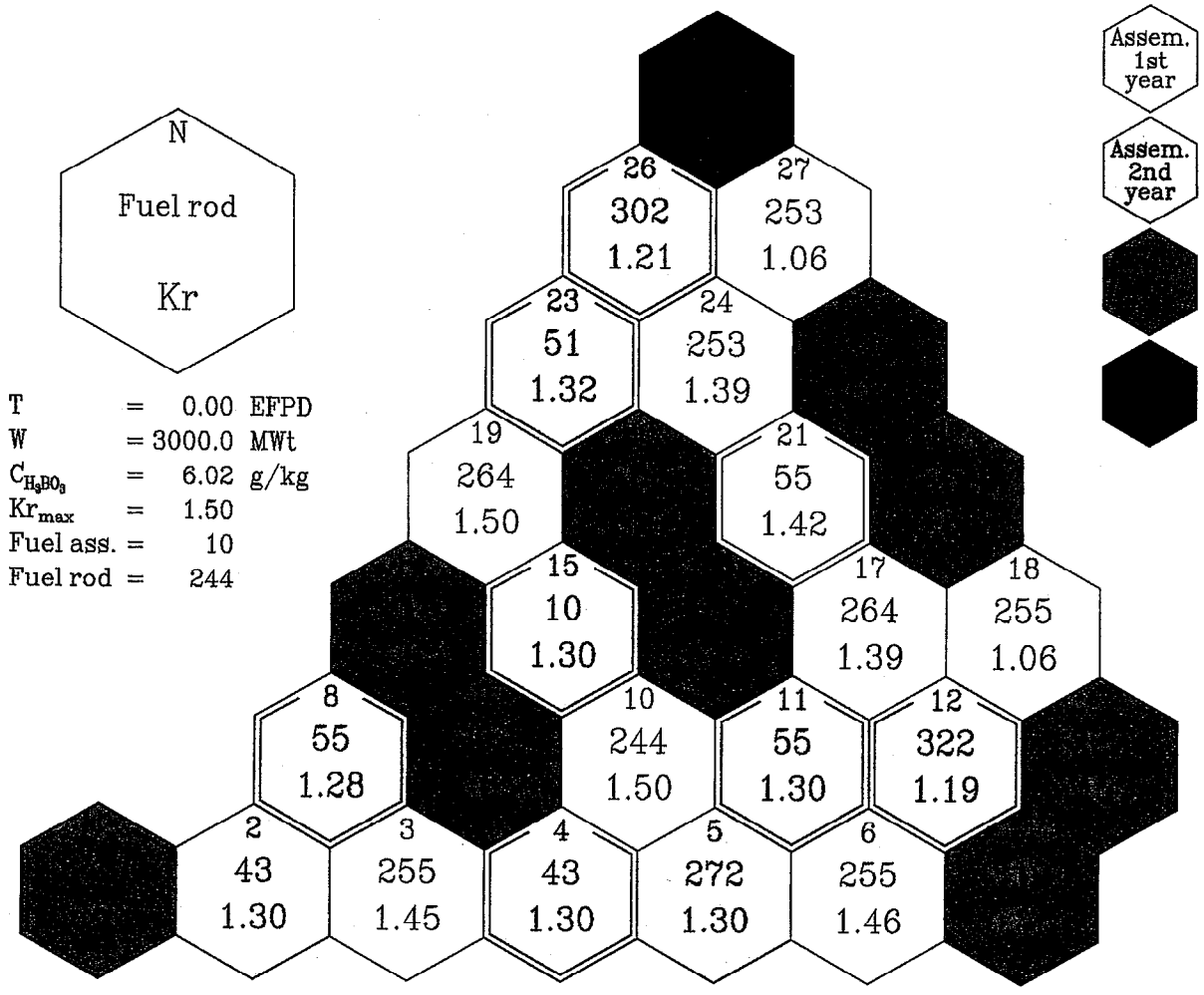

Figure 9. End of the Equilibrium Cycle for Reference Uranium Core. Assembly-by-Assembly Pin Power Peaking Factor, Core 60° Sector

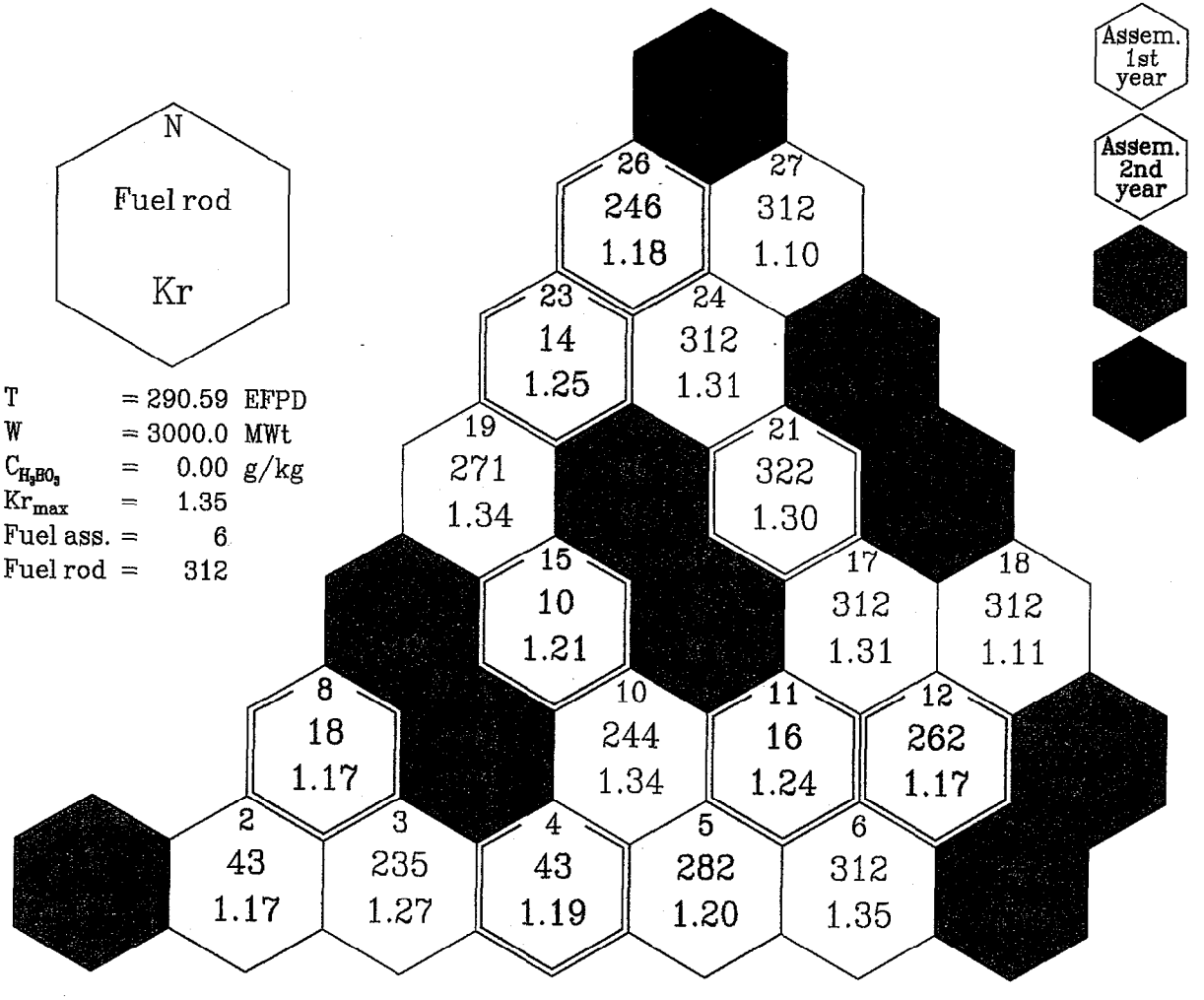

Figure 10. Beginning of the Equilibrium Cycle for Reference Uranium Core. Assembly-by-Assembly Maximum Pin Linear Power, Core 60° Sector

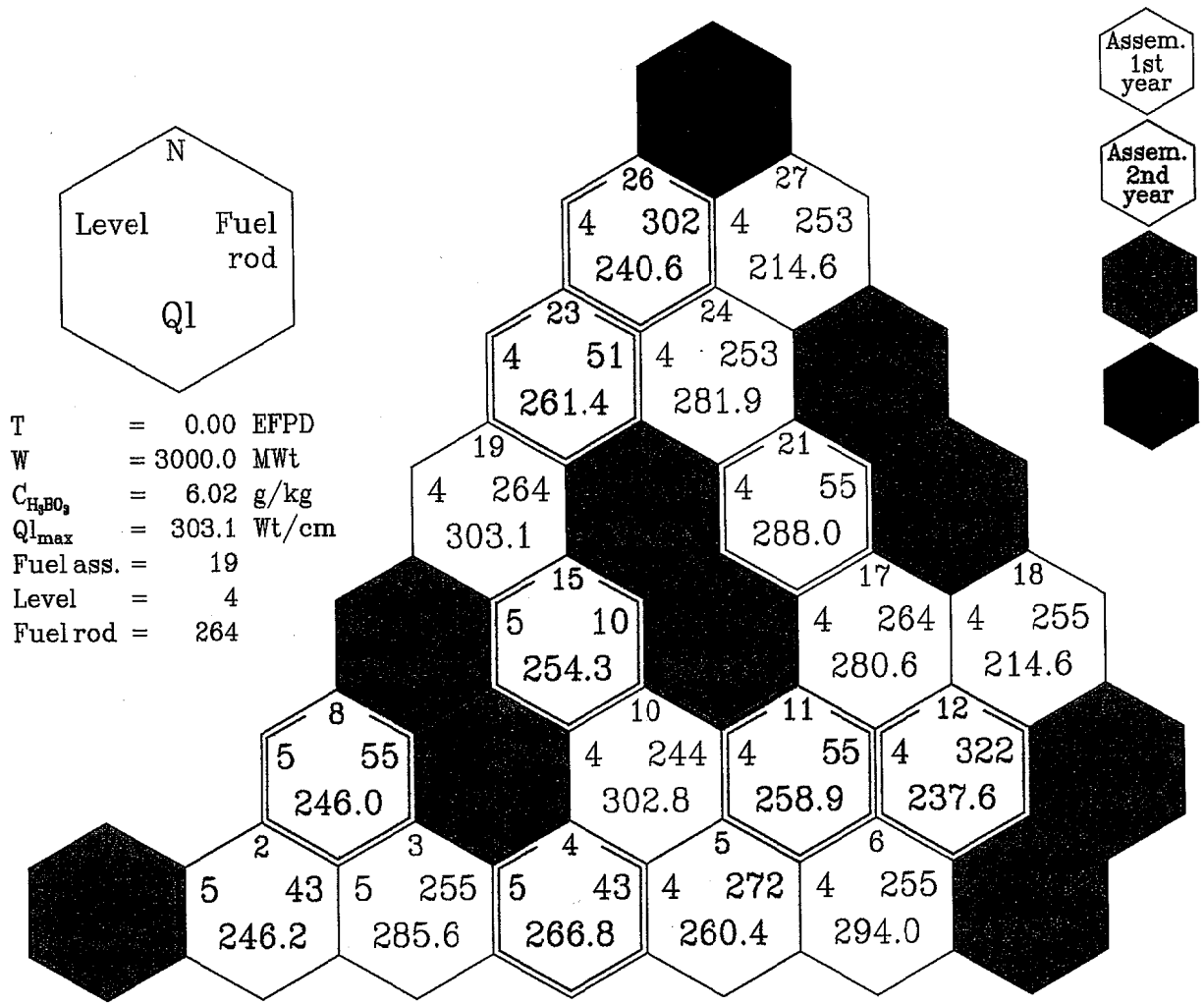

Figure 11. End of the Equilibrium Cycle for Reference Uranium Core. Assembly-by-Assembly Maximum Pin Linear Power, Core 60° Sector

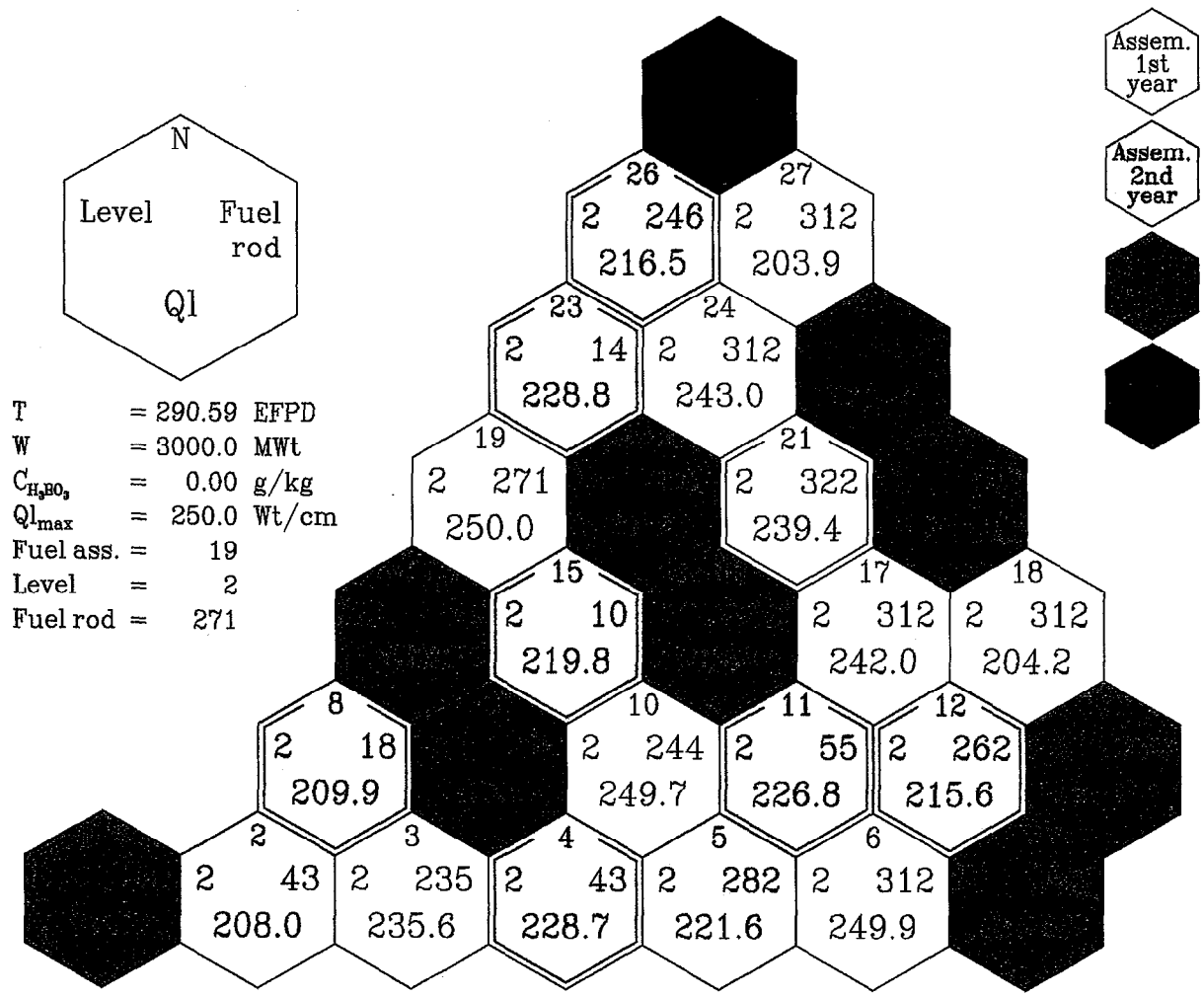

Figure 12. Beginning of the Equilibrium Cycle for Reference Uranium Core. Relative Power Distribution in the Most Powered Assembly

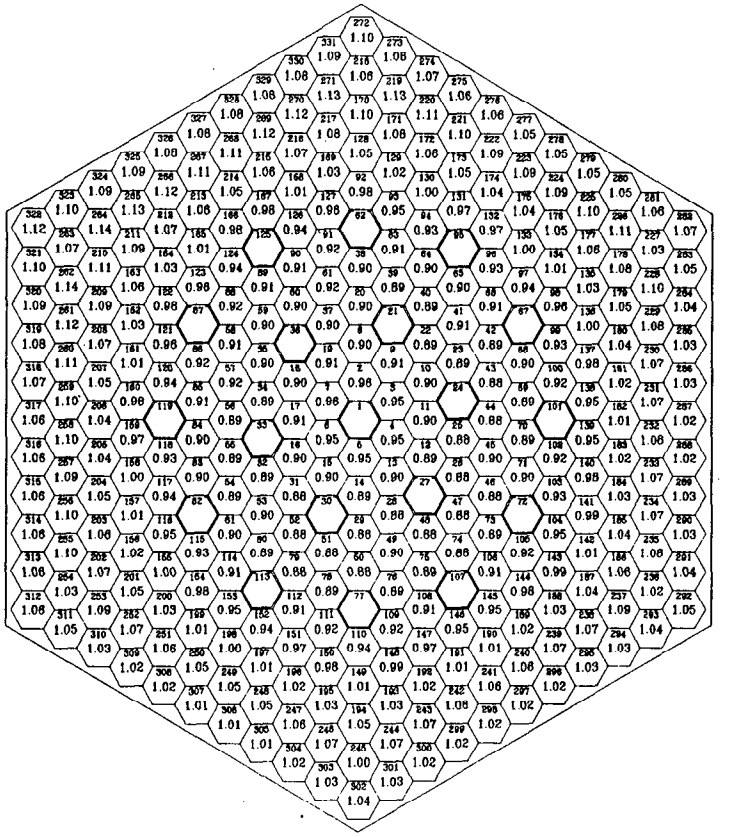

T	0.00	EFPD
W	3000.0	MWt
$C_{H_3BO_3}$	6.02	g/kg
Ql_{max}	303.1	Wt/cm
Fuel assembly	19	
Level	4	
Fuel rod	264	
Kk_{max}	1.14	

Figure 13. End of the Equilibrium Cycle for Reference Uranium Core. Relative Power Distribution in the Most Powered Assembly

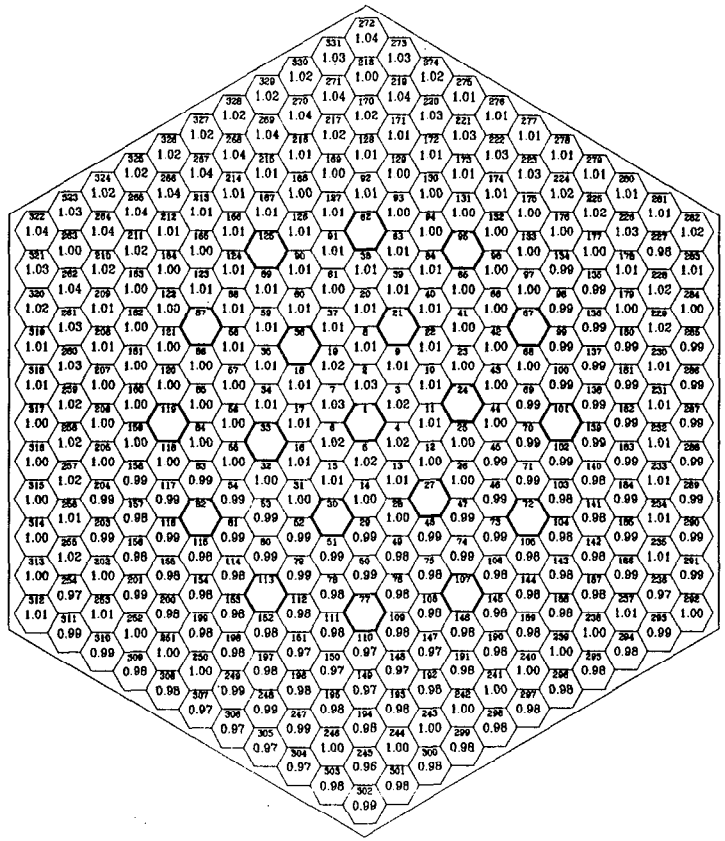

T	290.59	EFPD
W	3000.0	MWt
$C_{H_3BO_3}$	0.00	g/kg
Ql_{max}	250.0	Wt/cm
Fuel assembly	19	
Level	2	
Fuel rod	271	
Kk_{max}	1.04	

Figure 14. Loading Pattern for the First Cycle with 3 MOX LTAs

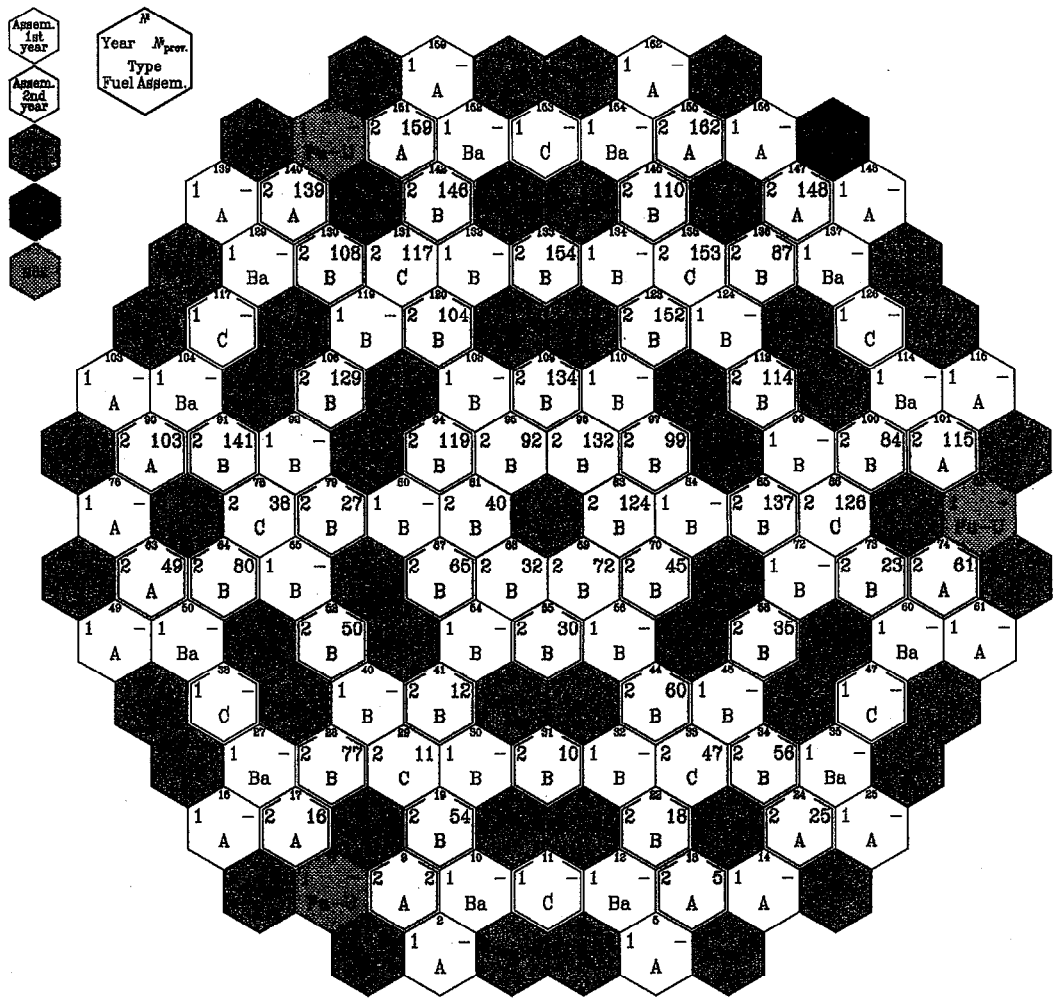

Figure 15. First Cycle with 3 MOX LTAs of "Island-2" Type (Pu3.8-2.8-U3.7). Assembly-by-Assembly Burnup Distribution

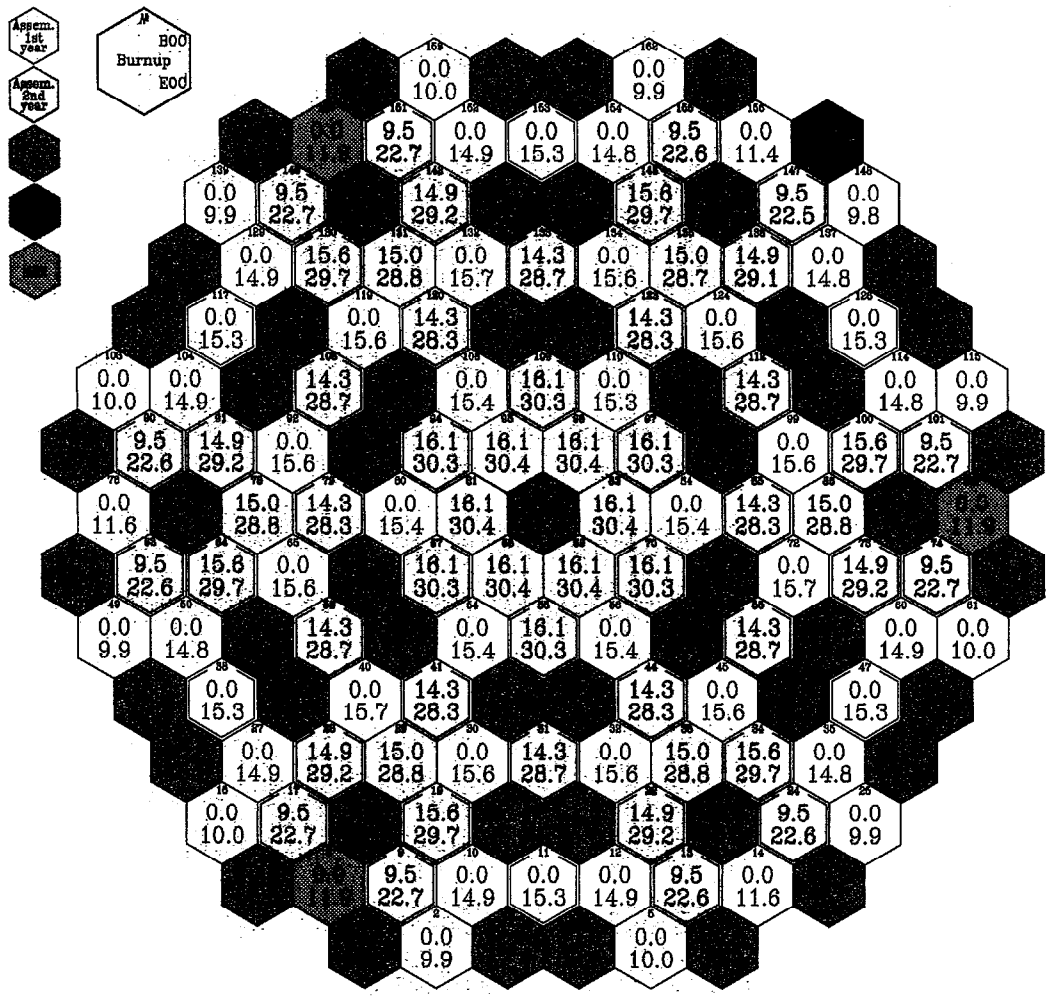

Figure 16. First Cycle with 3 MOX LTAs of "Island-2" Type (Pu3.8-2.8-U3.7). Assembly-by-Assembly Power Distribution

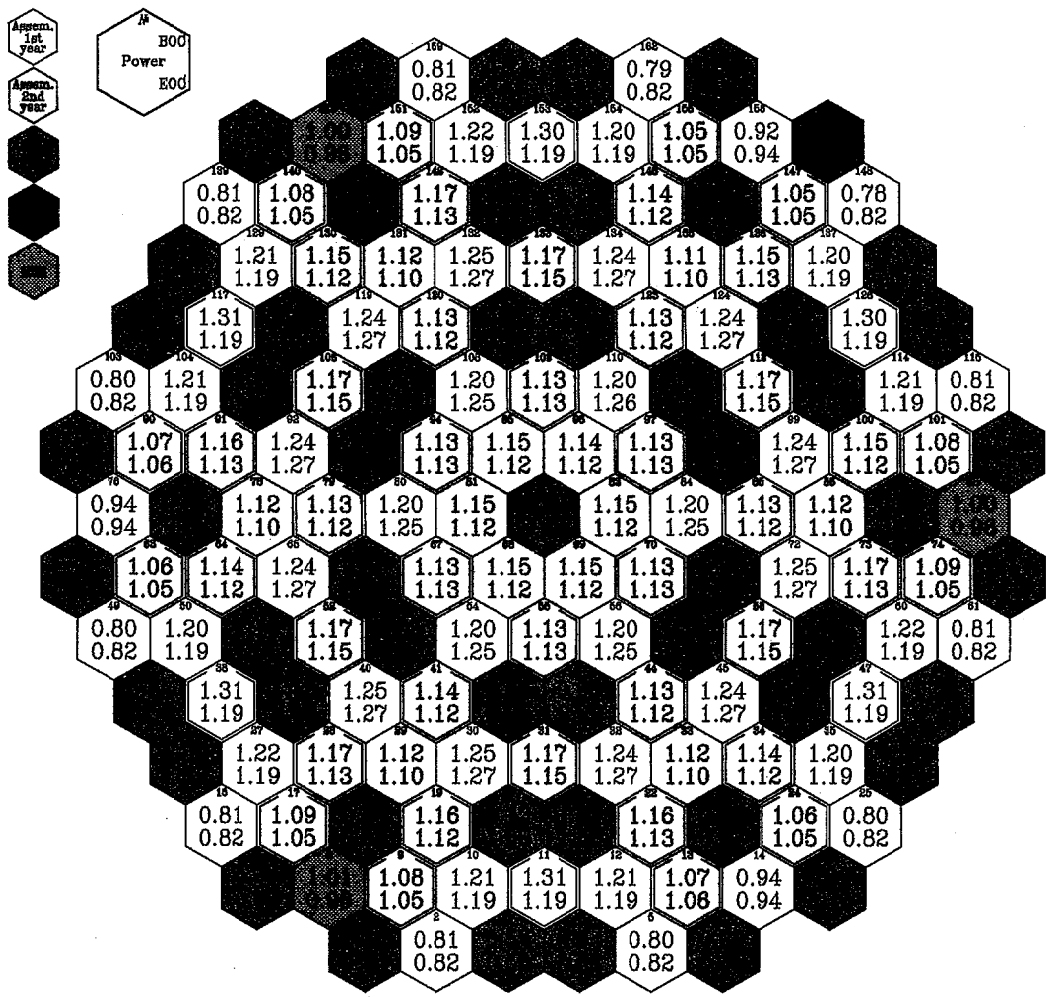

Figure 17. Beginnning of the First Cycle with 3 MOX LTAs of "Island-2" Type (Pu3.8-2.8-U3.7). Assembly-by-Assembly Pin Power Peaking Factor

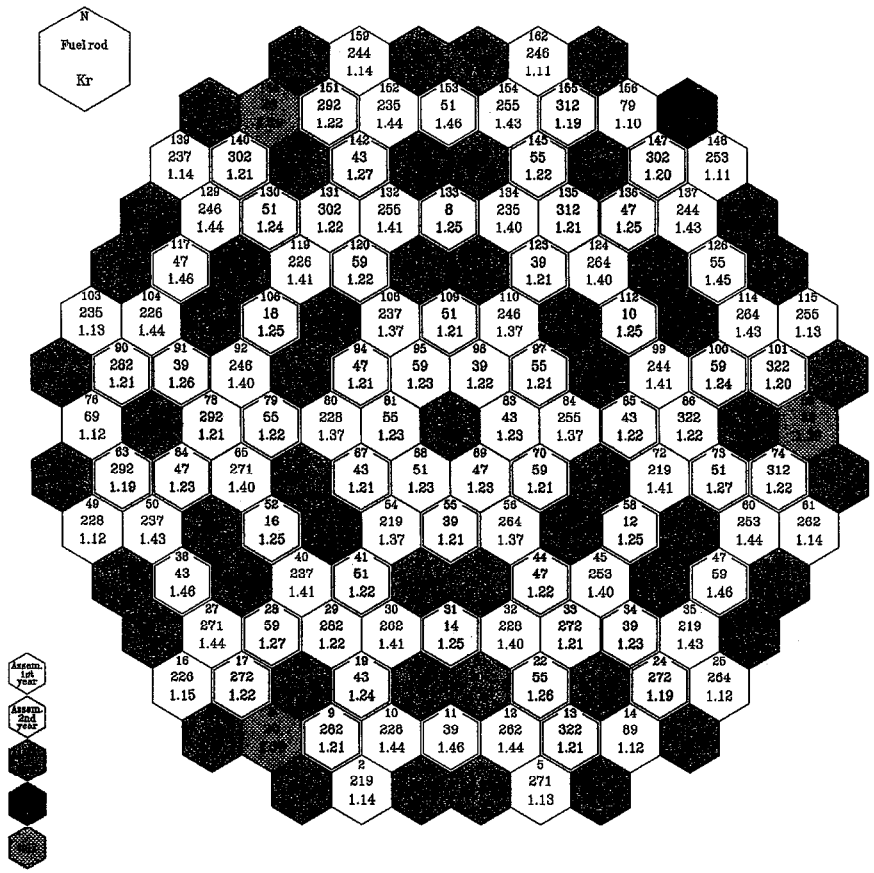

T	=	0.00	EFPD
W	=	3000.0	MWt
$C_{H_3BO_3}$	=	6.14	g/kg
Kr_{max}	=	1.46	
Fuel ass.	=	38	
Fuel rod	=	43	

Figure 18. End of the First Cycle with 3 MOX LTAs of "Island-2" Type (Pu3.8-2.8-U3.7). Assembly-by-Assembly Pin Power Peaking Factor

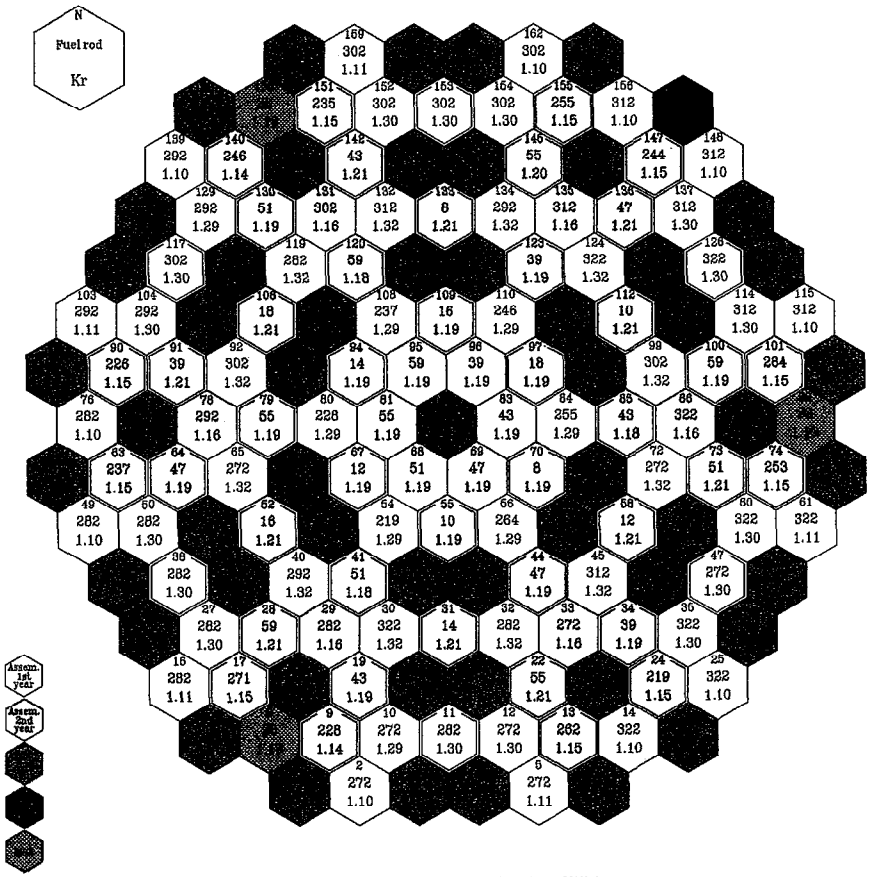

T	=	290.78 EFPD
W	=	3000.0 MWt
$C_{H_3BO_3}$	=	0.00 g/kg
Kr_{max}	=	1.32
Fuel ass.	=	134
Fuel rod	=	292

Figure 19. Beginning of the First Cycle with 3 MOX LTAs of "Island-2" Type (Pu3.8-2.8-U3.7). Assembly-by-Assembly Maximum Pin Linear Power

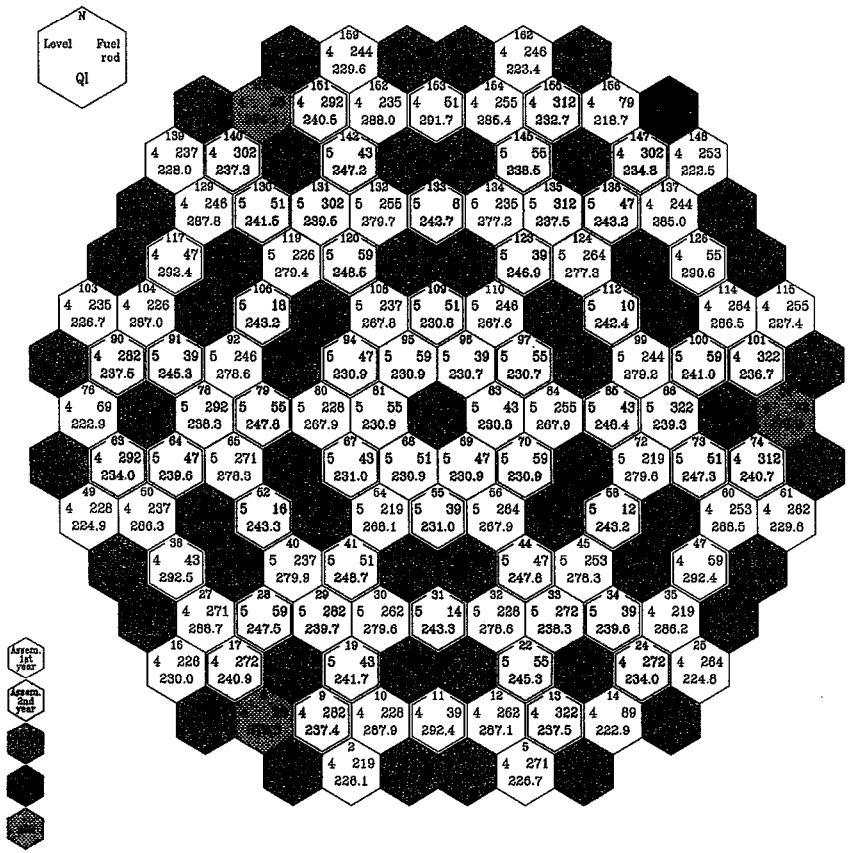

T	=	0.00	EFPD
W	=	3000.0	MWt
$C_{H_3BO_3}$	=	6.14	g/kg
Ql_{max}	=	292.5	Wt/cm
Fuel ass.	=	38	
Level	=	4	
Fuel rod	=	43	

Figure 20. End of the First Cycle with 3 MOX LTAs of "Island-2" Type (Pu3.8-2.8-U3.7). Assembly-by-Assembly Maximum Pin Linear Power

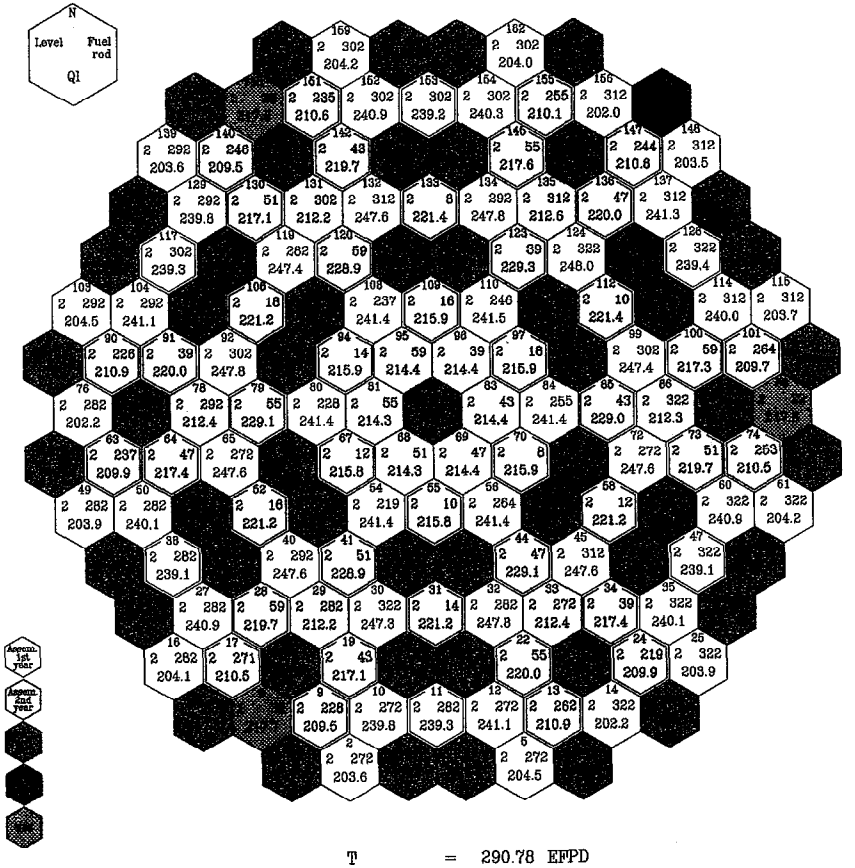

T	=	290.78	EFPD
W	=	3000.0	MWt
$C_{H_3BO_3}$	=	0.00	g/kg
Ql_{max}	=	248.0	Wt/cm
Fuel ass.	=	124	
Level	=	2	
Fuel rod	=	322	

Figure 21. Beginning of the First Cycle with 3 MOX LTAs of "Island-2" Type (Pu3.8-2.8-U3.7). Relative Power Distribution in the Most Powered Assembly

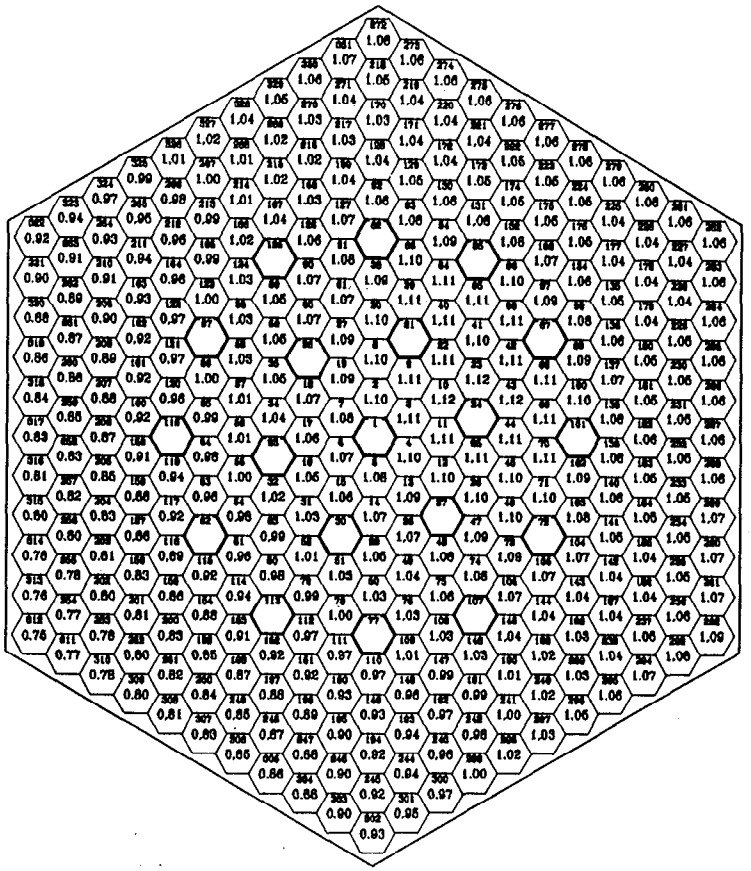

T	0.00	EFPD
W	3000.0	MWt
$C_{B(0)}$	6.14	g/kg
Ql_{max}	292.5	Wt/cm
Fuel assembly	36	
Level	4	
Fuel rod	43	
Kk_{max}	1.12	

Figure 22. End of the First Cycle with 3 MOX LTAs of "Island-2" Type (Pu3.8-2.8-U3.7). Relative Power Distribution in the Most Powered Assembly

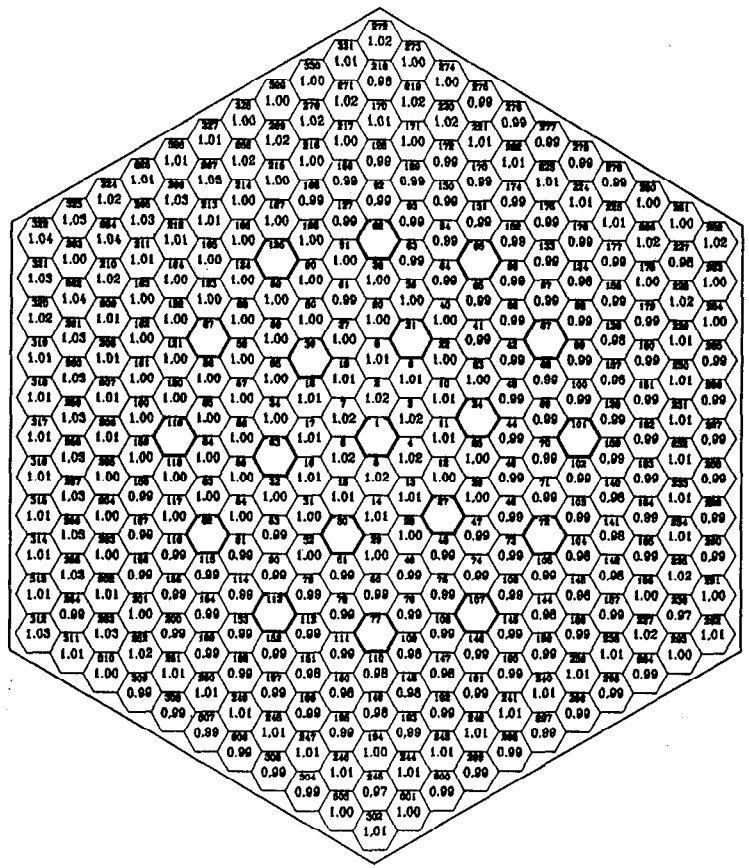

τ	290.78	EFPD
W	3000.0	MWt
$C_{B,ex}$	0.00	g/kg
Ql_{max}	246.0	Wt/cm
Fuel assembly	124	
Level	2	
Fuel rod	322	
Kk_{max}	1.04	

Figure 23. Beginning of the First Cycle with 3 MOX LTAs of "Island-2" Type (Pu3.8-2.8-U3.7). Relative Power Distribution in the MOX Assembly

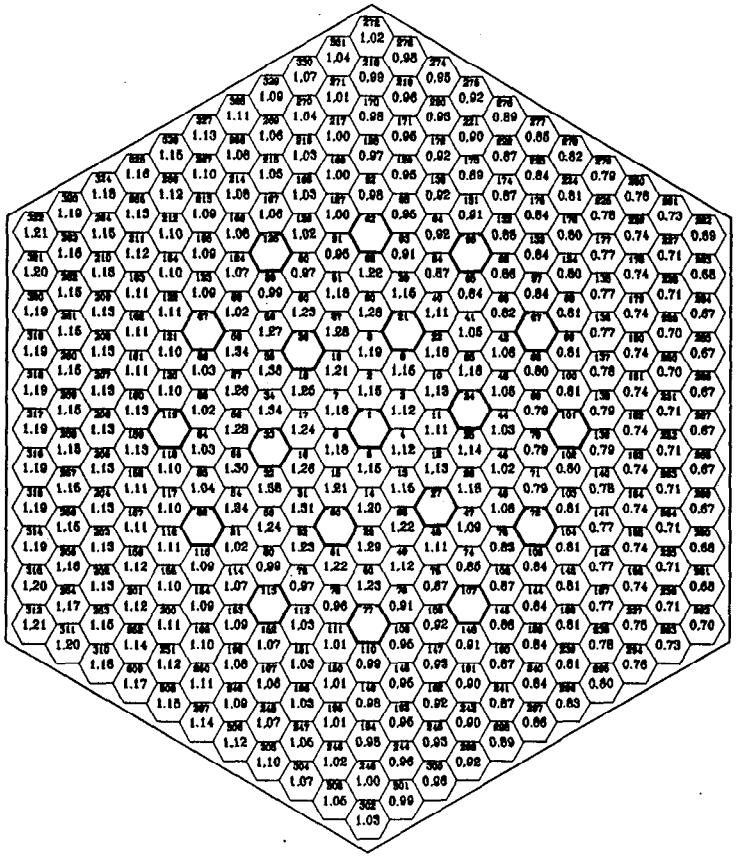

T	0.00	EFPD
W	3000.0	MWt
$C_{B,m}$	6.14	g/kg
Ql	275.9	Wt/cm
Fuel assembly	88	
Level	4	
Fuel rod	32	
Kk_{max}	1.38	

Figure 24. End of the First Cycle with 3 MOX LTAs of "Island-2" Type (Pu3.8-2.8-U3.7). Relative Power Distribution in the MOX Assembly

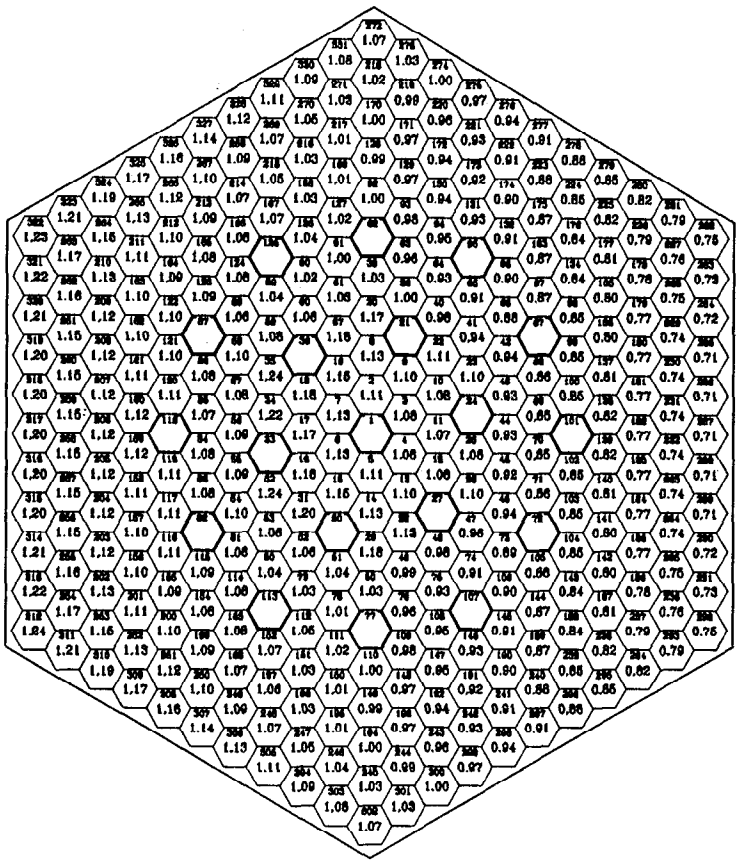

T	290.78	EFPD
W	3000.0	MWt
$C_{H_3BO_3}$	0.00	g/kg
Ql	207.0	Wt/cm
Fuel assembly	66	
Level	4	
Fuel rod	52	
Kk_{max}	1.24	

Figure 25. End of the First Cycle with 3 MOX LTAs of "Island-2" Type (Pu3.8-2.8-U3.7). Relative Burnup Distribution in the MOX Assembly

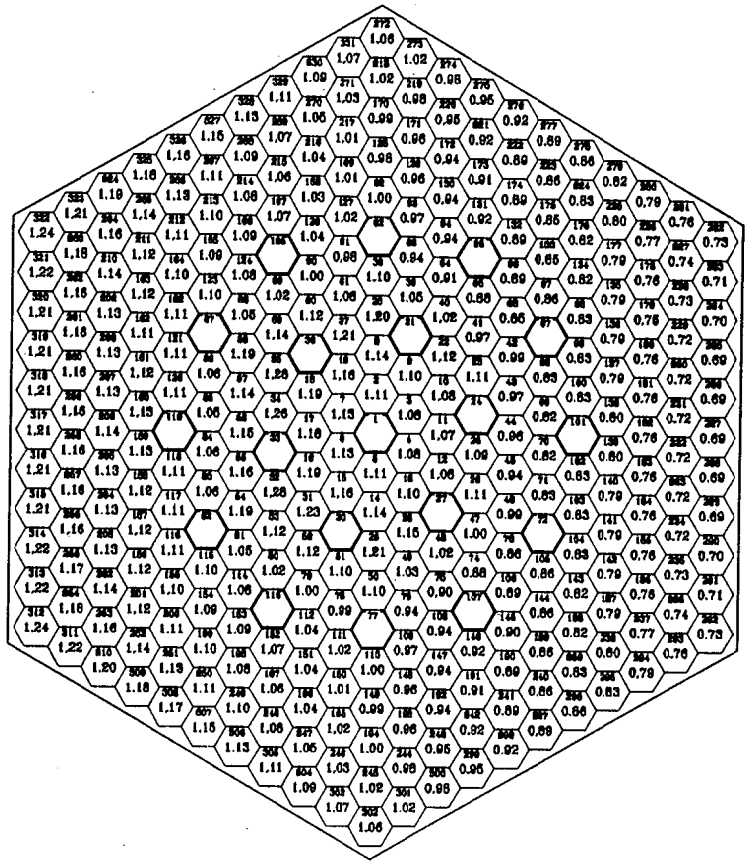

T	290.78	EFPD
W	3000.0	MWt
$C_{B_{ave}}$	0.00	g/kg
Burnup	16.9	
Fuel assembly	66	
Level	4	
Fuel rod	32	
Kb_{max}	1.28	

Figure 26. First Cycle with 3 MOX LTAs 100%Pu (4.2-3.0-2.0). Assembly-by-Assembly Burnup Distribution

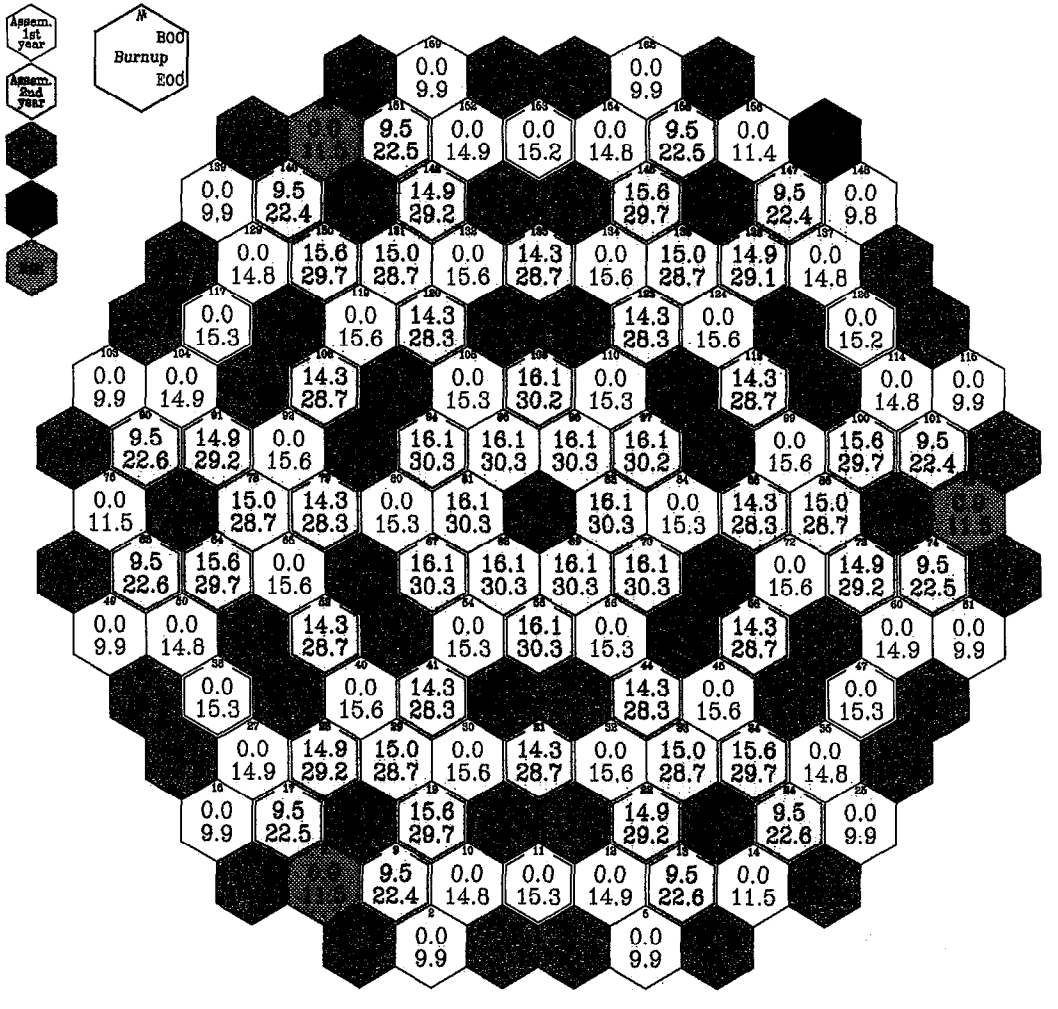

Figure 27. First Cycle with 3 MOX LTAs 100%Pu (4.2-3.0-2.0). Assembly-by-Assembly Power Distribution

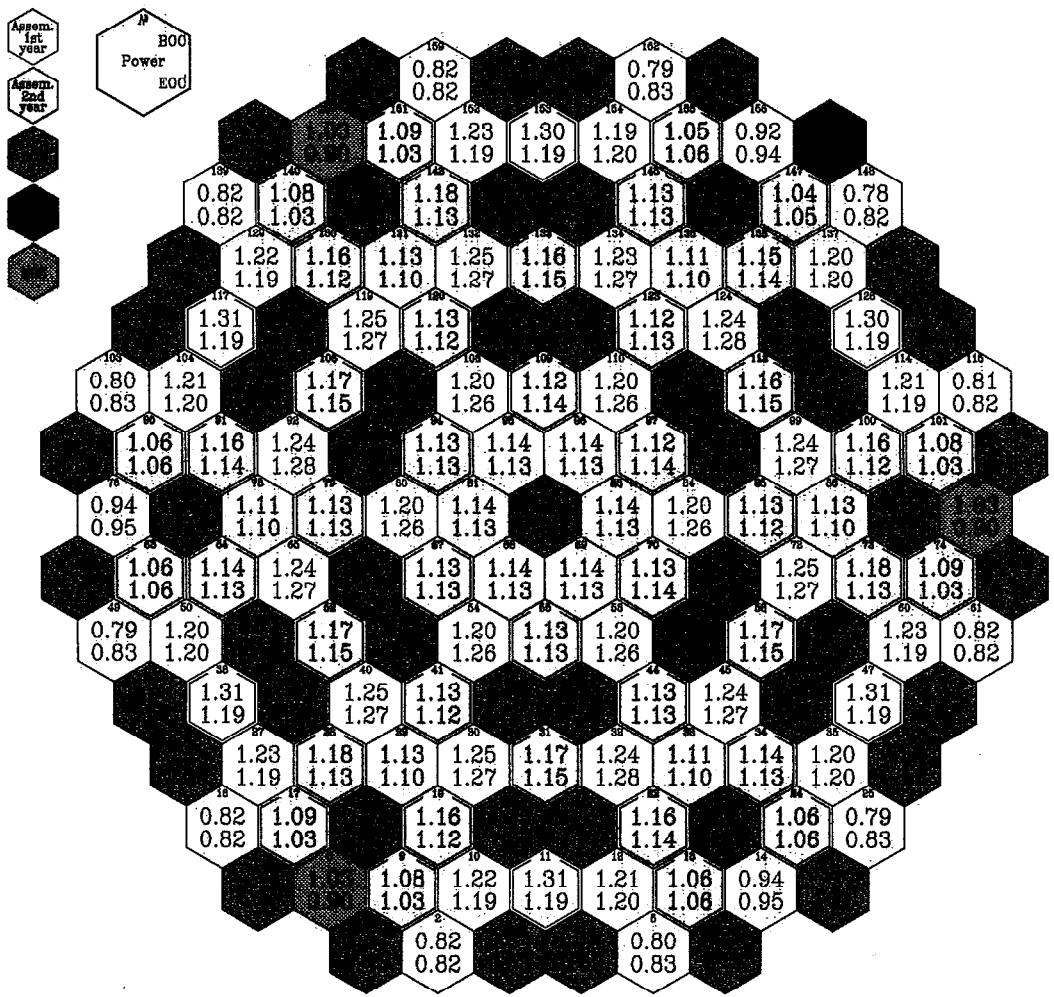

Figure 28. Beginning of the First Cycle with 3 MOX LTAs 100%Pu (4.2-3.0-2.0). Assembly-by-Assembly Pin Power Peaking Factor

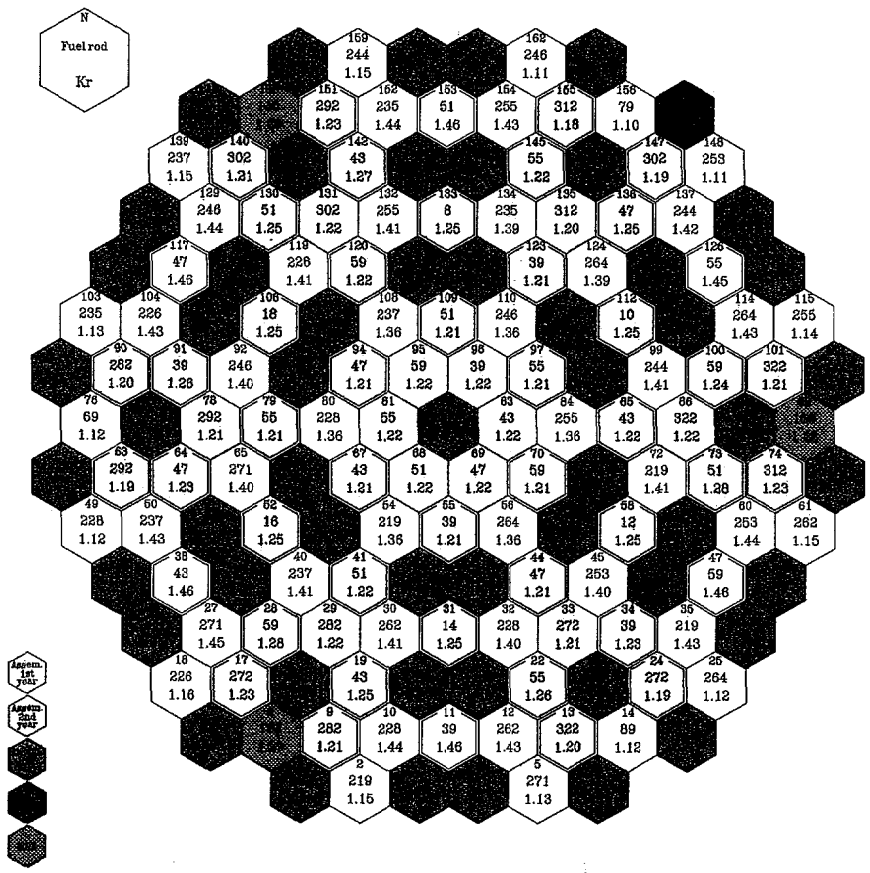

T	=	0.00	EFPD
W	=	3000.0	MWt
$C_{H_3BO_3}$	=	6.16	g/kg
Kr_{max}	=	1.46	
Fuel ass.	=	38	
Fuel rod	=	43	

Figure 29. End of the First Cycle with 3 MOX LTAs 100%Pu (4.2-3.0-2.0). Assembly-by-Assembly Pin Power Peaking Factor

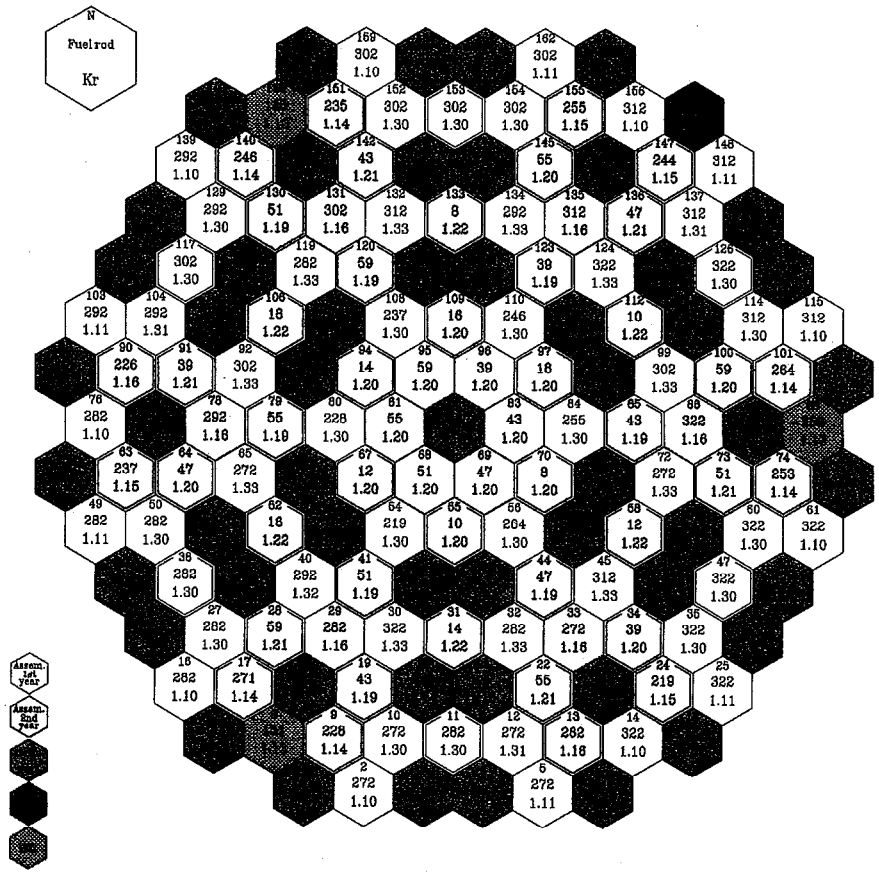

T	=	289.59	EFPD
W	=	3000.0	MWt
$C_{H_3BO_3}$	=	0.00	g/kg
Kr_{max}	=	1.33	
Fuel ass.	=	134	
Fuel rod	=	292	

Figure 30. Beginning of the First Cycle with 3 MOX LTAs 100%Pu (4.2-3.0-2.0). Assembly-by-Assembly Maximum Pin Linear Power

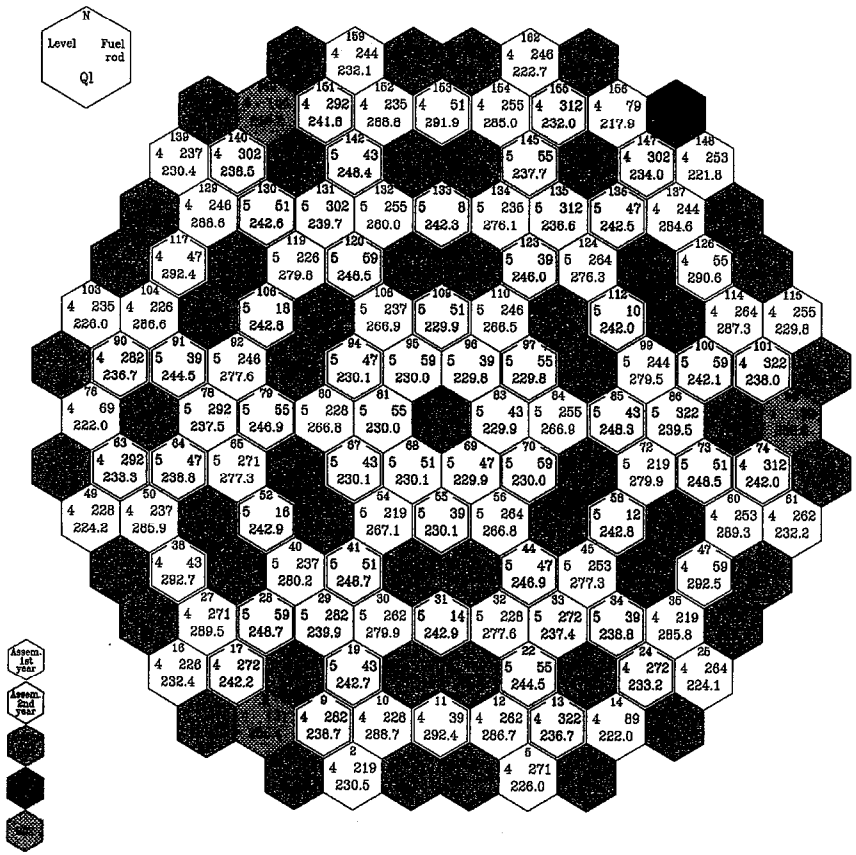

T	=	0.00	EFPD
W	=	3000.0	MWt
$C_{H_3BO_3}$	=	6.16	g/kg
Ql_{max}	=	292.7	Wt/cm
Fuel ass.	=	38	
Level	=	4	
Fuel rod	=	43	

Figure 31. End of the First Cycle with 3 MOX LTAs 100%Pu (4.2-3.0-2.0). Assembly-by-Assembly Maximum Pin Linear Power

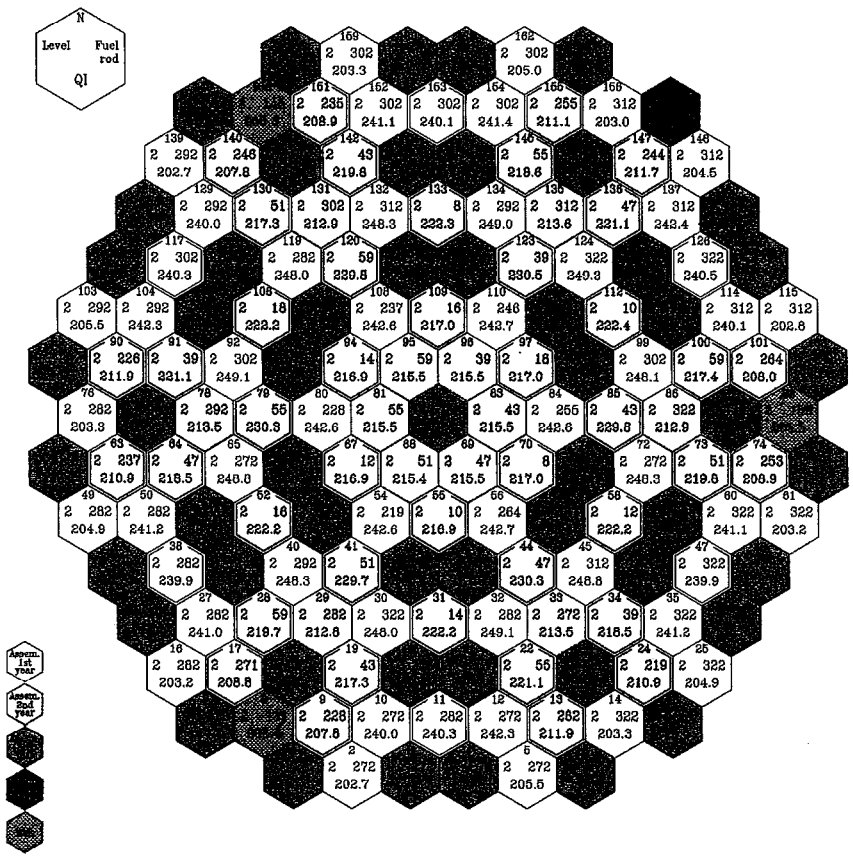

T	=	289.59 EFPD
W	=	3000.0 MWt
$C_{H_3BO_3}$	=	0.00 g/kg
Ql_{max}	=	249.3 Wt/cm
Fuel ass.	=	124
Level	=	2
Fuel rod	=	322

Figure 32. Beginning of the First Cycle with 3 MOX LTAs 100%Pu (4.2-3.0-2.0). Relative Power Distribution in the Most Powered Assembly

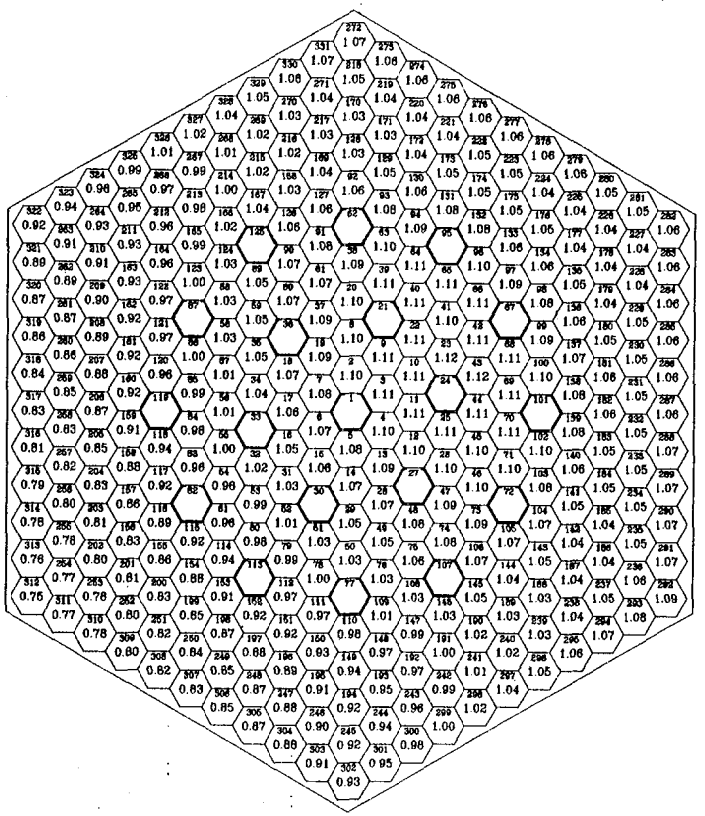

τ	0.00	EFPD
W	3000.0	MWt
$C_{B,ini}$	6.16	g/kg
Ql_{max}	292.7	Wt/cm
Fuel assembly	38	
Level	4	
Fuel rod	43	
Kk_{max}	1.12	

Figure 33. End of the First Cycle with 3 MOX LTAs 100%Pu (4.2-3.0-2.0). Relative Power Distribution in the Most Powered Assembly

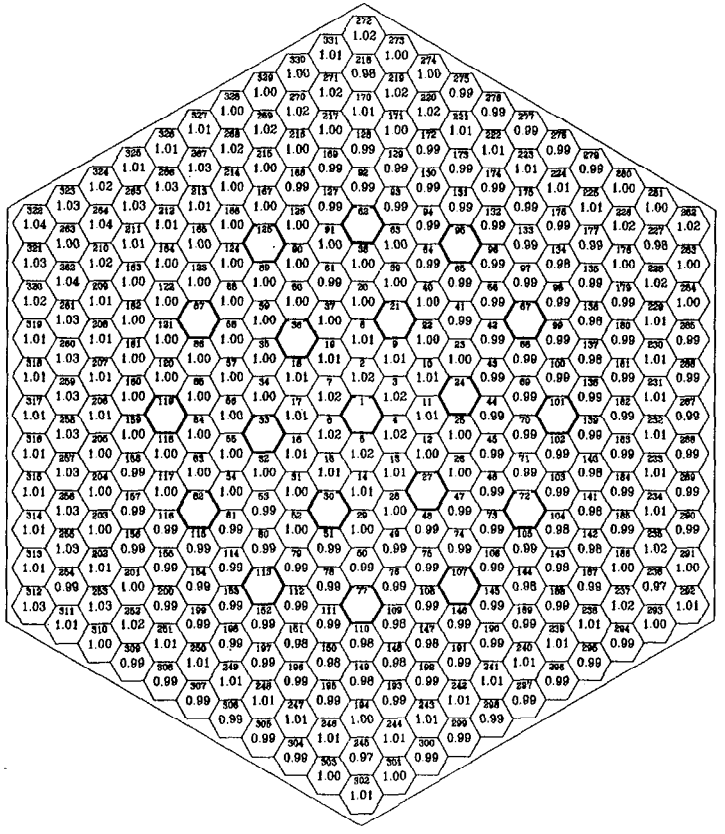

T	289.59	EFPD
W	3000.0	MWt
$C_{H_3BO_3}$	0.00	g/kg
Ql_{max}	249.3	Wt/cm
Fuel assembly	124	
Level	2	
Fuel rod	322	
Kk_{max}	1.04	

Figure 34. Beginning of the First Cycle with 3 MOX LTAs 100%Pu (4.2-3.0-2.0). Relative Power Distribution in the MOX Assembly

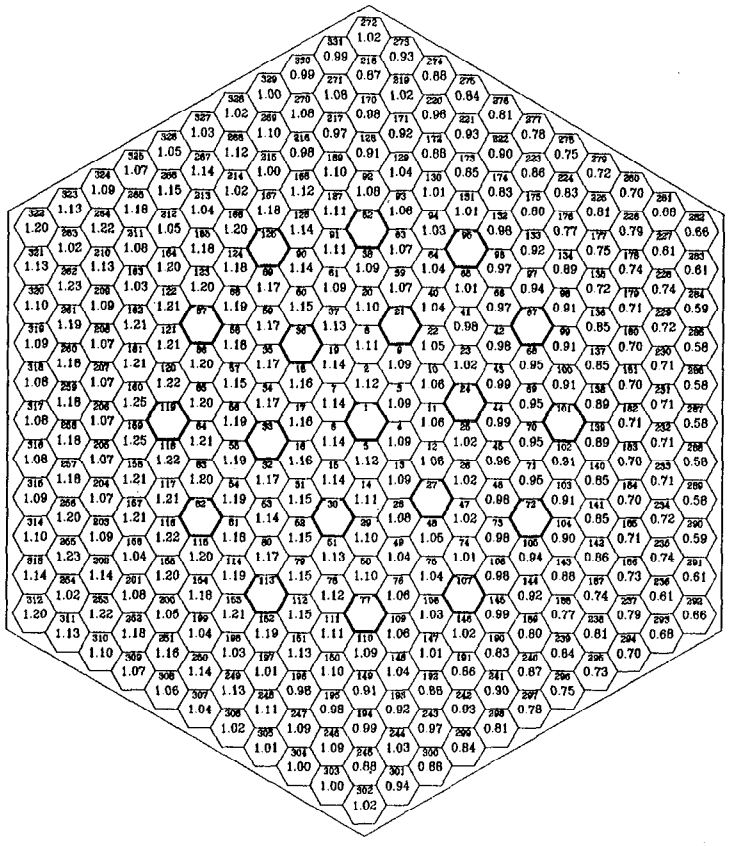

T	0.00	EFPD
W	3000.0	MWt
$C_{H_3BO_3}$	5 16	g/kg
Ql	256.0	Wt/cm
Fuel assembly	66	
Level	4	
Fuel rod	159	
Kk_{max}	1 25	

Figure 35. End of the First Cycle with 3 MOX LTAs 100%Pu (4.2-3.0-2.0). Relative Power Distribution in the MOX Assembly

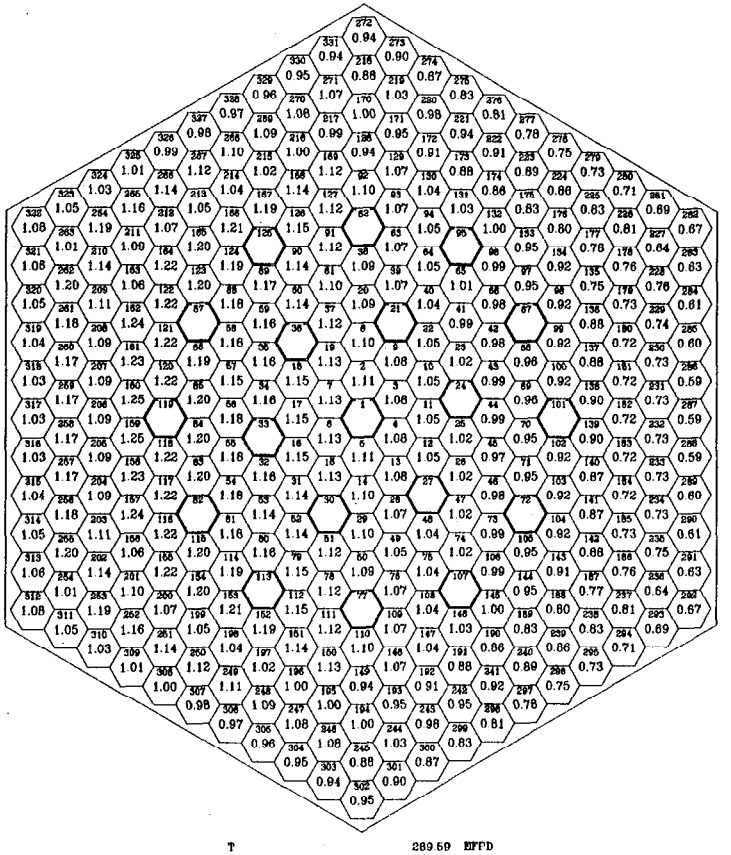

T	289.59	EFPD
W	3000.0	MWt
$C_{H_3BO_3}$	0.00	g/kg
Ql	196.2	Wt/cm
Fuel assembly	88	
Level	4	
Fuel rod	159	
Kk_{max}	1.25	

Figure 36. End of the First Cycle with 3 MOX LTAs 100%Pu (4.2-3.0-2.0). Relative Burnup Distribution in the MOX Assembly

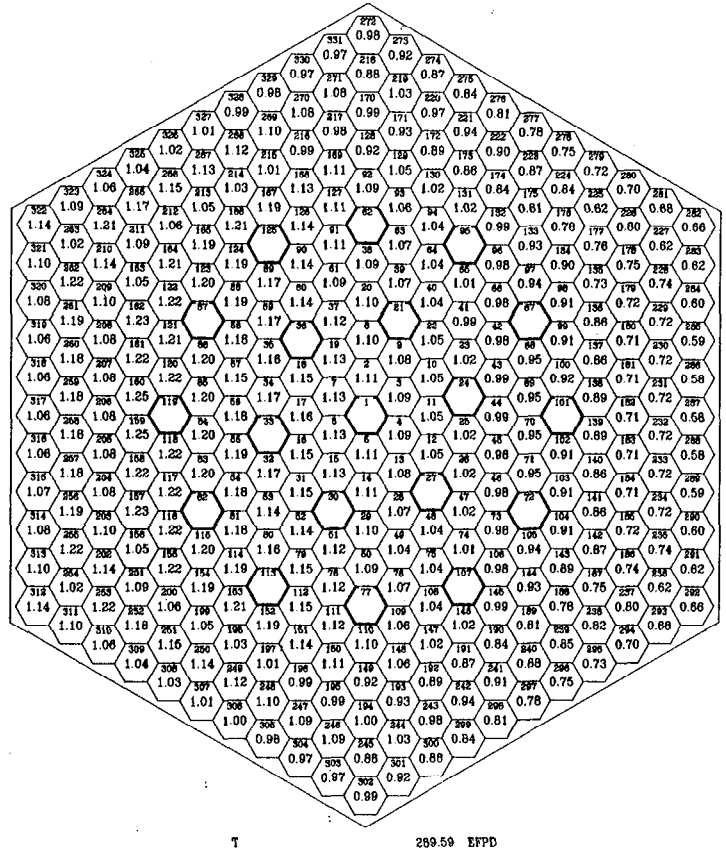

T	269.59	EFPD
W	3000.0	MWt
$C_{H_3BO_3}$	0.00	g/kg
Burnup	15.8	
Fuel assembly	88	
Level	4	
Fuel rod	159	
Kb_{max}	1.25	

Figure 37. Loading Pattern for the Second Cycle with 3 MOX LTAs

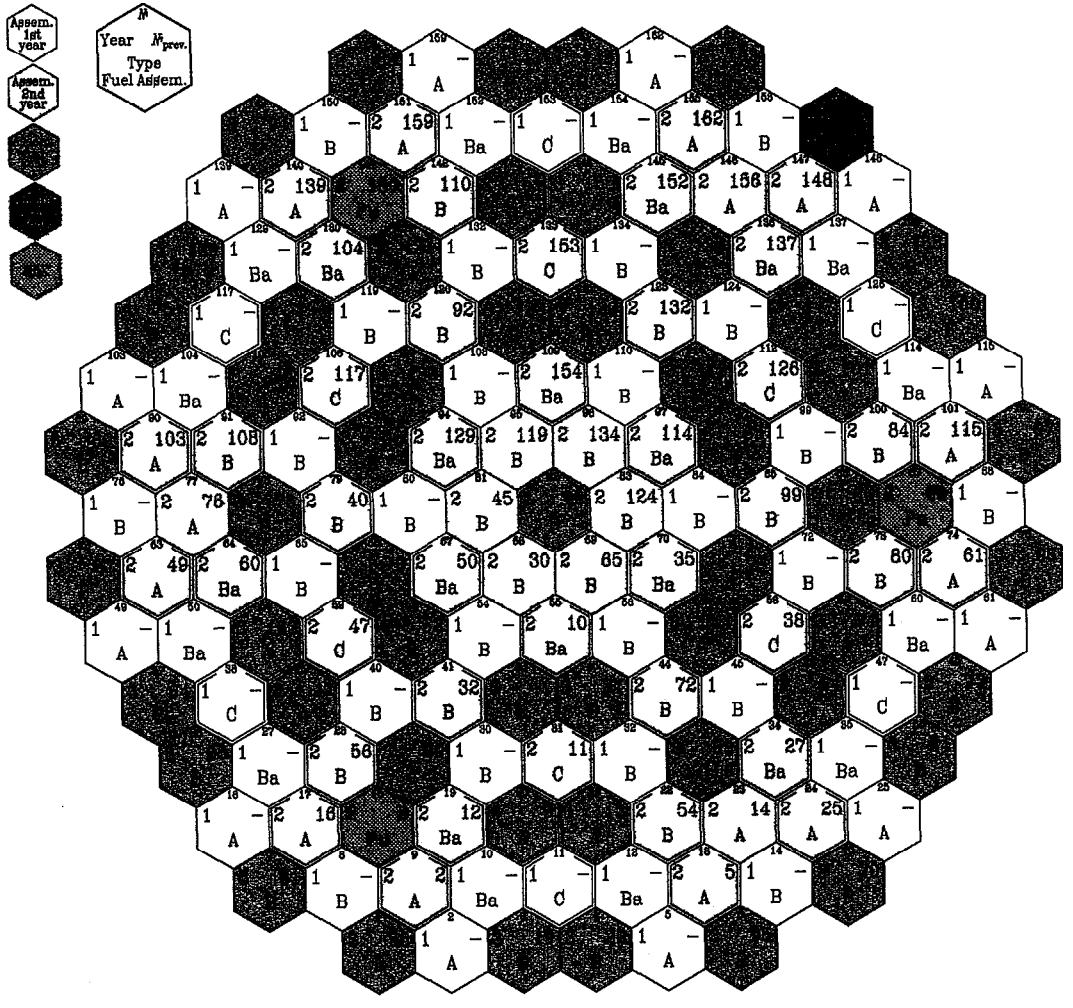

Figure 38. Second Cycle with 3 MOX LTAs 100%Pu (4.2-3.0-2.0). Assembly-by-Assembly Burnup Distribution

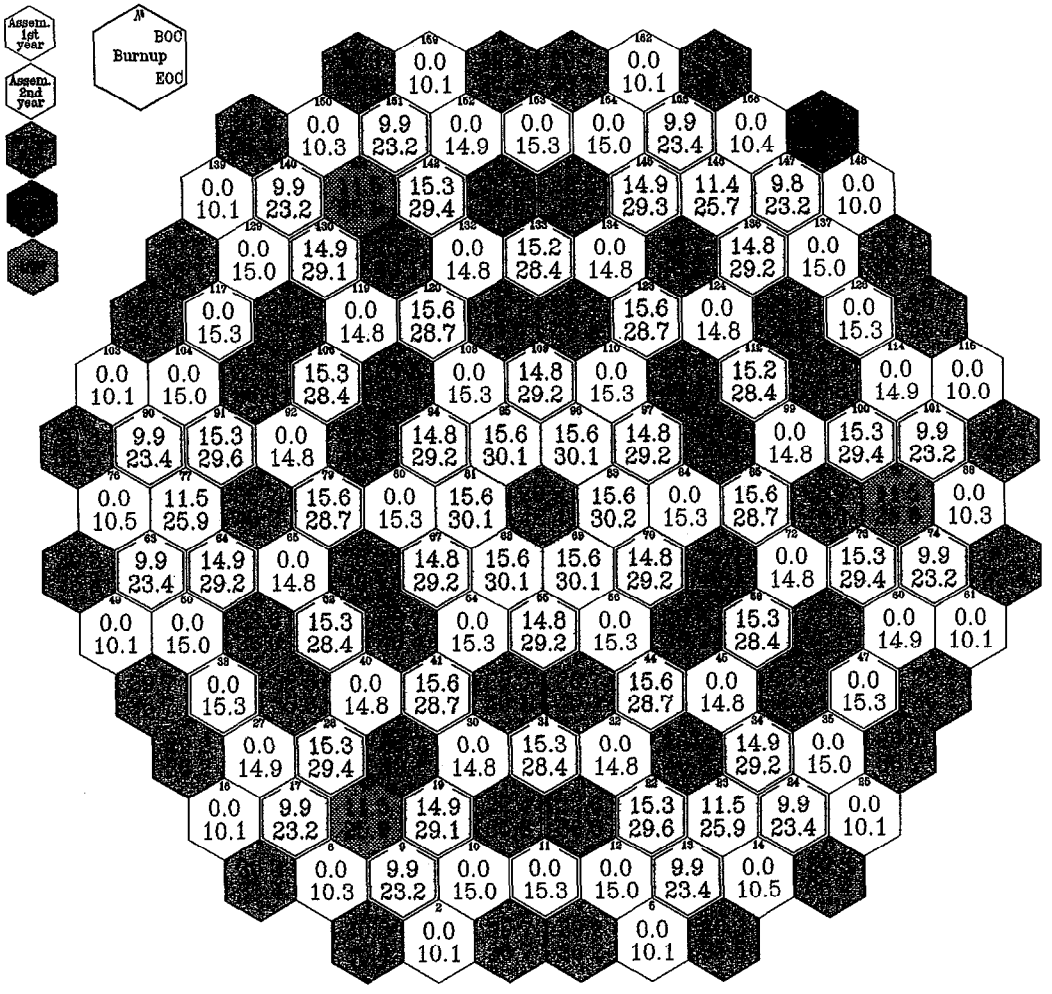

Figure 39. Second Cycle with 3 MOX LTAs 100%Pu (4.2-3.0-2.0). Assembly-by-Assembly Power Distribution

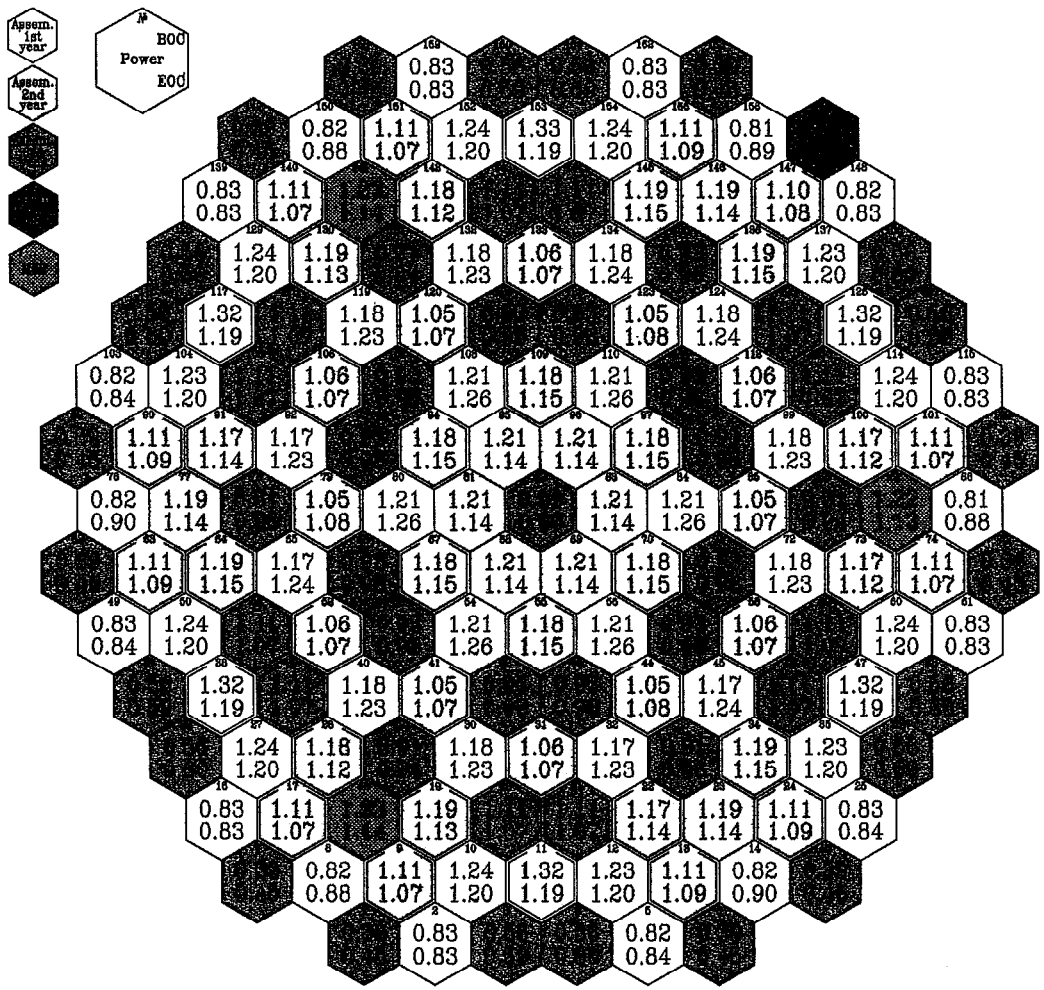

Figure 40. Beginning of the Second Cycle with 3 MOX LTAs 100%Pu (4.2-3.0-2.0). Assembly-by-Assembly Pin Power Peaking Factor

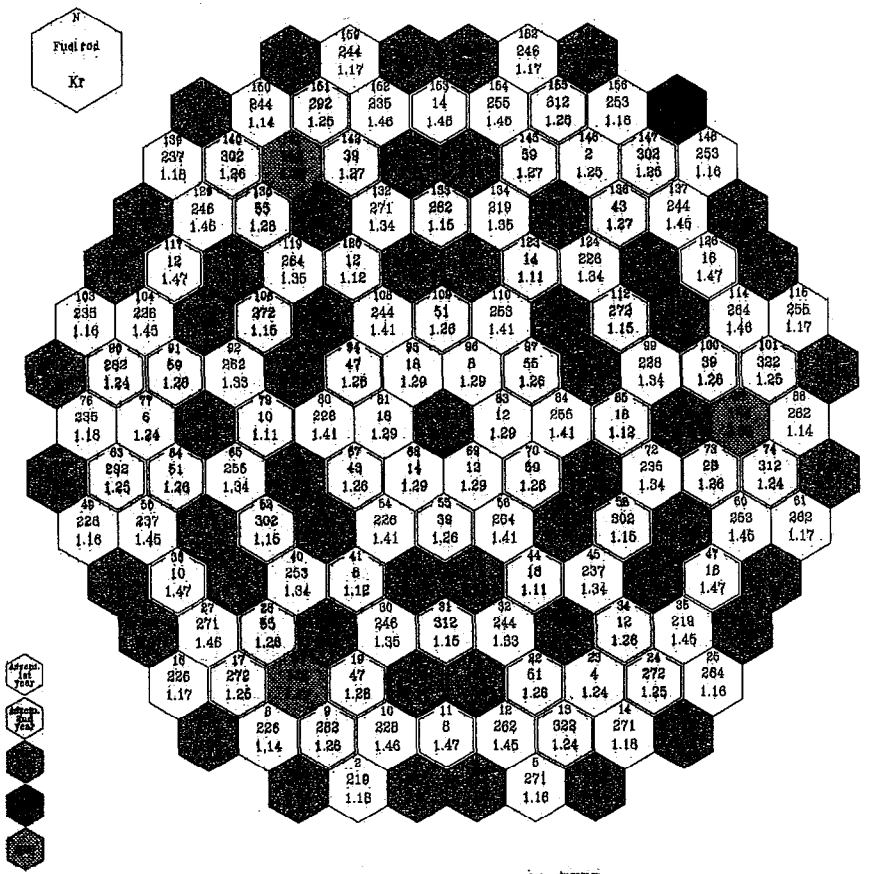

T	=	0.00	EFPD
W	=	3000.0	MWt
$C_{H_3BO_3}$	=	6.04	g/kg
Kr_{max}	=	1.48	
Fuel ass.	=	153	
Fuel rod	=	14	

Figure 41. End of the Second Cycle with 3 MOX LTAs 100%Pu (4.2-3.0-2.0). Assembly-by-Assembly Pin Power Peaking Factor

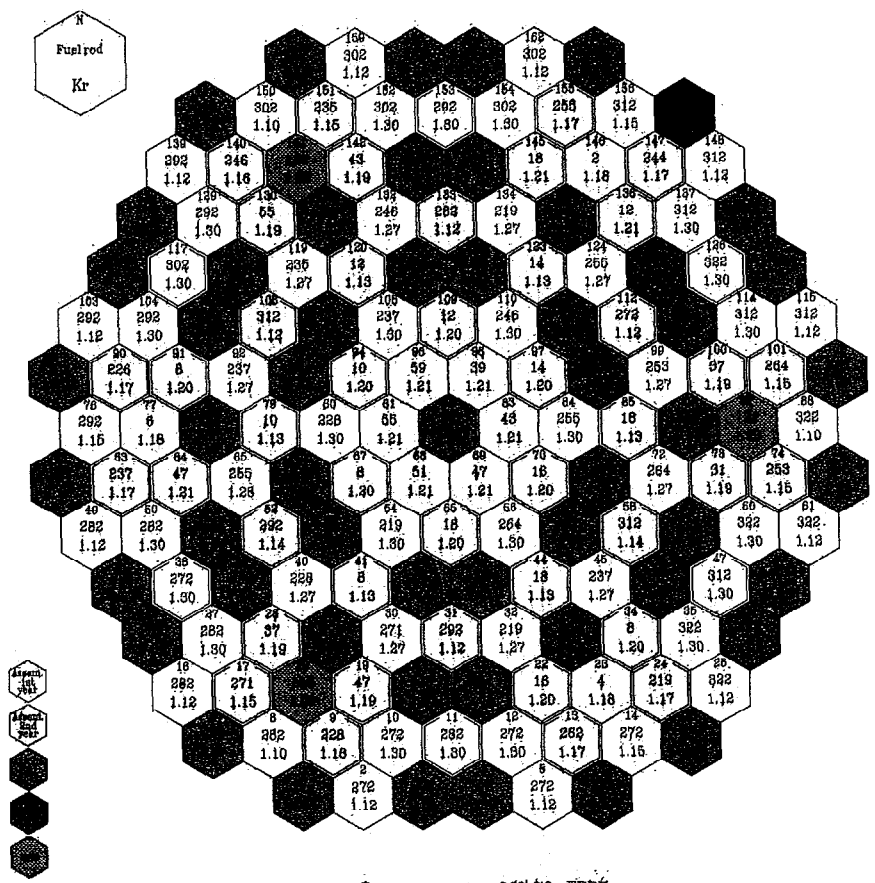

T	=	287.78 EFPD
W	=	3000.0 MWt
$C_{H_3BO_3}$	=	0,00 g/kg
Kr_{max}	=	1.30
Fuel ass.	=	50
Fuel rod	=	282

Figure 42. Beginning of the Second Cycle with 3 MOX LTAs 100%Pu (4.2-3.0-2.0). Assembly-by-Assembly Maximum Pin Linear Power

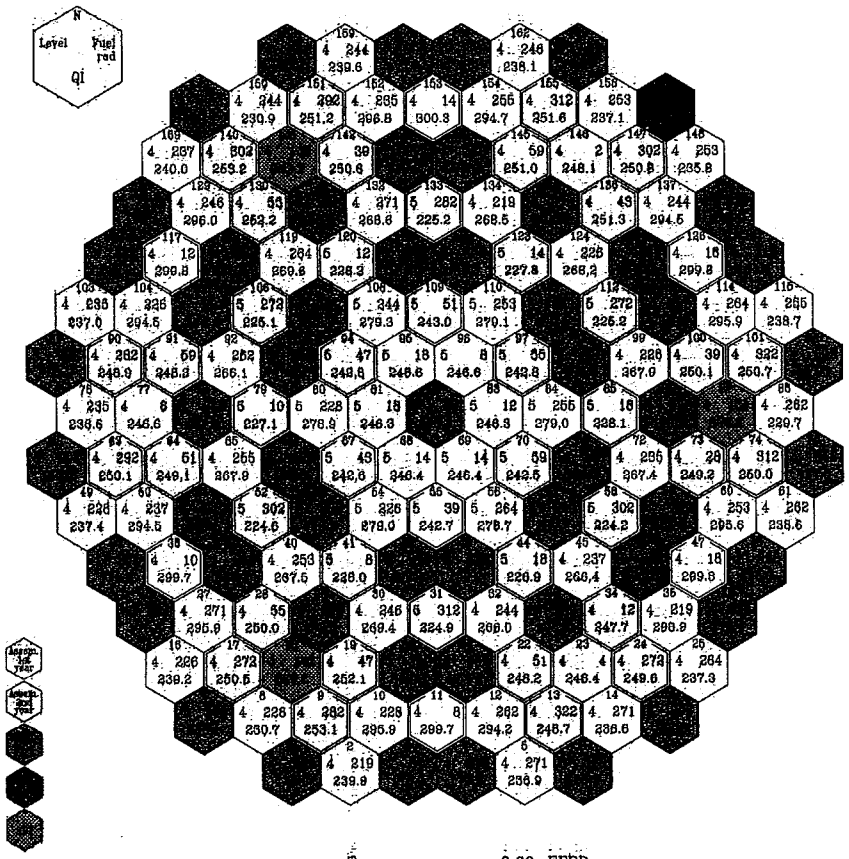

$\bar{T}$	=	0.00	EFPD
W	=	3000.0	MWt
$C_{H_3BO_3}$	=	6.04	g/kg
ql_{max}	=	300.3	Wt/cm
Fuel ass.	=	153	
Level	=	4	
Fuel rod	=	14	

Figure 43. End of the Second Cycle with 3 MOX LTAs 100%Pu (4.2-3.0-2.0). Assembly-by-Assembly Maximum Pin Linear Power

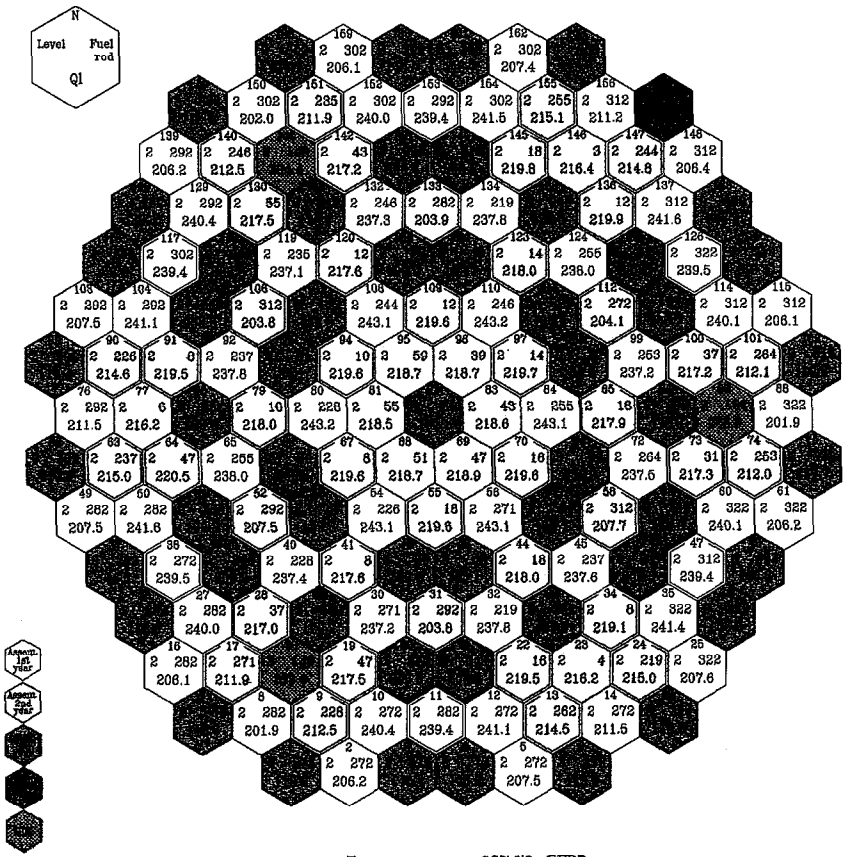

T	=	287.78	EFPD
W	=	3000.0	MWt
$C_{H_3BO_3}$	=	0.00	g/kg
Ql_{max}	=	243.2	Wt/cm
Fuel ass.	=	110	
Level	=	2	
Fuel rod	=	246	

Figure 44. Beginning of the Second Cycle with 3 MOX LTAs 100%Pu (4.2-3.0-2.0). Relative Power Distribution in the Most Powered Assembly

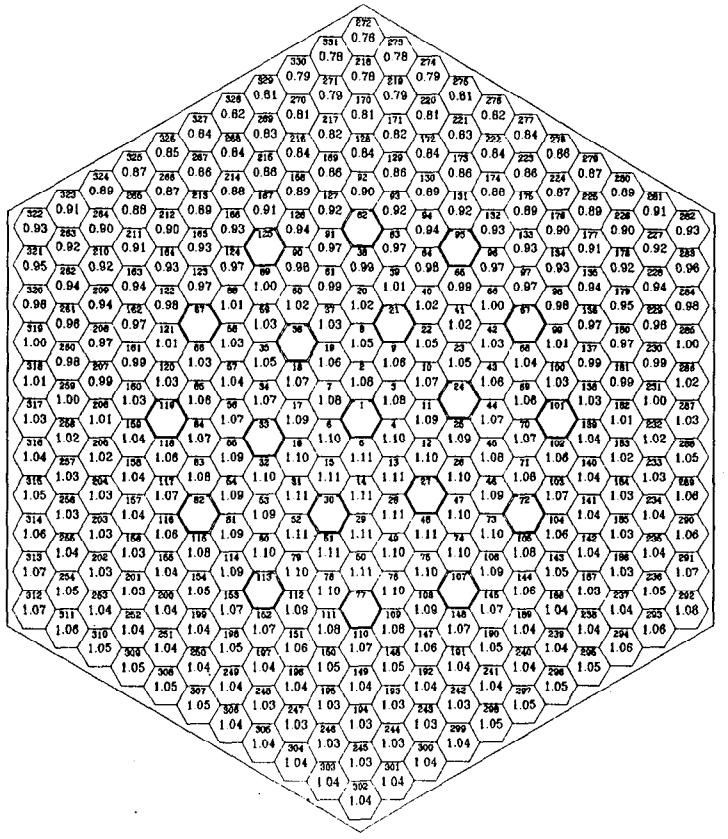

T	0.00	EFPD
W	3000.0	MWt
$C_{B,max}$	6.04	g/kg
Ql_{max}	300.3	Wt/cm
Fuel assembly	153	
Level	4	
Fuel rod	14	
Kk_{max}	1.11	

Figure 45. End of the Second Cycle with 3 MOX LTAs 100%Pu (4.2-3.0-2.0). Relative Power Distribution in the Most Powered Assembly

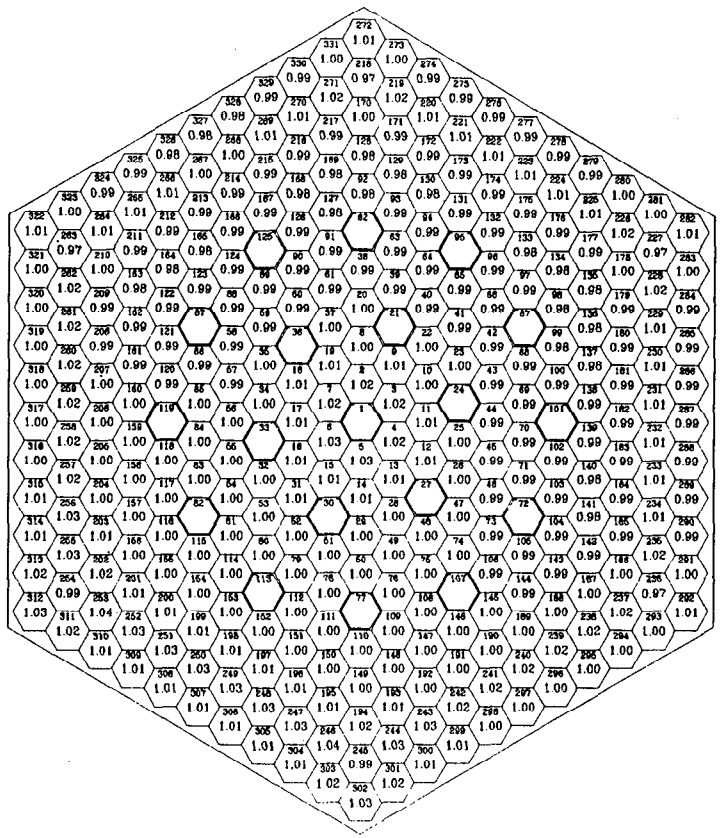

T	287.78	EFPD
W	3000.0	MWt
$C_{B,ppm}$	0.00	g/kg
Ql_{max}	243.2	Wt/cm
Fuel assembly	110	
Level	2	
Fuel rod	246	
Kk_{max}	1.04	

Figure 46. Beginning of the Second Cycle with 3 MOX LTAs 100%Pu (4.2-3.0-2.0). Relative Power Distribution in the MOX Assembly

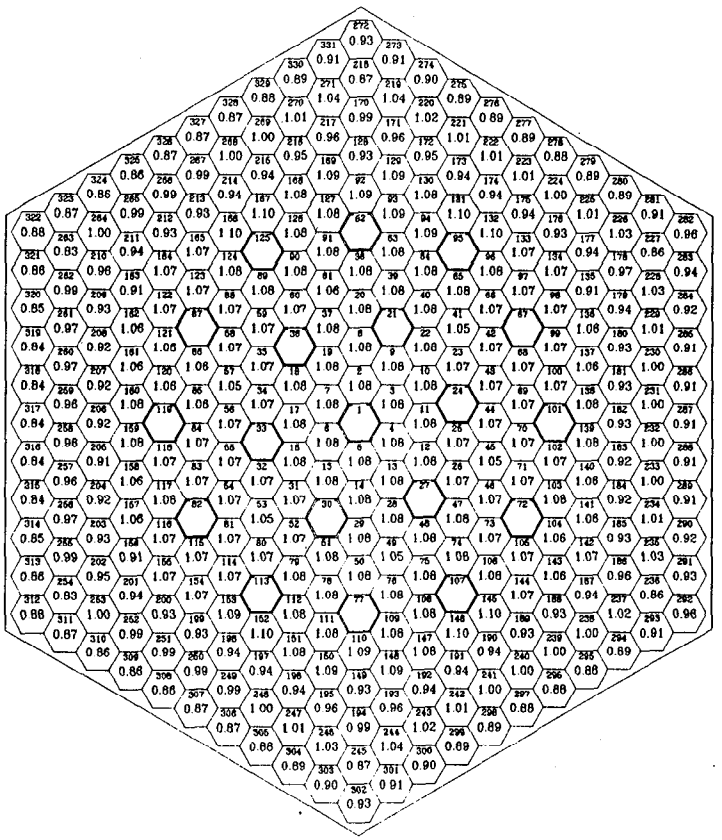

T	0.00	EFPD
W	3000.0	MWt
$C_{H_3BO_3}$	6.04	g/kg
Ql	268.8	Wt/cm
Fuel assembly	87	
Level	4	
Fuel rod	131	
KK_{max}	1.10	

Figure 46a. Beginning of the Second Cycle with 3 MOX LTAs of "Island" type (Pu3.8-2.8-U3.7). Relative Power Distribution in the MOX Assembly

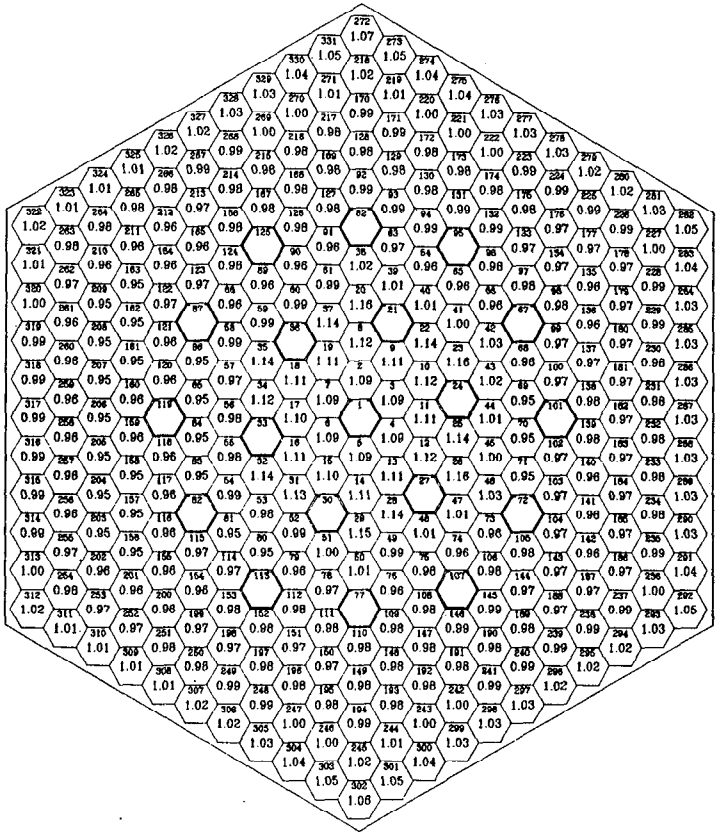

T	0.00	EFPD
W	3000.0	MWt
$C_{H_3BO_3}$	6.03	g/kg
Ql	282.5	Wt/cm
Fuel assembly	67	
Level	4	
Fuel rod	23	
Kk_{max}	1.16	

Figure 47. End of the Second Cycle with 3 MOX LTAs 100%Pu (4.2-3.0-2.0). Relative Power Distribution in the MOX Assembly

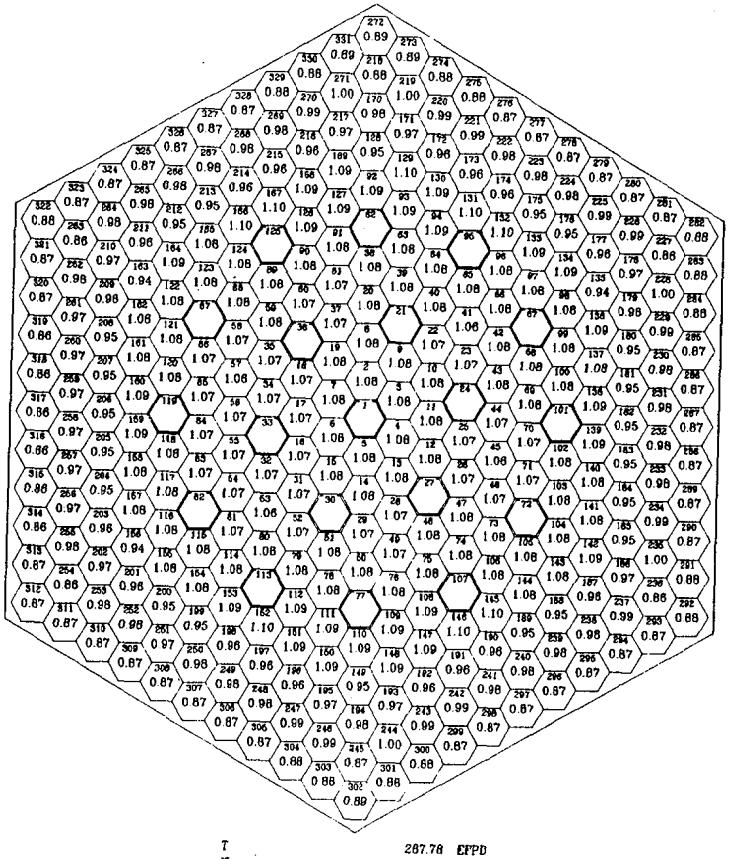

T	287.78	EFPD
W	3000.0	MWt
$C_{H_3BO_3}$	0.00	g/kg
QI	218.3	Wt/cm
Fuel assembly	87	
Level	4	
Fuel rod	131	
Kk_{max}	1.10	

Figure 47a. End of the Second Cycle with 3 MOX LTAs of "Island" type (Pu3.8-2.8-U3.7). Relative Power Distribution in the MOX Assembly

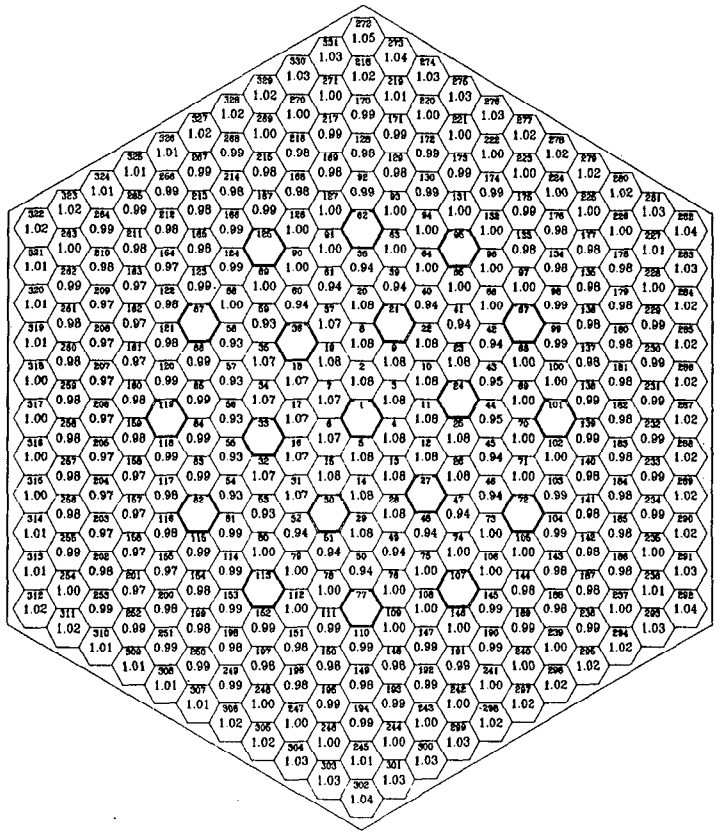

T.	288.55	EFPD
W	3000.0	MWt
$C_{B_2O_3}$	0.00	g/kg
Ql	218.9	Wt/cm
Fuel assembly	87	
Level	4	
Fuel rod	25	
Kk_{max}	1.08	

Figure 48. Beginning of the Second Cycle with 3 MOX LTAs 100%Pu (4.2-3.0-2.0). Relative Burnup Distribution in the MOX Assembly

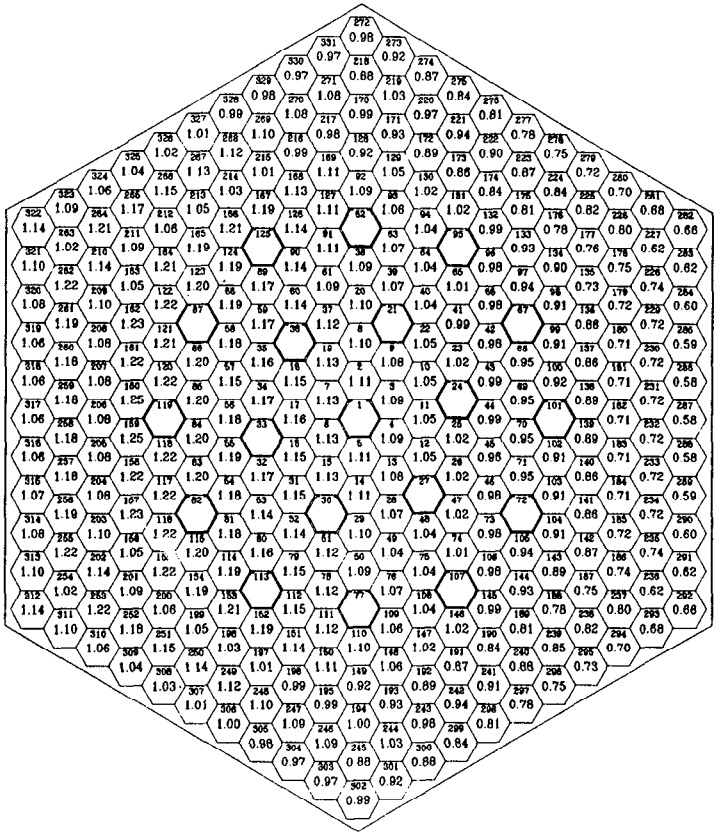

T	0.00	EFPD
W	3000.0	MWt
$C_{B_4C_1}$	6.04	g/kg
Burnup	15.8	
Fuel assembly	87	
Level	4	
Fuel rod	159	
Kb_{max}	1.25	

Figure 48a. Beginning of the Second Cycle with 3 MOX LTAs of "Island" type (Pu3.8-2.8-U3.7). Relative Burnup Distribution in the MOX Assembly

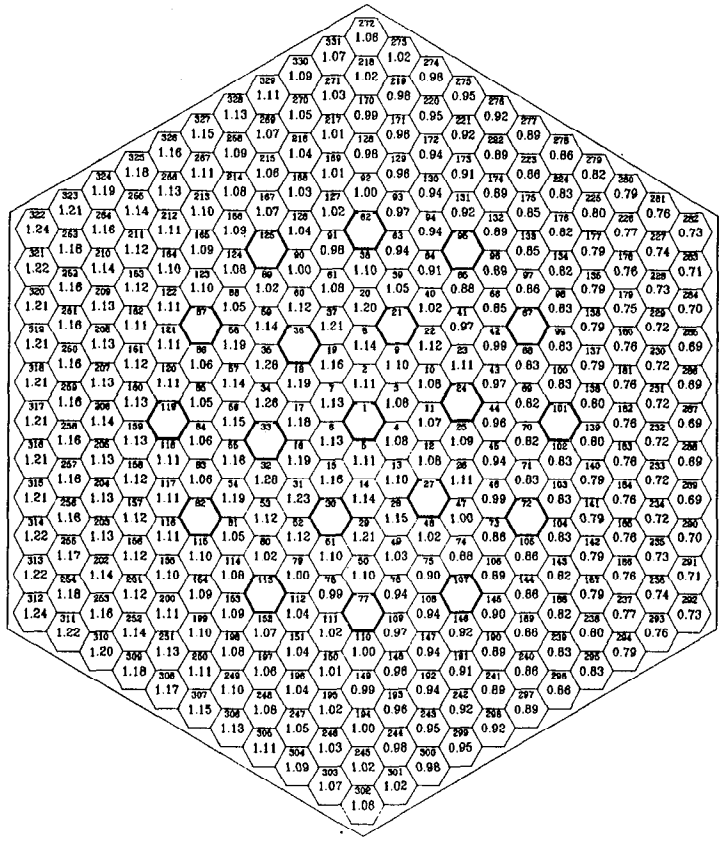

T	0.00	EFPD
W	3000.0	MWt
C_{B,ac_1}	6.03	g/kg
Burnup	16.9	
Fuel assembly	87	
Level	4	
Fuel rod	32	
Kb_{max}	1.28	

Figure 49. End of the Second Cycle with 3 MOX LTAs 100%Pu (4.2-3.0-2.0). Relative Burnup Distribution in the MOX Assembly

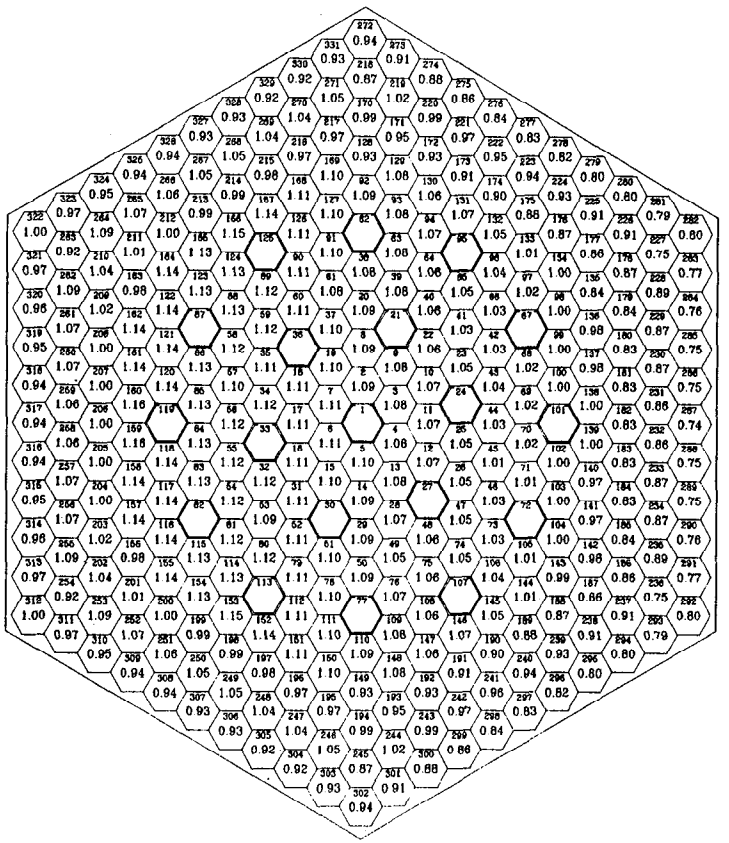

T	267.78	EFPD
W	3000.0	MWt
$C_{B_2O_3}$	0.00	g/kg
Burnup	33.0	
Fuel assembly	87	
Level	4	
Fuel rod	159	
Kb_{max}	1.16	

Figure 49a. End of the Second Cycle with 3 MOX LTAs of "Island" type (Pu3.8-2.8-U3.7). Relative Burnup Distribution in the MOX Assembly

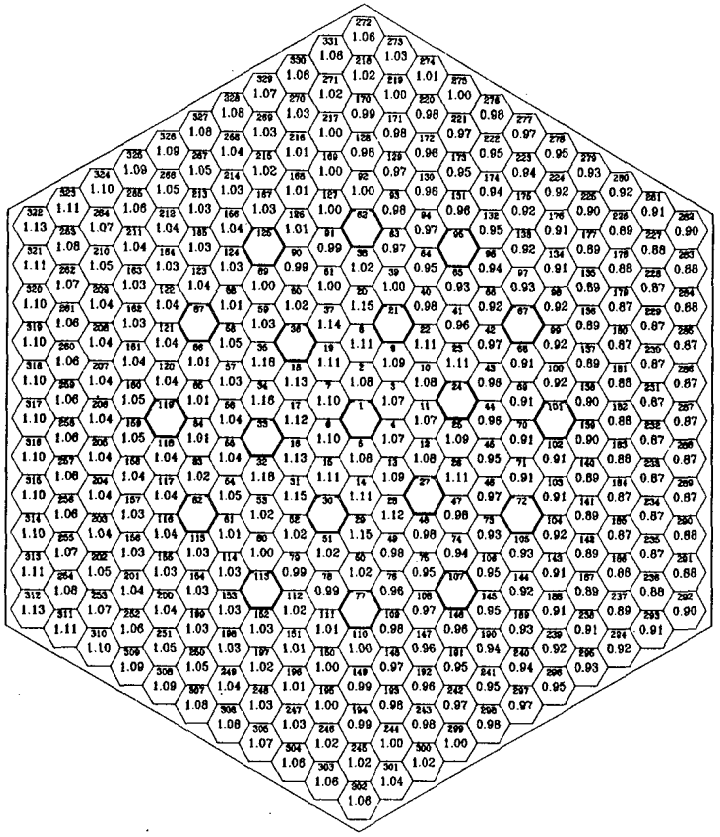

T	288.55	EFPD
W	3000.0	MWt
$C_{B_2O_3}$	0.00	g/kg
Burnup	34.3	
Fuel assembly	87	
Level	4	
Fuel rod	32	
Kb_{max}	1.18	

Figure 50. Loading Pattern for the Third Cycle with 3 MOX LTAs

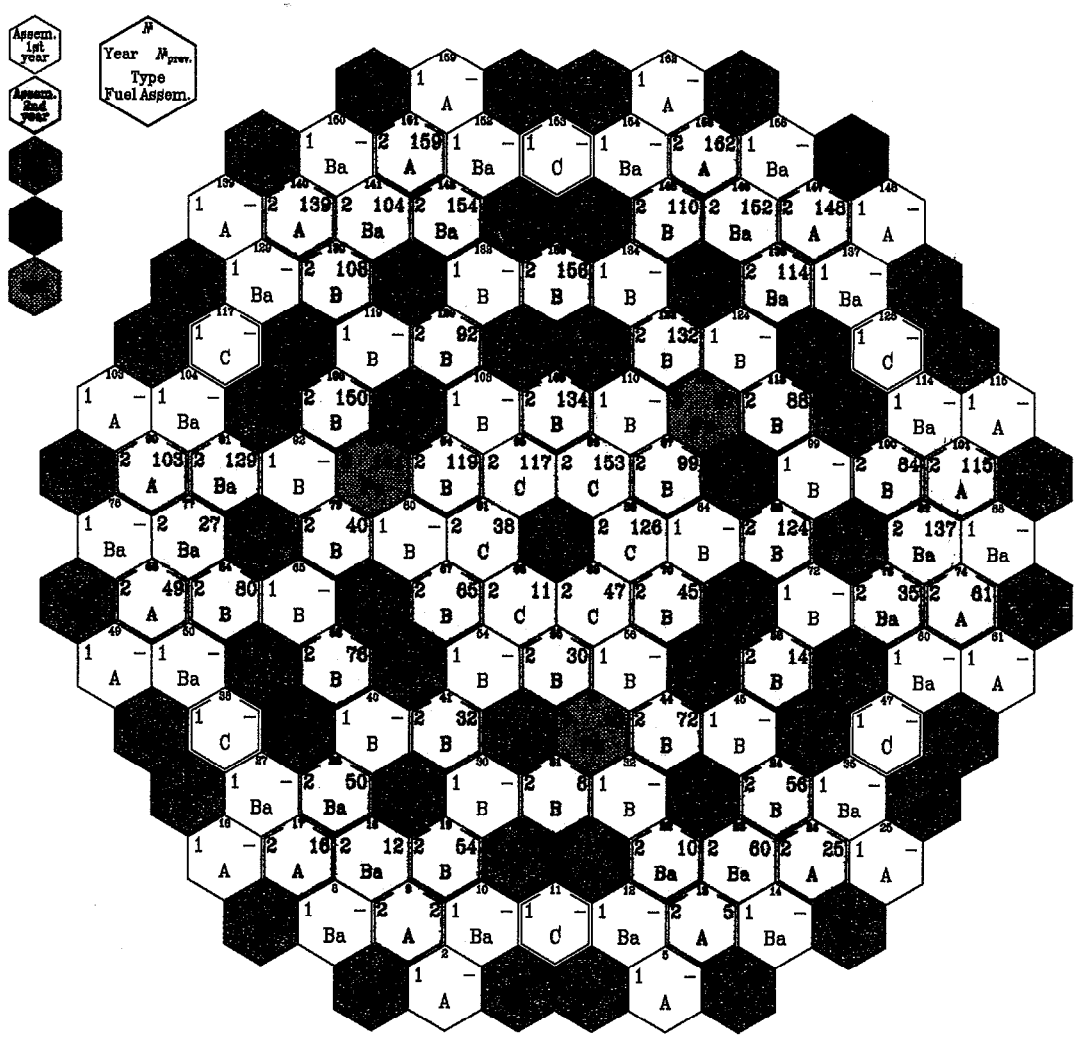

Figure 51. Third Cycle with 3 MOX LTAs 100%Pu (4.2-3.0-2.0). Assembly-by-Assembly Burnup Distribution

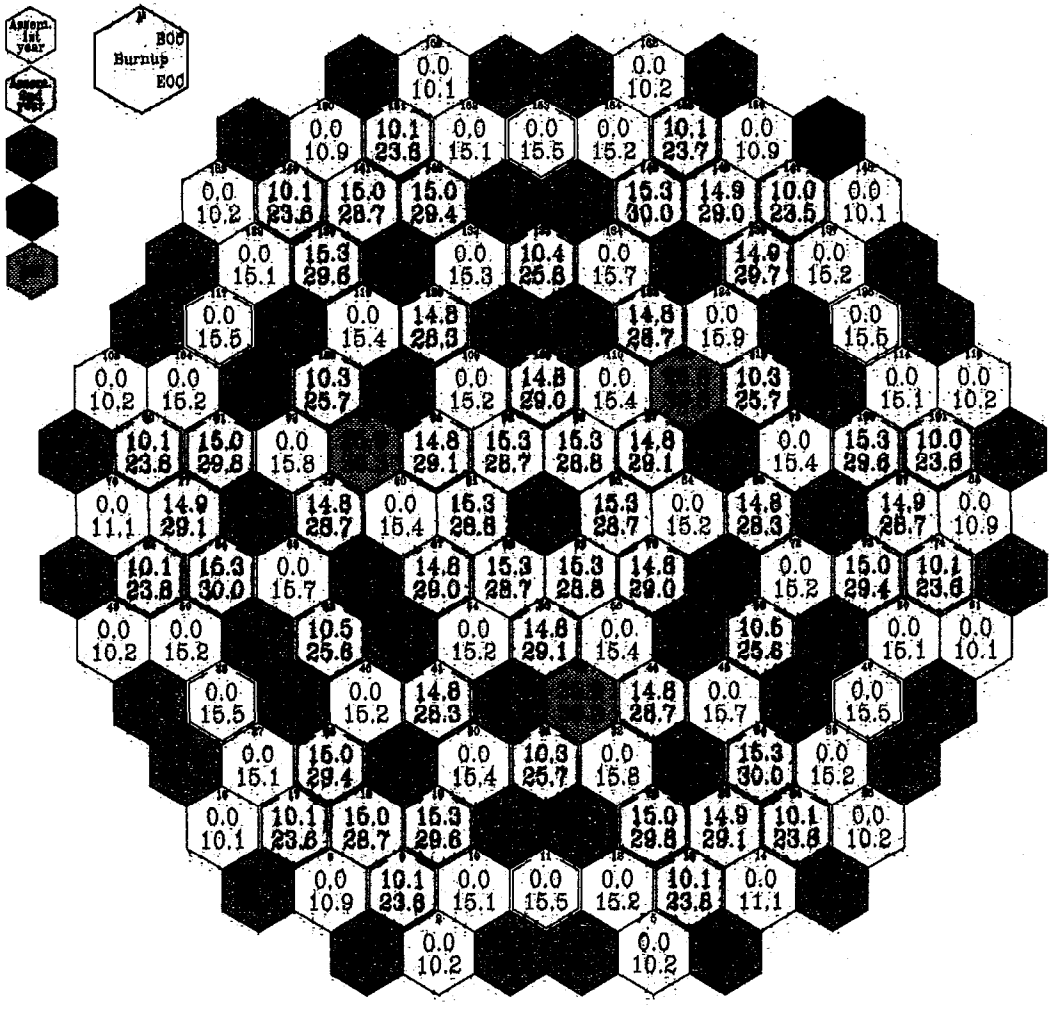

Figure 52. Third Cycle with 3 MOX LTAs 100%Pu (4.2-3.0-2.0). Assembly-by-Assembly Power Distribution

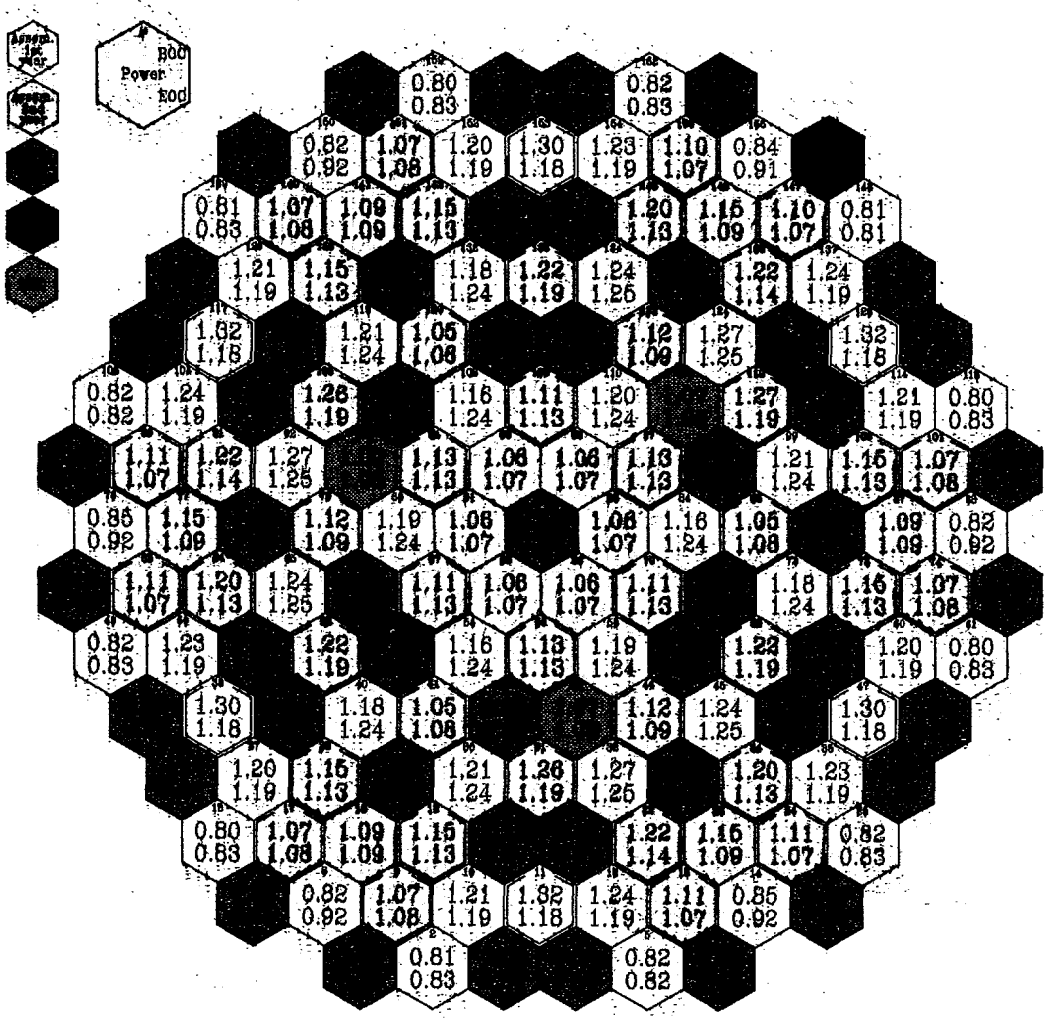

Figure 53. Beginning of the Third Cycle with 3 MOX LTAs 100%Pu (4.2-3.0-2.0). Assembly-by-Assembly Pin Power Peaking Factor

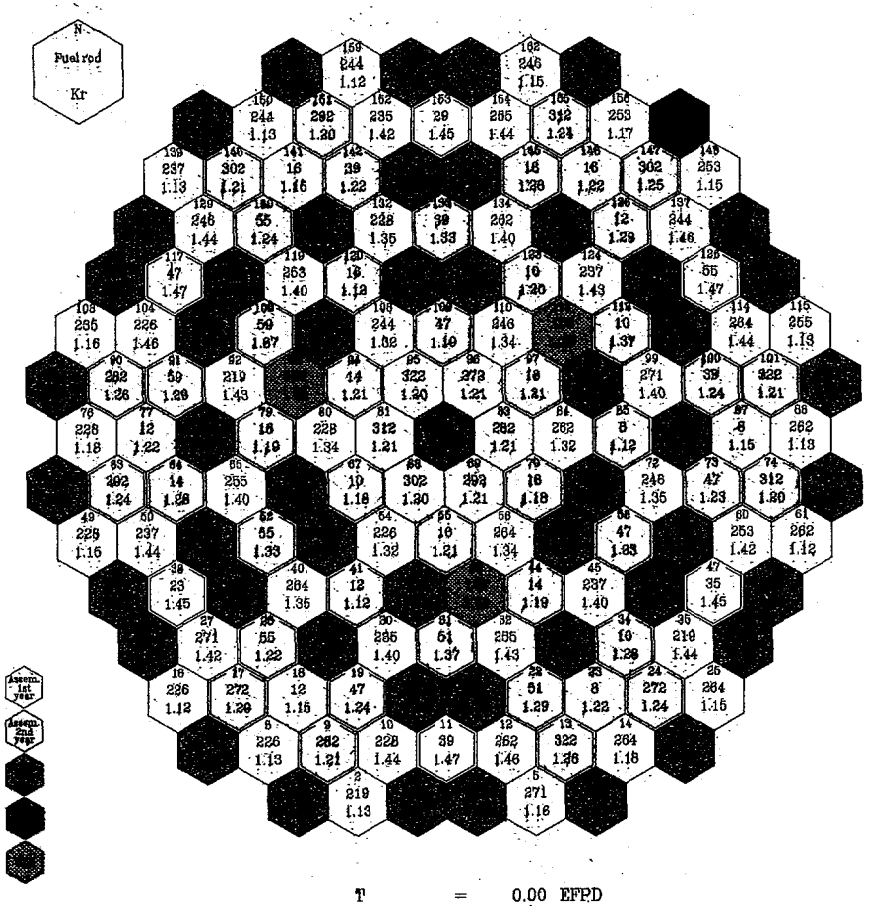

T	=	0.00	EFPD
W	=	3000.0	MWt
$C_{H_3BO_3}$	=	6.19	g/kg
Kr_{max}	=	1.47	
Fuel ass.	=	126	
Fuel rod	=	55	

Figure 54. End of the Third Cycle with 3 MOX LTAs 100%Pu (4.2-3.0-2.0). Assembly-by-Assembly Pin Power Peaking Factor

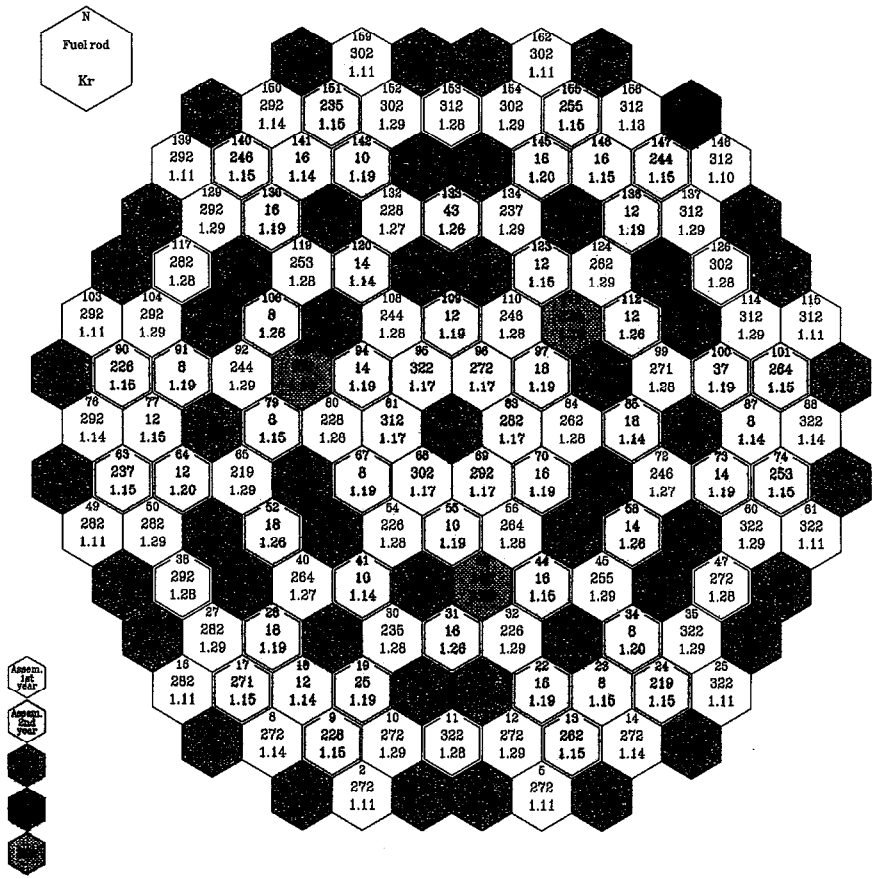

T	=	295.02	EFPD
W	=	3000.0	MWt
$C_{H_3BO_3}$	=	0.00	g/kg
Kr_{max}	=	1.29	
Fuel ass.	=	137	
Fuel rod	=	312	

Figure 55. Beginning of the Third Cycle with 3 MOX LTAs 100%Pu (4.2-3.0-2.0). Assembly-by-Assembly Maximum Pin Linear Power

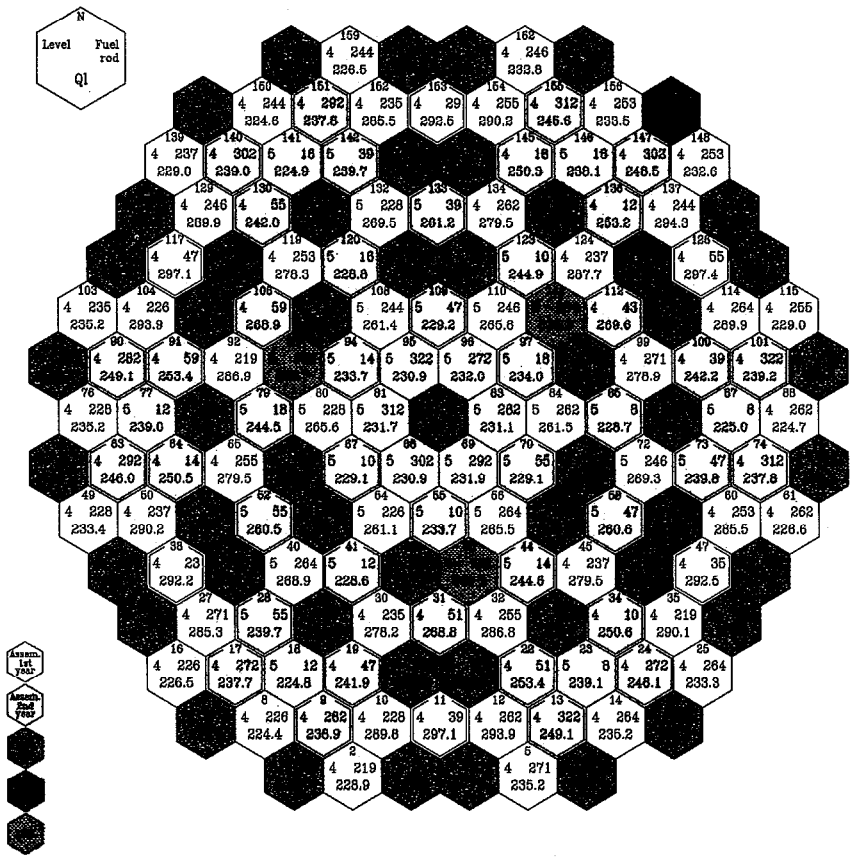

T	=	0.00	EFPD
W	=	3000.0	MWt
$C_{H_3BO_3}$	=	6.19	g/kg
Ql_{max}	=	297.4	Wt/cm
Fuel ass.	=	126	
Level	=	4	
Fuel rod	=	55	

Figure 56. End of the Third Cycle with 3 MOX LTAs 100%Pu (4.2-3.0-2.0). Assembly-by-Assembly Maximum Pin Linear Power

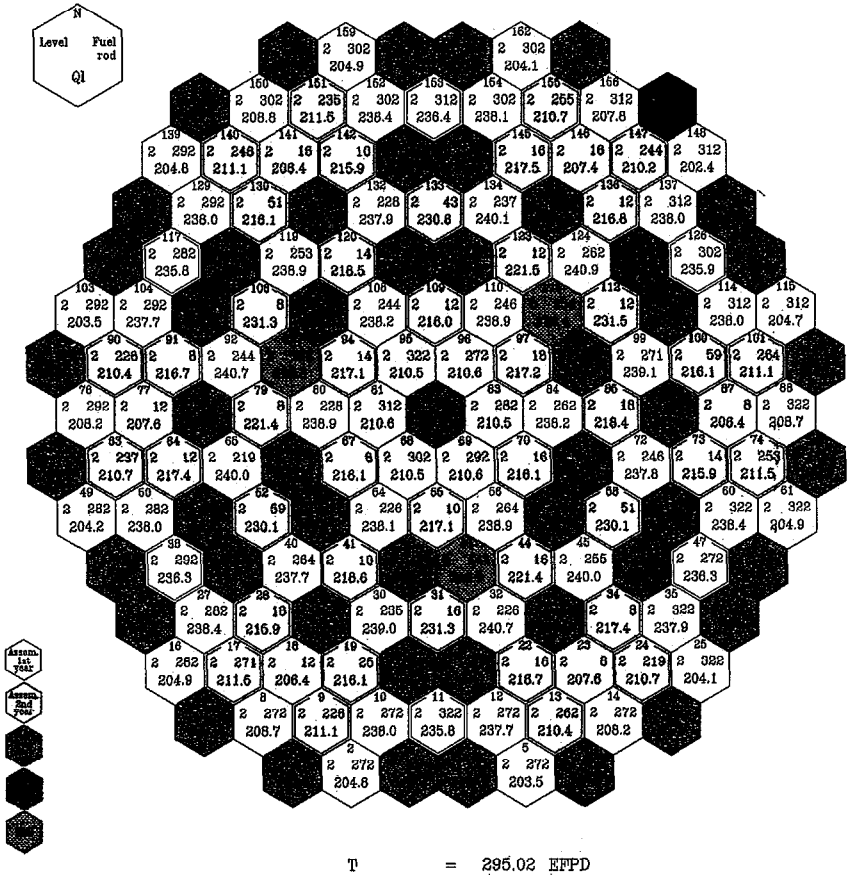

T	=	295.02	EFPD
W	=	3000.0	MWt
$C_{H_3BO_3}$	=	0.00	g/kg
Ql_{max}	=	240.9	Wt/cm
Fuel ass.	=	124	
Level	=	2	
Fuel rod	=	262	

Figure 57. Beginning of the Third Cycle with 3 MOX LTAs 100%Pu (4.2-3.0-2.0). Relative Power Distribution in the Most Powered Assembly

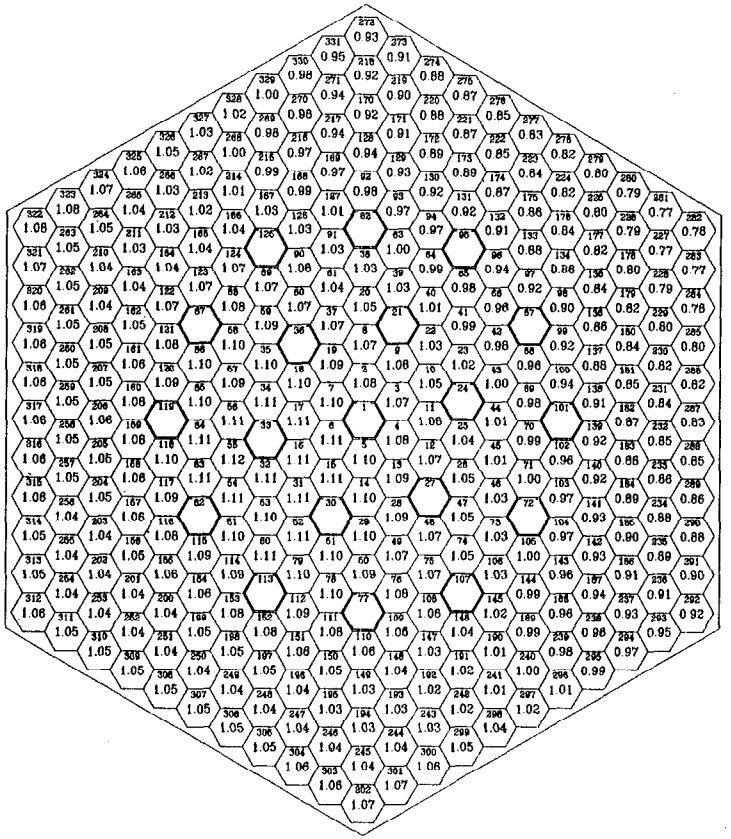

T	0.00	EFPD
W	3000.0	MWt
$C_{H_3BO_3}$	6.19	g/kg
Ql_{max}	297.4	Wt/cm
Fuel assembly	126	
Level	4	
Fuel rod	55	
Kk_{max}	1.12	

Figure 58. End of the Third Cycle with 3 MOX LTAs 100%Pu (4.2-3.0-2.0). Relative Power Distribution in the Most Powered Assembly

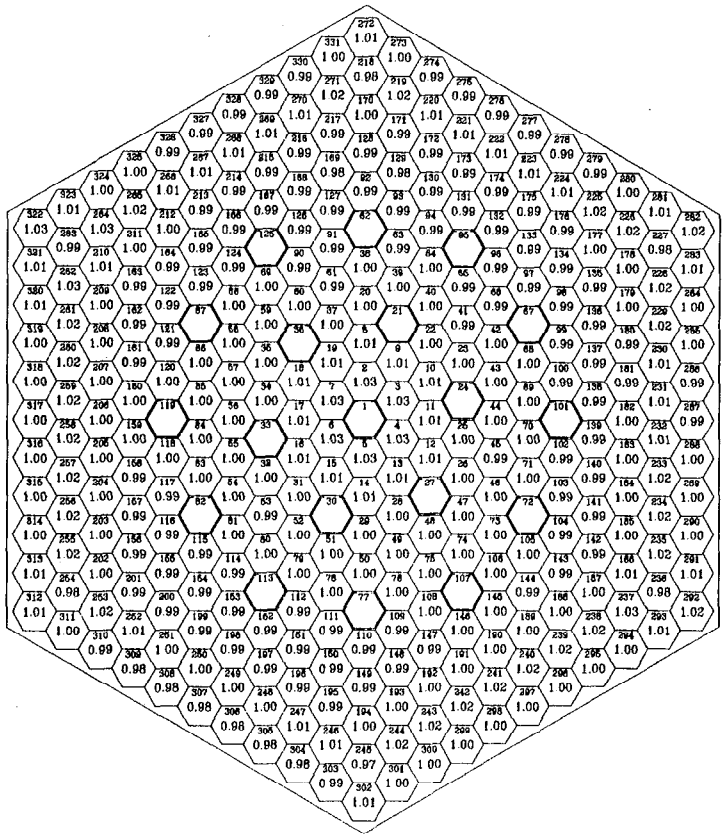

T	295.02	EFPD
W	3000.0	MWt
$C_{B_2O_3}$	0.00	g/kg
Ql_{max}	240.9	Wt/cm
Fuel assembly	124	
Level	2	
Fuel rod	262	
Kk_{max}	1.03	

Figure 59. Beginning of the Third Cycle with 3 MOX LTAs 100%Pu (4.2-3.0-2.0). Relative Power Distribution in the MOX Assembly

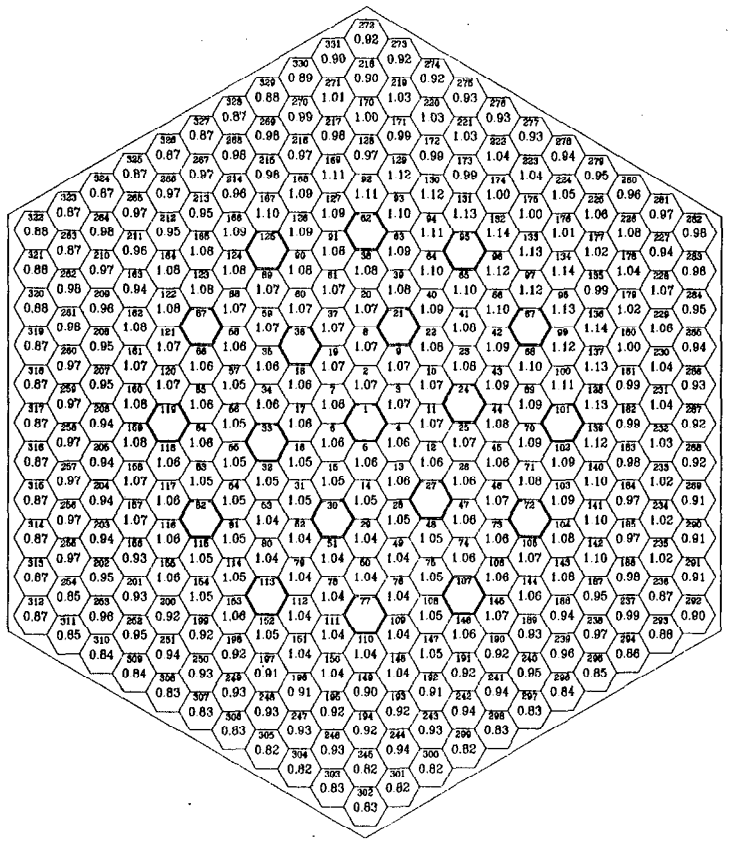

T	0.00	EFPD
W	3000.0	MWt
$C_{H_3BO_3}$	6.16	g/kg
Ql	229.1	Wt/cm
Fuel assembly	111	
Level	4	
Fuel rod	134	
Kk_{max}	1.14	

Figure 59a. Beginning of the Third Cycle with 3 MOX LTAs of "Island" type (Pu3.8-2.8-U3.7). Relative Power Distribution in the MOX Assembly

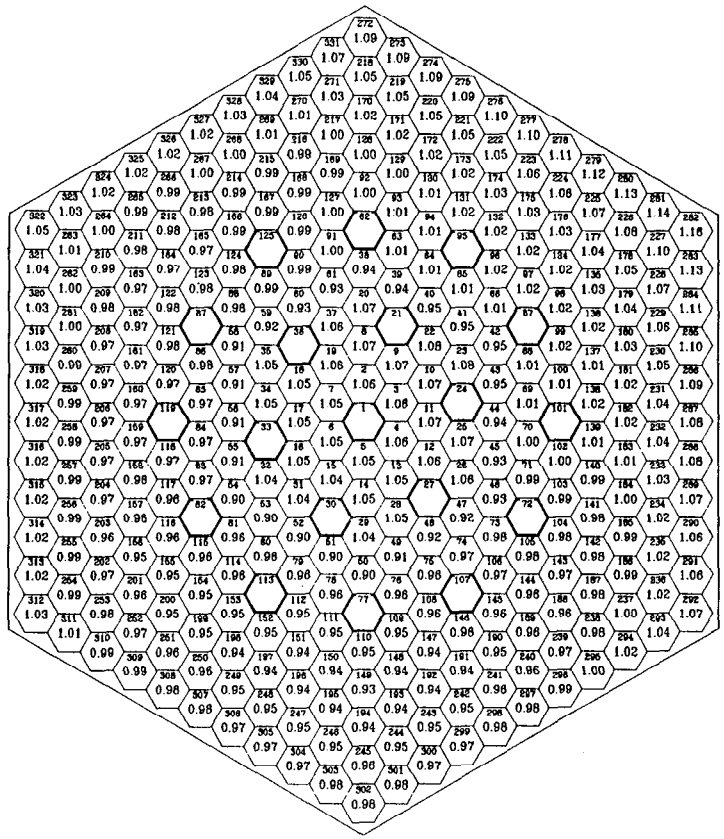

T	0.00	EFPD
W	3000.0	MWt
$C_{H_3BO_3}$	6.16	g/kg
Ql	233.5	Wt/cm
Fuel assembly	111	
Level	4	
Fuel rod	282	
Kk_{max}	1.16	

Figure 60. End of the Third Cycle with 3 MOX LTAs 100%Pu (4.2-3.0-2.0). Relative Power Distribution in the MOX Assembly

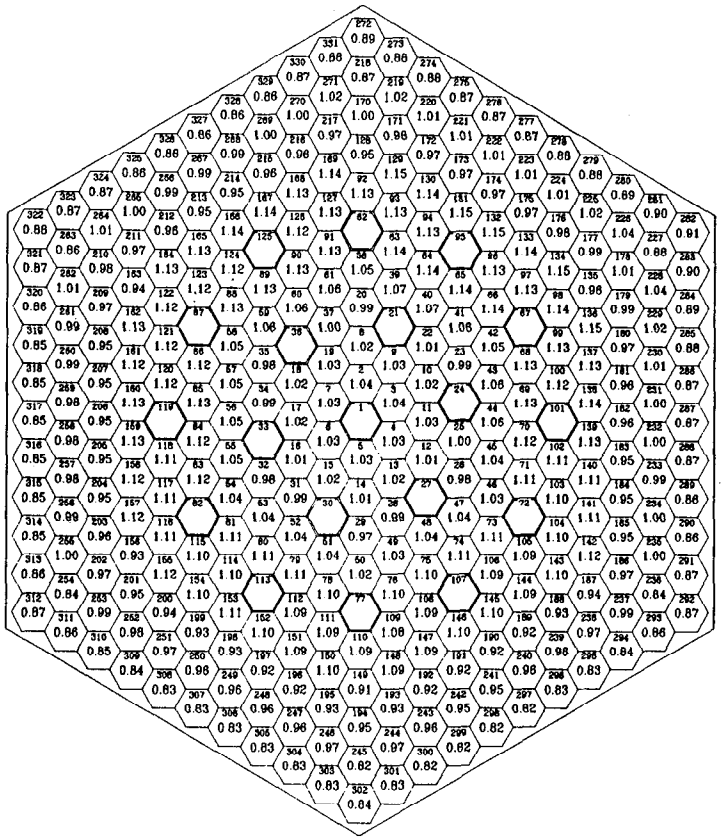

T	294.53	EFPD
W	3000.0	MWt
$C_{H_3BO_3}$	0.00	g/kg
Ql	207.0	Wt/cm
Fuel assembly	111	
Level	4	
Fuel rod	132	
Kk_{max}	1.15	

Figure 60a. End of the Third Cycle with 3 MOX LTAs of "Island" type (Pu3.8-2.8-U3.7). Relative Power Distribution in the MOX Assembly

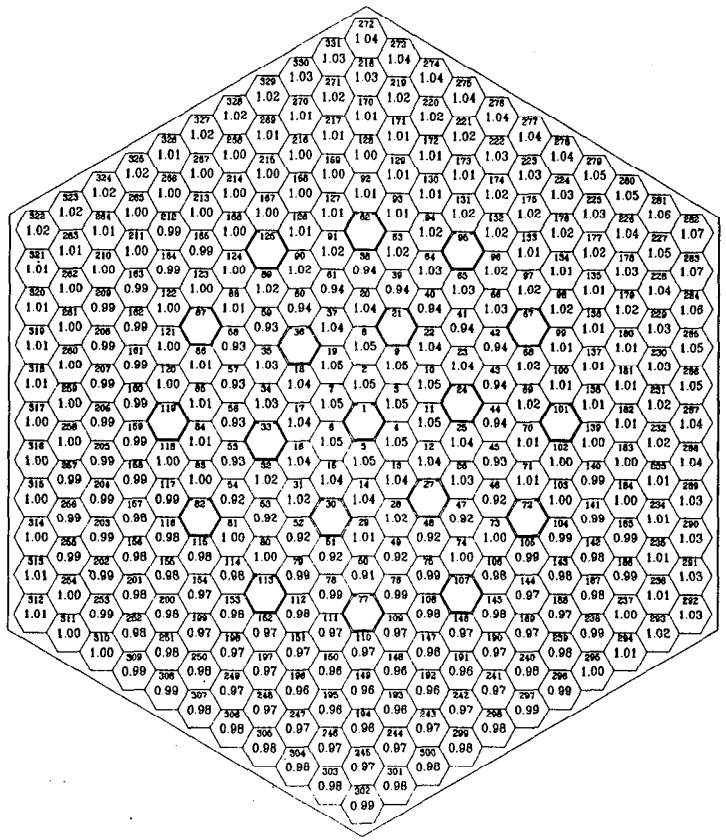

T	294.69	EFPD
W	3000.0	MWt
$C_{H_3BO_3}$	0.00	g/kg
Ql	195.0	Wt/cm
Fuel assembly	111	
Level	4	
Fuel rod	282	
Kk_{max}	1.07	

Figure 61. Beginning of the Third Cycle with 3 MOX LTAs 100%Pu (4.2-3.0-2.0). Relative Burnup Distribution in the MOX Assembly

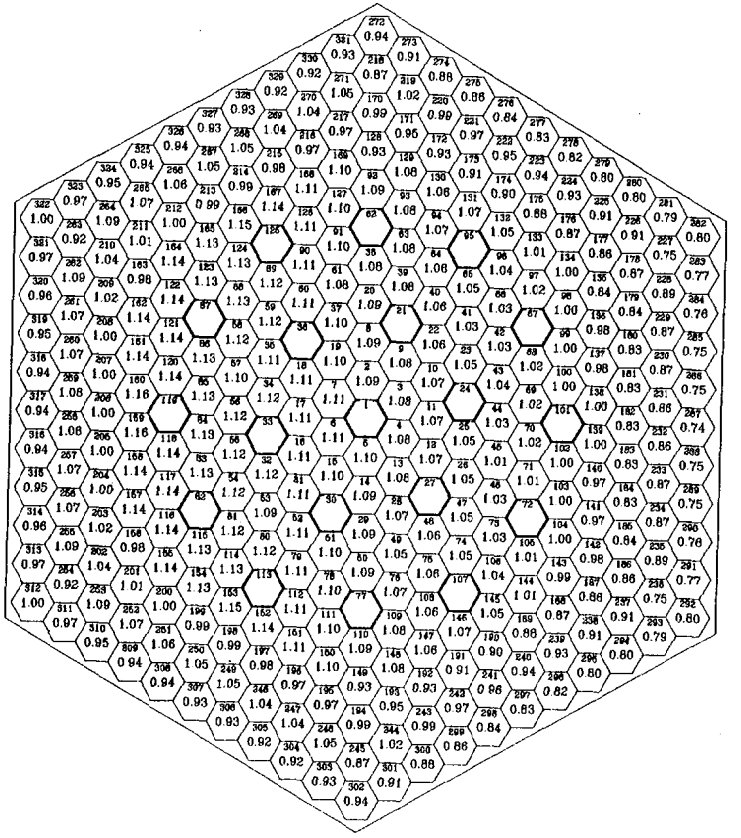

T	0.00	EFPD
W	3000.0	MWt
$C_{B_{max}}$	6 16	g/kg
Burnup	33.0	
Fuel assembly	111	
Level	4	
Fuel rod	159	
Kb_{max}	1 16	

Figure 61a. Beginning of the Third Cycle with 3 MOX LTAs of "Island" type (Pu3.8-2.8-U3.7). Relative Burnup Distribution in the MOX Assembly

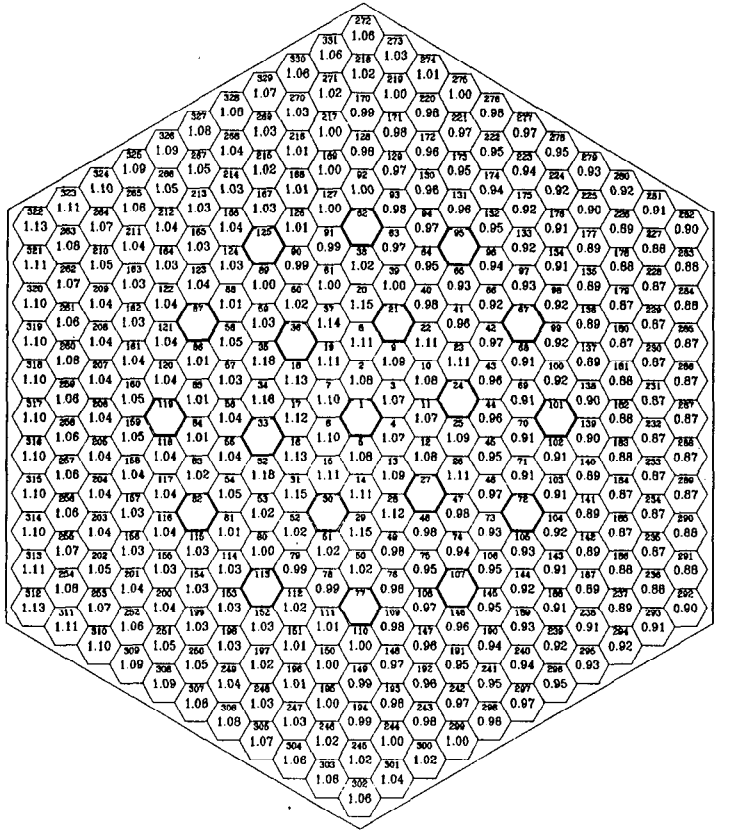

T	0.00	EFPD
W	3000.0	MWt
$C_{H_3BO_3}$	6.16	g/kg
Burnup	34.3	
Fuel assembly	111	
Level	4	
Fuel rod	32	
Kb_{max}	1.16	

Figure 62. End of the Third Cycle with 3 MOX LTAs 100%Pu (4.2-3.0-2.0). Relative Burnup Distribution in the MOX Assembly

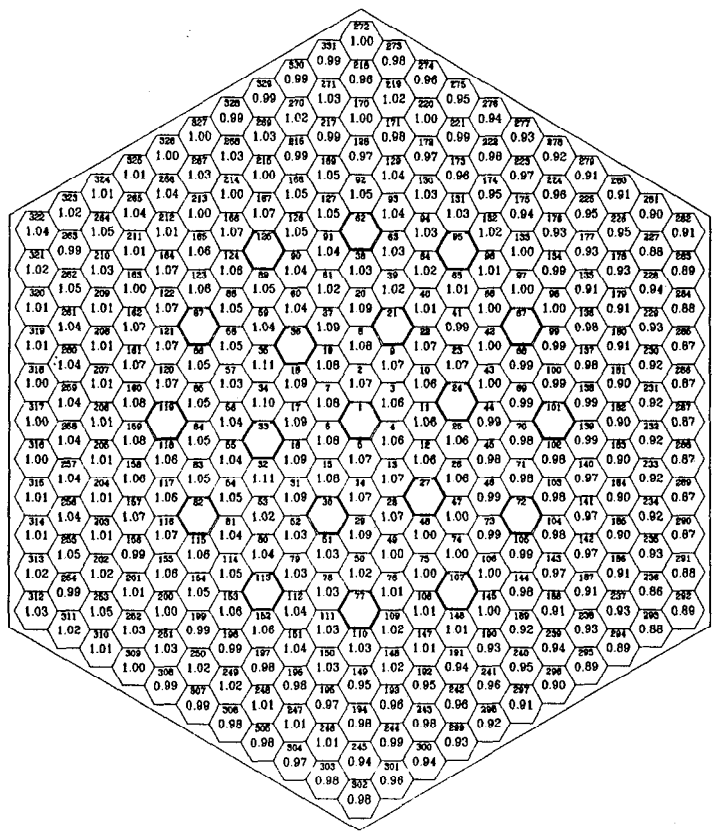

T	294.53	EFPD
W	3000.0	MWt
$C_{H_3BO_3}$	0.00	g/kg
Burnup	46.6	
Fuel assembly	111	
Level	4	
Fuel rod	35	
Kb_{max}	1.11	

Figure 62a. End of the Third Cycle with 3 MOX LTAs of "Island" type (Pu3.8-2.8-U3.7). Relative Burnup Distribution in the MOX Assembly

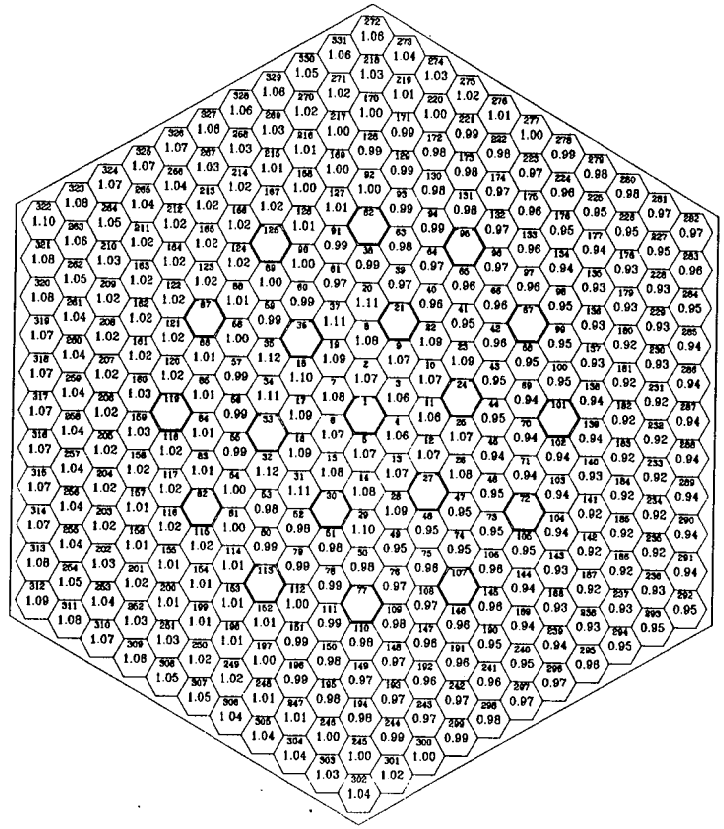

T	294.69	EFPD
W	3000.0	MWt
$C_{B_2O_3}$	0.00	g/kg
Burnup	48.8	
Fuel assembly	111	
Level	4	
Fuel rod	35	
Kb_{max}	1.12	

Figure 63. Control Rods Grouping and Positions of in-core self-powered detectors

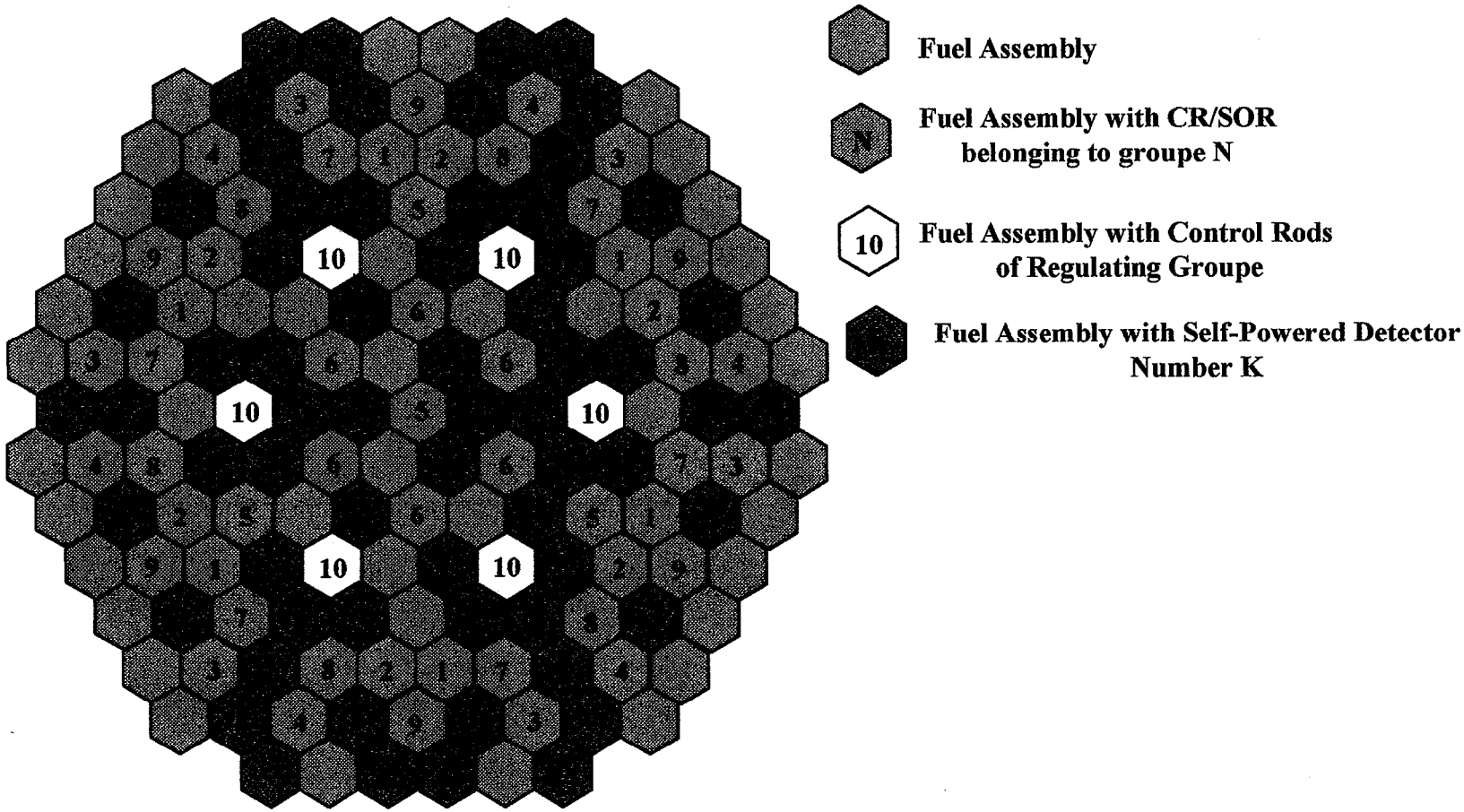

INTERNAL DISTRIBUTION

1–5. B. B. Bevard
6. J. J. Carbajo
7. E. D. Collins
8. B. S. Cowell
9. M. D. DeHart
10. F. C. Difilippo
11–15. J. C. Gehin
16. S. R. Greene
17. T. W. Horning
18. D. T. Ingersoll
19. H. T. Kerr
20. M. A. Kuliasha
21. G. T. Mays
22. G. E. Michaels
23. B. D. Murphy
24. D. L. Moses
25. C. V. Parks
26–30. R. T. Primm, III
31. I. Remec
32. C. C. Southmayd
33. B. A. Worley
34. B. S. Yarborough
35. G. L. Yoder, Jr.
36. Central Research Library
37–38. ORNL Laboratory Records (OSTI)
39. ORNL Laboratory Records–RC

EXTERNAL DISTRIBUTION

40. N. Abdurrahman, College of Engineering, Dept. of Mechanical Engineering, University of Texas, Austin, Texas 78712
41. M. L. Adams, Department of Nuclear Engineering, Texas A&M University, Zachry 129, College Station, TX 77843
42. H. Akkurt, College of Engineering, Dept. of Mechanical Engineering, University of Texas, Austin, TX 78712
43. D. Alberstein, Los Alamos National Laboratory, MS-E502, P.O. Box 1663, Los Alamos, NM 87545
44. J. Baker, Office of Fissile Materials Disposition, U. S. Department of Energy, MD-3, 1000 Independence Avenue SW, Washington, DC 20585
45. H. R. Canter, Office of Fissile Materials Disposition, U. S. Department of Energy, MD-1/2, 1000 Independence Avenue SW, Washington DC 20585
46. A. Caponiti, Office of Fissile Materials Disposition, U. S. Department of Energy, MD-3, 1000 Independence Avenue SW, Washington DC 20585
47. K. Chidester, Los Alamos National Laboratory, MS-E502, P.O. Box 1663, Los Alamos, NM 87545
48. W. Danker, U. S. Department of Energy, MD-3, 1000 Independence Avenue SW, Washington DC 20585
49. T. Gould, Lawrence Livermore National Laboratory, P.O. Box 808, MS-L186, Livermore, CA 94551
50. L. Jardine, Lawrence Livermore National Laboratory, P.O. Box 808, MS-L166, Livermore, CA 94551
51. Dr. Alexander Kalashnikov, Institute of Physics and Power Engineering, 1 Bondarenko Square, Obninsk, Kaluga Region, Russia 249020
52–57. D. E. Klein, Associate Vice Chancellor for Special Engineering Programs, The University of Texas System, 210 West Sixth Street, Austin, TX 78701
58. J. O. Nulton, Office of Fissile Materials Disposition, U.S. Department of Energy, MD-3, 1000 Independence Avenue SW, Washington, DC 20585
59. S. L. Passman, Sandia National Laboratories, 1401 Wilson Blvd., Suite 1050, Arlington, VA 22209
60–65. Dr. Alexander Pavlovitchev, Russian Research Center "Kurchatov Institute", Institute of Nuclear Reactors VVER Division, VVER Physics Department, 123182, Kurchatov Square, 1, Moscow, Russia
66. K. L. Peddicord, Associate Vice Chancellor, Texas A&M University, 120 Zachry, College Station, TX 77843-3133
67. G. Radulescu, Framatom Cogema Fuels, 1261 Town Center Drive, MS-423, Las Vegas, Nevada 89143
68. W. D. Reece, Texas A&M University, Department of Nuclear Engineering, Zachry 129, College Station, TX 77843-3133
69. P. T. Rhoads, Office of Fissile Materials Disposition, U.S. Department of Energy, MD-4, 1000 Independence Avenue SW, Washington, DC 20585
70. J. Thompson, Office of Fissile Materials Disposition, U.S. Department of Energy, MD-4, 1000 Independence Avenue SW, Washington, DC 20585
71. M. Yavuz, 7201 Wood Hollow Drive, #475, Austin, TX 78731